Cardiac c-Kit Biology Revealed by Inducible Transgenesis

Natalie A. Gude,* Fareheh Firouzi,* Kathleen M. Broughton, Kelli Ilves, Kristine P. Nguyen, Christina R. Payne, Veronica Sacchi, Megan M. Monsanto, Alexandria R. Casillas, Farid G. Khalafalla, Bingyan J. Wang, David E. Ebeid, Roberto Alvarez, Walter P. Dembitsky, Barbara A. Bailey, Jop van Berlo, Mark A. Sussman

Rationale: **Biological significance of c-Kit as a cardiac stem cell marker and role(s) of c-Kit+ cells in myocardial development or response to pathological injury remain unresolved because of varied and discrepant findings. Alternative experimental models are required to contextualize and reconcile discordant published observations of cardiac c-Kit myocardial biology and provide meaningful insights regarding clinical relevance of c-Kit signaling for translational cell therapy.**

Objective: **The main objectives of this study are as follows: demonstrating c-Kit myocardial biology through combined studies of both human and murine cardiac cells; advancing understanding of c-Kit myocardial biology through creation and characterization of a novel, inducible transgenic c-Kit reporter mouse model that overcomes limitations inherent to knock-in reporter models; and providing perspective to reconcile disparate viewpoints on c-Kit biology in the myocardium.**

Methods and Results: **In vitro studies confirm a critical role for c-Kit signaling in both cardiomyocytes and cardiac stem cells. Activation of c-Kit receptor promotes cell survival and proliferation in stem cells and cardiomyocytes of either human or murine origin. For creation of the mouse model, the cloned mouse c-Kit promoter drives Histone2B-EGFP (enhanced green fluorescent protein; H2BEGFP) expression in a doxycycline-inducible transgenic reporter line. The combination of c-Kit transgenesis coupled to H2BEGFP readout provides sensitive, specific, inducible, and persistent tracking of c-Kit promoter activation. Tagging efficiency for EGFP+/c-Kit+ cells is similar between our transgenic versus a c-Kit knock-in mouse line, but frequency of c-Kit+ cells in cardiac tissue from the knock-in model is 55% lower than that from our transgenic line. The c-Kit transgenic reporter model reveals intimate association of c-Kit expression with adult myocardial biology. Both cardiac stem cells and a subpopulation of cardiomyocytes express c-Kit in uninjured adult heart, upregulating c-Kit expression in response to pathological stress.**

Conclusions: **c-Kit myocardial biology is more complex and varied than previously appreciated or documented, demonstrating validity in multiple points of coexisting yet heretofore seemingly irreconcilable published findings. (*Circ Res*. 2018;123:57-72. DOI: 10.1161/CIRCRESAHA.117.311828.)**

Key Words: c-Kit protein ■ myocardium ■ myocytes, cardiac ■ signal transduction ■ stem cell

Cardiovascular research has struggled to advance the field of regenerative medicine, due in part to the lack of a unique and unequivocal marker for resident adult cardiac stem cells capable of mediating repair. In fact, the concept of myocardial regeneration that was initially advanced over a decade ago used the stem cell marker c-Kit to identify presumptive cardiac stem cells.[1,2] During the ensuing years, the c-Kit+ cardiac stem cell population has become the focus of intense and diverse investigation by hundreds of laboratories worldwide at both the basic and clinical levels.[3–10] At present, the presence and participation of c-Kit+ cells in myocardial development and response to pathological stress or injury are indisputable.[2,4,8,10–12] However, controversy persists on the roles(s) that cells expressing c-Kit play in cardiac biology. Such divergent perspectives suggest that fundamental understanding has not been achieved and that additional study is warranted to provide sorely needed novel insight(s). The present study was conceived and initiated to examine myocardial c-Kit biology with fresh perspective using a unique approach yielding novel findings.

Editorial, see p 9
In This Issue, see p 2
Meet the First Author, see p 3

Original received August 2, 2017; revision received March 24, 2018; accepted April 9, 2018. In March 2018, the average time from submission to first decision for all original research papers submitted to *Circulation Research* was 10.69 days.

From the SDSU Heart Institute, Department of Biology (N.A.G., F.F., K.M.B., K.I., K.P.N., C.R.P., V.S., M.M.M., A.R.C., F.G.K., B.J.W., D.E.E., R.A., M.A.S.) and SDSU Department of Mathematics and Statistics (B.A.B.), San Diego State University, CA; Sharp Memorial Hospital, San Diego, CA (W.P.D.); and Department of Medicine, University of Minnesota, Minneapolis (J.v.B.).

*N.A.G. and F.F. contributed equally to this article.

The online-only Data Supplement is available with this article at http://circres.ahajournals.org/lookup/suppl/doi:10.1161/CIRCRESAHA.117.311828/-/DC1.

Correspondence to Mark A. Sussman, PhD, SDSU Heart Institute and Department of Biology, San Diego State University, 5500 Campanile Dr NLS426, San Diego, CA 92182. E-mail heartman4ever@icloud.com

Novelty and Significance

What Is Known?

- The mammalian heart has a limited capacity for self-renewal and repair. The identity of cells responsible for this regenerative activity remains an area of active investigation.
- c-Kit is a receptor tyrosine kinase used to identify cardiac stem and progenitor cell populations. c-Kit signaling promotes cell proliferation and survival.
- The cardiac c-Kit cell population is heterogeneous; it contributes to myocardial development and participates in the myocardial response to injury.
- Experimental animal models designed to identify and study the biological function of c-Kit–expressing cells produce varying and discrepant results likely in part because of variations in promoter and reporter design.

What New Information Does This Article Contribute?

- c-Kit expression increases in mouse and human cardiac progenitor cells in response to cellular stress.
- c-Kit is expressed in adult cardiac myocytes, and its abundance increases after cellular stress.
- c-Kit signaling promotes proliferation and survival in mouse and human cardiac progenitor cells.
- The novel, transgenic, inducible c-Kit reporter mouse model characterized in this study reveals previously unrecognized heterogeneous, dynamic c-Kit expression and biology in the postnatal myocardium.

The biological role of cardiac c-Kit has been largely overlooked in the cardiovascular research community because of overemphasis on the use of c-Kit as a marker for stem cells. The protective and proproliferative effects of c-Kit signaling in cardiac cells are central to their regenerative potential and their role in cardiac formation and repair. Heterogeneity of the cardiac c-Kit+ cell population including c-Kit activity in cardiac myocytes, confirmed with our novel transgenic reporter mouse, reconcile and extend prior divergent reports and point toward new horizons for c-kit biology in the myocardium. The biological role(s) for cardiac progenitor cells, including those expressing c-kit, in maintaining cardiac homeostasis and promoting repair is clearly more nuanced and complex than previously represented in the evolving field of myocardial regeneration.

Nonstandard Abbreviations and Acronyms

ACM	adult cardiac myocytes
BAC	bacterial artificial chromosome
bFGF	basic fibroblast growth factor
BMSC	bone marrow stem cell
BrdU	bromodeoxyuridine
CKH2B	c-KitrtTA/H2BEGFP mouse line
CKmCm	c-Kit-MerCreMer /R26-NG mouse line
DAPI	4',6-diamidino-2-phenylindole
EGF	epidermal growth factor
EGFP	enhanced green fluorescent protein
EPO	erythropoietin
ERK	extracellular signal–regulated kinase
ES-FBS	embryonic stem cell–qualified fetal bovine serum
FACS	fluorescence-activated cell sorting
hCPC	human cardiac progenitor cell
HUVEC	human umbilical vein endothelial cells
IHC-P	immunohistochemistry-paraffin
LIF	leukemia inhibitory factor
LVAD	left ventricular assist device
MACs	magnetic-activated cell sorting
MAPK	mitogen-activated protein kinase
mCPC	mouse cardiac progenitor cell
mTOR	mammalian target of rapamycin
NMC	nonmyocyte cardiac cell
PDGF	platelet-derived growth factor receptor
PI3K	phosphatidylinositide 3-kinase
rtTA	reverse tetracycline-controlled transactivator
SCF	stem cell factor
TRE	tet-responsive element
WGA	wheat germ agglutinin

Phenotypically, c-Kit serves as a marker of multiple cell types including stem cells, most often associated with hematopoietic progenitor cells, but in fact is present from early embryogenesis and persists in wide distribution throughout various adult tissues.[13,14] Functionally, c-Kit protein is a kinase that, upon activation by its cognate ligand stem cell factor (SCF), serves to induce cell proliferation, survival, and transcriptional activation.[14] Variation in temporal appearance and expression level of c-Kit in multiple cell types and in response to environmental stimuli is indicative of a dynamically regulated protein that does not necessarily respect traditional nomenclature of a stem cell marker. Despite years of study, details of c-Kit signaling cascades and downstream targets remain obscure,[15] and the respective activities for surface-expressed versus internal c-Kit remain poorly characterized.[16] In the cardiac context, c-Kit expression has been documented in multiple cell types including (but not necessarily limited to) myocytes, endothelial cells, cardiac progenitor cells (CPCs), and mesenchymal stem cells.[17,18] Indeed, observations of c-Kit protein induction suggest that stress responses and myocyte remodeling serve as inductive stimuli for expression of this stem cell marker in cardiomyocytes.[4,19]

Given the heterogeneous expression pattern for c-Kit that is not restricted solely to a canonical cardiac stem cell, the complex and varied findings derived from study of various genetically engineered c-Kit lineage-tracing models might indeed even be an expected outcome.[18] Furthermore, every experimental approach to define c-Kit+ cell fate possesses inherent strengths and weaknesses to be considered when deriving conclusions. Although the advantages of a genetically engineered knock-in model are well known,[20] the inevitable silencing of one c-Kit allele perturbs endogenous c-Kit biology with potentially significant consequences for stem cell function. Furthermore, imperfect tagging efficiency in

hemizygous knock-in mice allows for covert existence of an invisible c-Kit+ subpopulation in the myocardium comprising 25% to 30% of all c-Kit+ expressing cells[9] that cannot be followed. Consequently, c-Kit knock-in mice may harbor c-Kit–dependent biological defects, impaired reporter sensitivity, and attendant uncertainty of the functional impact resulting from c-Kit allele hemizygosity that could affect proliferation and survival in culture.

An alternative approach to c-Kit+ tracking by knock-in techniques and associated allele inactivation is the use of transgenesis to introduce a cloned construct carrying a c-Kit promoter fragment driving expression of a long-lived reporter protein. The cloned c-Kit promoter used as a driver for reporter gene expression has been extensively characterized both in vitro and in vivo[3,21,22] but has never been adopted to serve for inducible tracing of cell fate in the myocardial context. Transgenesis minimizes allele inactivation and potential deleterious consequences of impaired c-Kit activity that could influence interpretation of c-Kit expression and relevance in myocardial biology. For the current study, we use a doxycycline-inducible transgenic mouse model to tag c-Kit+ cells with a long-lived, tetracycline-responsive H2BEGFP (CKH2B) reporter.[23] Endogenous c-Kit remains unperturbed, and ≈80% of nonmyocyte cardiac c-Kit+ cells express H2BEGFP reporter, similar to c-Kit coincidence with EGFP (enhanced green fluorescent protein) in a c-Kit/mER-Cre-mEr knock-in reporter model (CKmCm). A heterogeneous CKH2B cell population is revealed after induction with doxycycline, including tagging of select adult cardiomyocytes (ACM) in vivo, a finding consistent with expression of c-Kit mRNA and protein in isolated ACMs. Increased expression of CKH2B in cultured ACM in response to stress is consistent with a role for c-Kit expression in cardiomyocyte survival, a finding recapitulated by acute pathological injury in vivo. Similarly, c-Kit activation in cultured mouse CPCs (mCPCs) and human CPCs (hCPCs) enhances proliferation and survival, in line with previous reports establishing the role of c-Kit signaling in human cardiac stem cells.[19] Collectively, data presented here support validity of the c-Kit reporter model, pointing to heterogeneous and dynamic c-Kit expression in the postnatal myocardium that facilitates reconciliation of seemingly disparate observations from published literature and resolves multiple aspects of the controversial role for c-Kit in cardiac biology.

Methods

The authors declare that all supporting data are available within the article [and its online supplementary files].

Mice

c-Kit/rtTA (reverse tetracycline-controlled transactivator) transgenic mice expressing the rtTA transactivator under control of the c-Kit promoter clone 2[21] were generated using standard genomics techniques and stabilized by breeding several generations into the FVB/N background. The CKH2B line was created by crossing c-Kit/rtTA mice with tet-responsive element (TRE)-H2BEGFP mice purchased from Jaxmice (stock number: 005104/pTRE-H2BEGFP). Copy number of the c-KitrtTA transgene per cell was determined by a quantitative polymerase chain reaction (qPCR) as described[24] with the following modifications. c-KitrtTA plasmid injected for transgenesis was used to establish the standard curve ranging in concentration from 5 fg to 5 ng of plasmid template per reaction. Genomic DNA was extracted from livers of mice hemizygous for the c-KitrtTA transgene or from non-rtTA controls. The qPCR mix consisted of iQSYBR Green master mix, 50-ng genomic DNA, and primers specific for rtTA and 18S, and was performed using a CFX Connect Bio-Rad cycler for 40 two-step cycles at 95 and 60°C. A logarithmic standard curve was generated and copy number calculated per cell based on the assumption that each cell contains 6-pg genomic DNA or that 1-ng DNA is the equivalent of 167 diploid cells. Genotyping of mice to detect rtTA and EGFP transgenic sequences in genomic tail DNA was performed by standard PCR using target-specific primers. All primers for measuring copy number and genotyping are listed in Online Table I. c-Kit-MerCreMer/R26-NG (CKmCm) mice were created by crossing the Kit-MerCreMer driver line[9] to the FVB.Cg-Gt(ROSA)26Sortm1(CAG-lacZ,EGFP)Glh/J from Jaxmice (stock number 012429)[25].

Animal Procedures

All procedures and experiments involving mice were approved by the SDSU Institutional Animal Care and Use Committee. Acute diffuse injury was achieved by administering a single subcutaneous injection of 150 mg/kg isoproterenol. H2BEGFP reporter expression was induced in vivo with 0.2 mg/mL doxycycline in the drinking water for up to 4 days. CKmCm, 3-month-old, male mice were fed normal chow or chow containing tamoxifen citrate for 4 weeks to induce EGFP reporter expression, after which hearts were retroperfused and fixed in formalin for paraffin processing. For flow cytometry analysis of heart and bone marrow, CKmCm mice were fed tamoxifen chow for 4 weeks followed by 4 weeks chow with no tamoxifen.

Cell Isolation and Expansion

Murine CPCs and ACMs were simultaneously isolated from transgenic hearts using a modified isolation protocol.[26] Briefly, hearts were cannulated via the aortic arch and perfused for 15 minutes at 37°C in digestion buffer containing Liberase, then physically dissociated in digestion buffer at 37°C. Myocytes were filtered through a 100-µm nylon mesh and separated from nonmyocyte cardiac cells (NMC) by gravity sedimentation. Fractions of myocytes and NMC were collected from 3 subsequent steps of digestion, sedimentation, and filtration. Myocytes were plated on laminin-coated slides or dishes. The nonmyocyte fraction was either analyzed for EGFP and c-Kit expression by flow cytometry or filtered through a 40-µm nylon mesh and subjected to magnetic cell sorting to deplete the CD45+ population and enrich for c-Kit–expressing cells using the Miltenyi magnetic sorting system (catalog number 130-090-312; mouse CD45 microbeads catalog number 130-052-301; and mouse CD117 microbeads catalog number 130-091-224). CPCs were expanded in a humidified incubator at 37°C, 5% CO_2 in growth media consisting of 1:1 DMEM/Ham F12 (DMEM/F12; Life Technologies) and Neurobasal Media (Life Technologies) containing 10% ES-FBS (embryonic stem cell–qualified fetal bovine serum; Life Technologies), LIF (leukemia inhibitory factor; 10 ng/mL; Millipore), bFGF (basic fibroblast growth factor; 10 ng/mL; Peprotech), EGF (epidermal growth factor; 20 ng/mL; Peprotech), 1× insulin–transferrin–selenium (ITS 500×; Lonza) 1% penicillin/streptomycin/2 mmol/L glutamine (100× PSG; Life Technologies), supplemented with B27 and N2 (Life Technologies). hCPCs were isolated from human LVAD (left ventricular assist device) discard tissue and expanded as previously described.[27] Briefly, tissue was digested with collagenase, nonmyocyte cells were separated by low-speed centrifugation (350*g* for 5 minutes), sequentially filtered through 100- and 40-µm filters, and cultured for 1 day at 37°C, 5% CO_2 in hCPC growth media (HAM's F12 supplemented with 10% ES-FBS, 5 mU/mL human EPO [erythropoietin], 10 ng/mL human bFGF, 0.2 mmol/L glutathione, 1× penicillin/streptomycin/glutamine), after which the c-Kit+ population was selected by incubating with magnetic bead conjugated c-Kit antibodies (Miltenyi Biotec catalog number 130-091-332) and MAC (magnetic-activated cell sorting) sorting.

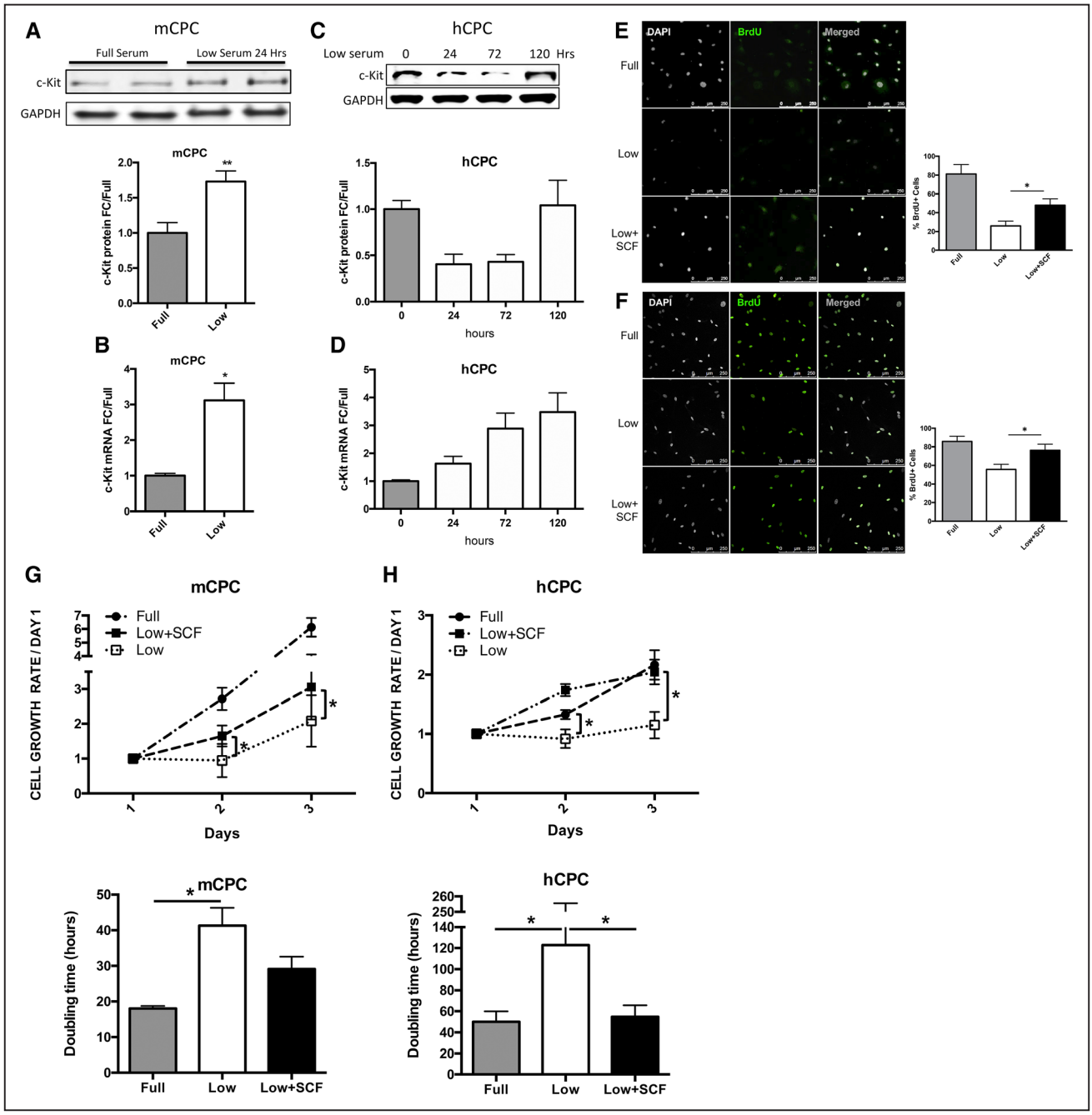

Figure 1. c-Kit signaling promotes proliferation and survival in cardiac progenitor cells (CPCs). c-Kit protein and RNA were quantified in mouse CPCs (mCPCs) and human CPCs (hCPCs) cultured in full or low serum media. c-Kit protein levels increase 2-fold in mCPCs cultured for 24 h in low serum vs full growth media as measured by immunoblotting (**A**). c-Kit RNA levels in mCPCs exposed to low serum increase 3-fold as measured by quantitative polymerase chain reaction (**B**). hCPC culture for 5 days in low serum exhibit an initial decrease in c-Kit protein levels, which return to full serum levels by 5 d (**C**), whereas c-Kit mRNA increases steadily over time (**D**). Decreased proliferation in mCPCs and hCPCs cultured in low serum is partially rescued by SCF treatment as indicated by BrdU (bromodeoxyuridine) incorporation (green=BrdU, **E** [mCPC] and **F** [hCPC]) and daily cell counts (**G** and **H**). Doubling time of CPCs calculated from growth rates increases after serum depletion but is restored with addition of stem cell factor (SCF; **G** and **H**). (*Continued*)

Magnetically separated cells were expanded for at least 5 passages in hCPC growth media before use in experiments. Adult hCPCs were used at passages 6 to 10 in all experiments.

Statistics

Two-tailed *t* tests were used to compare to 2 groups for all analyses other than the linear mixed model for Figure 5 as described below. $P<0.05$ is considered statistically significant.

To formally test the difference in the means of the knock-in versus transgenic, the repeated measures of c-Kit for each animal are modeled using a linear mixed model. A post hoc Tukey 2-sided test for comparison of means indicates some evidence to suggest a significant difference in means of CKH2B+Doxy versus CKmCm+Tx ($P=0.0838$). (See Supplementary Material section in the Online Data Supplement for description and details of the statistical analyses.)

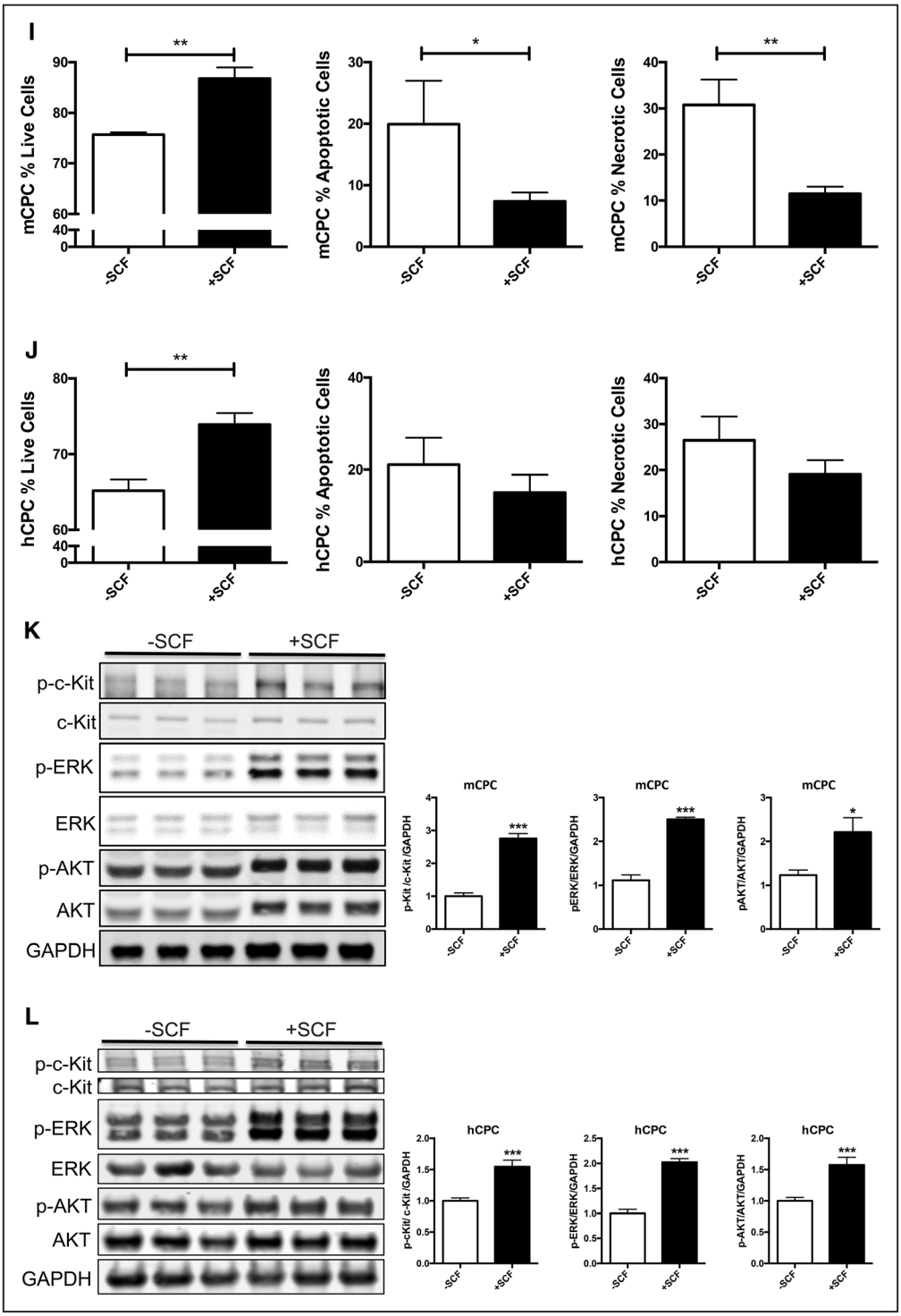

Figure 1 Continued. Viability is higher, whereas apoptosis and necrosis are lower in SCF-treated CPCs as measured by AnnexinV/PI flow cytometry analysis (**I** and **J**). Specific activation of c-Kit in mCPCs and hCPCs is confirmed by increased phosphorylation of c-Kit, ERK (extracellular signal–regulated kinase), and AKT after SCF treatment (**K** and **L**). n=3 for all experiments. $P<0.05$ denotes statistical significance. Statistical significance between 2 groups was determined by unpaired *t* test for all data except (**J**), which was analyzed by paired *t* test. *$P<0.05$, **$P<0.01$, and ***$P<0.001$.

To formally test the difference of c-Kit density per unit area, the repeated measures of c-Kit for each animal are modeled using a linear mixed model. On the basis of the significant results of the mice strain factor, a post hoc Tukey 2-sided test for multiple comparison of means indicates a significant difference in means of CKmCm-Tx versus CKH2B+Doxy (P=0.00769), CKH2B+Doxy versus CKmCm+Tx (P=0.00542), and no significant difference in means of CKmCm-Tx versus CKmCm+Tx (P=0.90577). (See Supplementary Material section in the Online Data Supplement for description and details of statistical analyses.) Online Table III provides values for efficiency of coexpression assessed with c-Kit+/EGFP+ coincidence in 3 experiments using CKH2B and CKmCm mouse heart samples.

Results

c-Kit Signaling Promotes Proliferation and Survival in CPCs

c-Kit signaling stimulates proliferation and enhances survival in multiple cell types,[28–30] including human cardiac stem cells.[19] Mouse and human CPCs were assayed for c-Kit expression, proliferation, and cell death in response to low serum culture conditions. Serum starvation for 24 hours induces a significant 73% increase in c-Kit protein and 3-fold higher levels of c-Kit mRNA in mCPC (Figure 1A and 1B), whereas c-Kit protein levels in hCPC initially decrease by 60% at 24 hours and return to full serum levels after 5 days of starvation, as measured in 3 distinct lines (Figure 1C). Interestingly, c-Kit mRNA levels increase by 63% in hCPCs after 24 hours and rise to >3-fold by 5 days in low serum (Figure 1D). Treatment of serum-starved mCPC and hCPC with c-Kit ligand SCF significantly enhances BrdU (bromodeoxyuridine) incorporation by 84% and 37%, respectively (Figure 1E and 1F). Similarly, SCF treatment increases cell growth rate and shortens doubling time in serum-starved cells (Figure 1G and 1H), confirming the proproliferative activity of c-Kit signaling in CPCs. Viability in serum-starved mCPCs is significantly higher, and cell death significantly blunted in cells treated with SCF, as measured by a 14% increase in cell survival and 63% decrease in both apoptosis and necrosis using flow cytometry, indicative of protective c-Kit signaling in these cells. Likewise, SCF-treated hCPC exhibit a significant 13% increase in viability, and 29% and 28% downward trends in apoptosis and necrosis, respectively (Figure 1I and 1J). Activation of c-Kit by SCF is verified in mouse and human CPCs as evidenced by

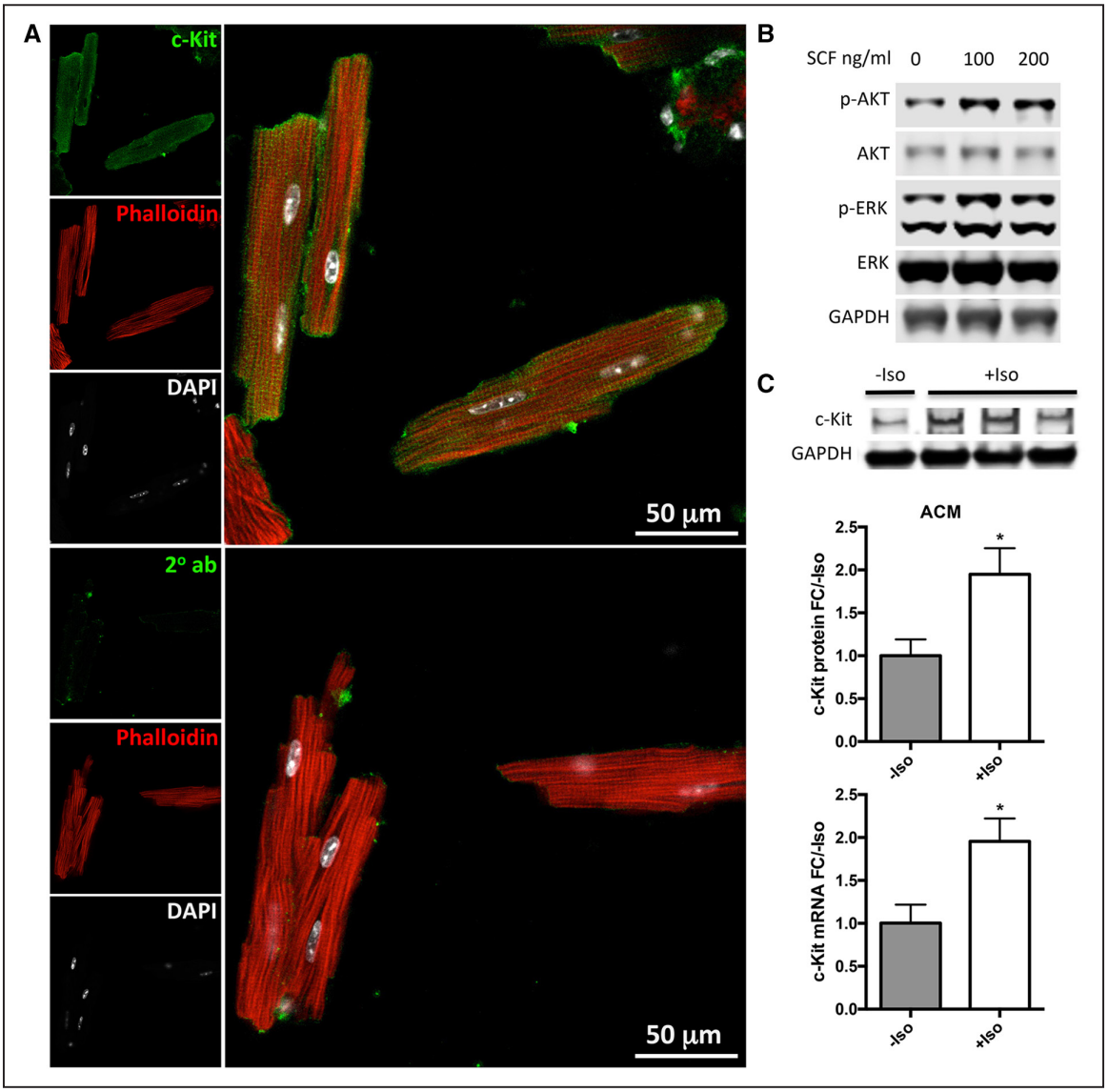

Figure 2. Cardiac myocytes express active c-Kit and upregulate c-Kit expression in response to stress in vitro. Adult mouse cardiac myocytes (ACM) were isolated, fixed, and immunolabeled for c-Kit (green) colocalized with phalloidin (red) and DAPI (4',6-diamidino-2-phenylindole; white; **A**). Activation of c-Kit by stem cell factor (SCF) was confirmed by immunoblotting for phospho-ERK (extracellular signal–regulated kinase) and phospho-AKT (**B**). ACM were treated with isoproterenol to induce cellular stress. c-Kit mRNA and protein levels were measured by quantitative polymerase chain reaction (qPCR) and immunoblotting, respectively. c-Kit protein and mRNA levels increased significantly in isoproterenol-treated ACMs as measured by immunoblotting and qPCR, respectively (**C**). n=3 experiments for **A** and **B**. **P*<0.05 as measured by *t* test.

significant upregulation of phospho-c-Kit and of downstream targets phospho-ERK1/2 (extracellular signal–regulated kinase 1/2) and phospho-AKT (Figure 1K and 1L). Inhibition of c-Kit with Imatinib or with c-Kit–specific antibody blunts phosphorylation of c-Kit, ERK, and AKT, demonstrating specificity of SCF-mediated c-Kit pathway activation in mCPCs (Online Figure IA and IB) and hCPCs (Online Figure IC). To determine whether macrophages or mast cells contribute to c-Kit signaling in mCPCs, freshly isolated NMC and cultured mCPCs were analyzed for macrophage (F4/80, CD206), mast cell (FceR1), and hematopoietic (CD45) markers by flow cytometry (Online Figure ID and IE). These populations comprise between 7% and 12% of the whole nonmyocyte population (Online Figure ID) but are absent above baseline in mCPCs (Online Figure IE), indicating that cardiac progenitors, not cultured mast or macrophage cells, drive c-Kit signaling in these cells. Consistent with previous reports, live cultured mCPCs express stromal markers (CD105, CD90.1, and PDGFRα [platelet-derived growth factor receptor alpha]). Surface c-Kit expression does decrease with culture as measured by flow cytometry in unfixed mCPCs (Online Figure IF); nevertheless, c-Kit is detected in the majority of fixed mCPCs assessed by flow cytometry (Online Figure IF) and immunofluorescence (Online Figure X). Collectively, these data demonstrate that the c-Kit pathway is active in mouse and human CPCs and that c-Kit signaling promotes CPC proliferation and survival in low serum conditions.

Cardiac Myocytes Express Active c-Kit and Upregulate c-Kit in Response to Stress In Vitro

Prior studies have reported increased cardiac c-Kit expression in myocytes after myocardial injury.[4] Isolated ACM immunolabeled for c-Kit confirms myocyte-specific c-Kit protein expression (Figure 2A; Online Figure IIB and IIC). c-Kit was detected in most ACM, whether fixed immediately after isolation or plated for 2 hours and then fixed. Using either method, c-Kit staining was found in the majority of ACM (79.25%, or 42 out of 53 immediately fixed ACM). Upregulation of phospho-ERK and phoshpo-AKT in ACM treated with SCF verifies activation of c-Kit activity in these cells (Figure 2B; Online Figure IIA). Finally, c-Kit protein and mRNA levels are elevated 2-fold in isoproterenol-treated ACMs (Figure 2C). Taken together, these results indicate that mouse ACMs express c-Kit mRNA and protein, exhibit c-Kit pathway activation by SCF, and upregulate c-Kit expression in response to cellular stress in vitro.

H2BEGFP Reporter Is Expressed in Transgenic Cardiac and Noncardiac c-Kit+ Cells In Vivo

An inducible transgenic c-Kit reporter mouse was created to further probe cardiac c-Kit biology in vivo. The rtTA transcription factor was cloned downstream of a previously characterized 14 kb fragment of the mouse c-Kit promoter[3,21] to generate the c-KitrtTA mouse line (Online Figure

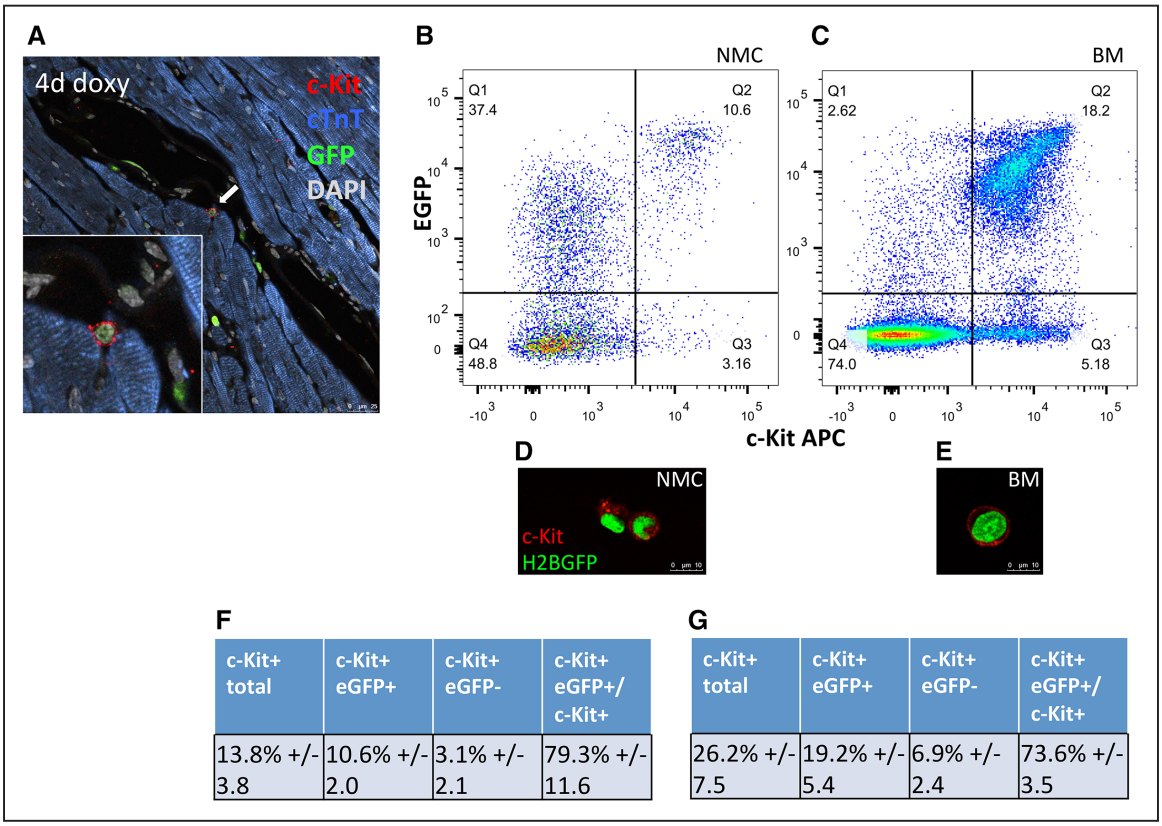

F

c-Kit+ total	c-Kit+ eGFP+	c-Kit+ eGFP-	c-Kit+ eGFP+/ c-Kit+
13.8% +/- 3.8	10.6% +/- 2.0	3.1% +/- 2.1	79.3% +/- 11.6

G

c-Kit+ total	c-Kit+ eGFP+	c-Kit+ eGFP-	c-Kit+ eGFP+/ c-Kit+
26.2% +/- 7.5	19.2% +/- 5.4	6.9% +/- 2.4	73.6% +/- 3.5

Figure 3. H2BEGFP reporter expression is induced in c-Kit+ cells in vivo. Cardiac c-Kit+ cells from CKH2B mice express H2BEGFP reporter (white arrow) after administration of doxycycline, as visualized by immunolabeling (**A**, red=c-Kit, green=EGFP, blue=cTnT (cardiac troponin T), and gray=DAPI [4',6-diamidino-2-phenylindole]). Coexpression of c-Kit and H2BEGFP is detected in fresh isolates of nonmyocyte (NMC) cardiac cells (**B**) and whole bone marrow (BM; **C**) from doxycycline-treated CKH2B mice as measured by flow cytometry and illustrated by corresponding representative confocal images (red=c-Kit; green=H2BEGFP). Tabulation of flow cytometry analysis of c-Kit+ and H2BEGFP in CKH2B NMC (**F**) and BM (**G**). n=4 animals.

III). c-KitrtTA mice were crossed with mice harboring the tetracycline-responsive H2BEGFP reporter construct (TRE-H2BJ/eGFP; Online Figure IIIB)[23] to create a double transgenic line in which doxycycline treatment induces H2BEGFP expression in cells harboring an active c-KitrtTA construct (CKH2B; Online Figure IIIC and IIID). c-KitrtTA transgene copy number was calculated to be ≈4 copies per diploid genome in hemizygous animals, as measured by qPCR of genomic DNA using a previously described method (Online Figure IV).[24] Transgene expression was validated in CKH2B mice treated with doxycycline (Figure 3). Cardiac c-Kit+ cells from doxycycline-treated CKH2B mice express the H2BEGFP reporter in the nucleus, as illustrated by immunolabeling of paraffin sections (Figure 3A) and freshly isolated, unfixed NMC immunolabeled for c-Kit and analyzed by flow cytometry (Figure 3B and 3D). Likewise, noncardiac tissues exhibit H2BEGFP induction in c-Kit+ cells as measured by flow cytometry of bone marrow (Figure 3C and 3E) and immunostaining in c-Kit+ rich tissues, such as intestinal crypts and cryptopatches, and pancreatic islet of Langerhans (Online Figure VIIIA through VIIIC). Furthermore, H2BEGFP is expressed in vascular and stromal cardiac cells, as indicated by colocalization with CD31 and vimentin by IHC-P (immunohistochemistry-paraffin; Online Figure VA and VB) and with CD105, CD90.1, and PDGFRα as measured by flow cytometry (Online Figures VE and XI). Vascular smooth muscle does not seem to express H2BEGFP (Online Figure VD), and CD45+/EGFP+ cells were rarely observed in uninjured tissue sections; however, flow cytometry reveals a higher percentage of CD45+/H2BEGFP nonmyocyte cells (Online Figure VE).

c-Kit+ cells comprise 13.8±3.8% of all freshly isolated nonmyocyte, most of which (79.3±11.6%) coexpress the H2BEGFP reporter in CKH2B doxycycline-treated hearts (Figure 3F). Freshly isolated, unfixed whole bone marrow from the same animals exhibit a higher percentage of c-Kit cells in the overall population (26.2±7.5%), 82.4% of the H2BEGFP bone marrow (BM), more c-Kit+EGFP+ cells overall (19.2±5.4% in total BM versus 10.6±2.0% in total nonmyocyte, and 82.4% of H2BEGFP+ BM versus 29.5% of the H2BEGFP nonmyocyte population; Online Figure VE), but a similar proportion of c-Kit+EGFP+ cells within the total c-Kit population (73.6±3.5%), reflective of higher overall endogenous c-Kit expression levels in bone marrow versus nonmyocyte, but similar tagging efficiency in the 2 c-Kit+ tissues (Figure 3G). To correlate EGFP+ signal with c-Kit mRNA expression in c-Kit-nonmyocyte, EGFP+ NMC were FACS (fluorescence-activated cell sorting) sorted for positive or negative c-Kit protein expression and analyzed for c-Kit mRNA levels by qPCR (Online Figure VG). c-Kit mRNA was detected above negative control levels in the EGFP+/c-Kit- population and at one-third the level seen in EGFP+/c-Kit+ cells. These results serve as additional evidence that the H2BEGFP reporter reflects c-Kit promoter activity and further validates the CKH2B model.

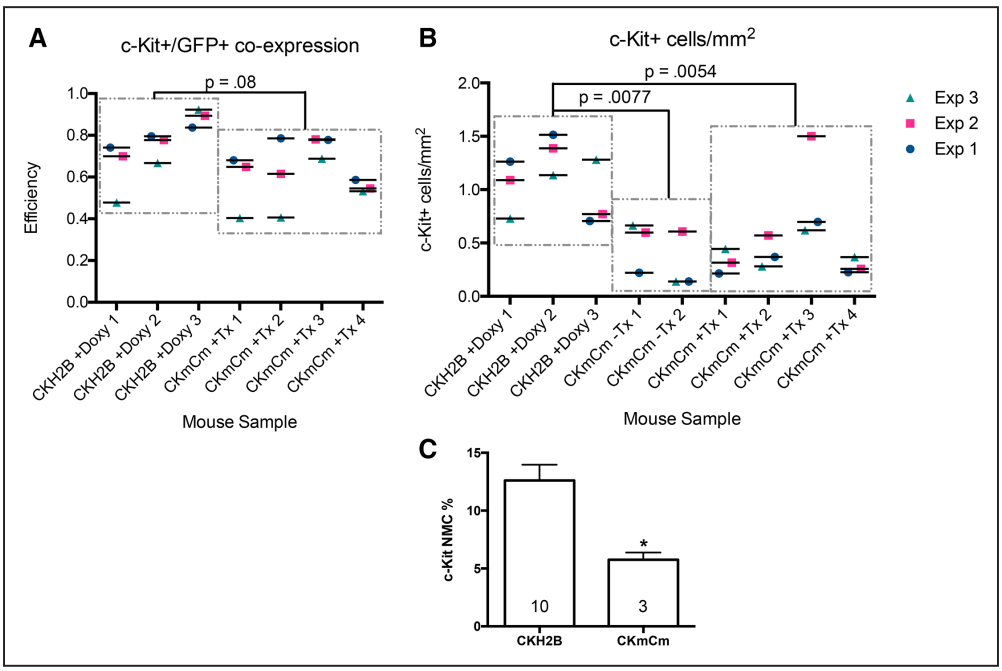

Figure 4. Similar c-Kit+/EGFP+ colocalization but decreased total cardiac c-Kit+ cells per area in CKmCm knock-in mice vs CKH2B transgenic mice. Paraffin sections were immunolabeled for c-Kit and EGFP to quantify reporter coexpression in cardiac c-Kit+ cells in situ. EGFP colocalization with c-Kit+ cells in hearts of CKmCm and CKH2B mice is comparable (P=0.0838; **A**). Significantly fewer c-Kit+ cells per area were present in CKmCm+Tx and CKmCm-Tx mice compared with doxycycline-treated CKH2B mice (P=0.0054 and P=0.0077, respectively). No statistical differences were found between CKmCm-Tx and CKmCm+Tx mice (0.9058; **B**). CKH2B hearts n=3, CKmCm-Tx hearts n=2, and CKmCm+Tx hearts n=4. Significance determined by mixed linear modeling as described in the Statistics section and the Statistical Analysis section in the Online Data Supplement. P<0.05 denotes significance. **C**, Comparative flow cytometry analysis of nonmyocytes (NMC) isolated from CKmCm+Tx vs CKH2B+doxycycline hearts reveals significantly lower percentage of c-Kit+ NMC in CKmCm hearts. n=10 CKH2B; n=3 CKmCm; statistical significance determined by 2-tailed t test, *P<0.05.

Differences in Coincidence of c-Kit/EGFP Tagging and c-Kit+ Cell Frequency Assessed by Comparative Analysis of Transgenic Versus Knock-In Reporter Mouse Models

Various tagging strategies have been developed to identify the c-Kit cell population in vivo using mouse models.[4,9,10,21,31] An established c-Kit/EGFP knock-in reporter construct from a Cre-mediated inducible knock-in line (CKmCm)[9] was compared with the CKH2B model for both colocalization of c-Kit with EGFP and frequency of c-Kit+ cells in myocardial tissue sections. Paraffin sections were immunolabeled for c-Kit, EGFP, and DAPI (4',6-diamidino-2-phenylindole), along with WGA (wheat germ agglutinin) to mark cell boundaries and cTnT (cardiac troponin T) to identify myocytes (representative images, Online Figure VIA and VIB). The total number of c-Kit+ cells was counted per area of tissue, and percentage of c-Kit cells expressing reporter determined by colocalization of c-Kit, EGFP, and DAPI signals. Efficiency of coincident tagging between c-Kit and EGFP in cardiac c-Kit+/EGFP+ cells exhibited a trend but was not significantly higher in heart tissue sections from CKH2B+Doxy versus CKmCm+Tx mice (Figure 4A; P=0.08; 75.7±6.9% SD versus 62±4.5% SD, respectively; Online Table III), consistent with flow cytometry data for CKH2B+Doxy nonmyocyte (Figure 3F and 3G) or CKmCm+Tx bone marrow cells.[9] Moreover, density of c-Kit+ cells per unit area is significantly higher in CKH2B versus CKmCm heart tissue sections (Figure 4B). This rigorous, blinded analysis reveals that the transgenic (CKH2B) reporter mice possess 2.2-fold higher cardiac c-Kit+ cell population density and a trend toward higher EGFP tagging of c-Kit+ cells relative to the knock-in (CKmCm) mice. However, neither model successfully tags all c-Kit+ cells with EGFP, demonstrating a similarity consistent with heterogeneity of the endogenous cardiac c-Kit cell population. Additionally, NMC were isolated from tamoxifen-treated CKmCm mice and analyzed for c-Kit and EGFP+ by flow cytometry. Consistent with findings in paraffin sections, the percentage of c-Kit+ NMC is approximately

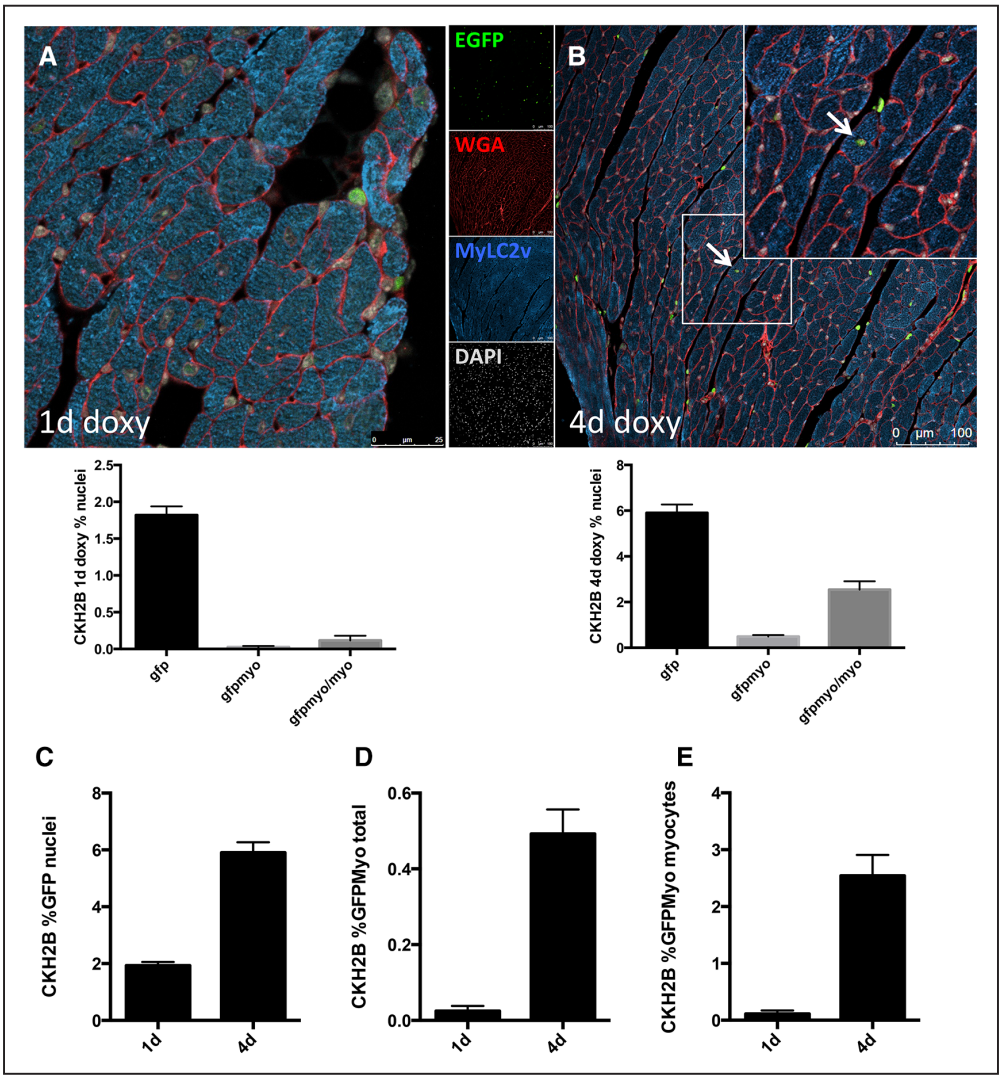

Figure 5. H2BEGFP reporter accumulates in cardiac myocytes in vivo. EGFP (enhanced green fluorescent protein) is detected and quantified in nuclei of immunolabeled CKH2B hearts treated for 1 d (**A**) or 4 d (**B**) with doxycycline (red=wheat germ agglutinin, green=H2BEGFP, blue=myosin light chain 2v [MYLC2V], and gray=DAPI [4',6-diamidino-2-phenylindole]). Quantification of the increase in EGFP+ cells per total nuclei (**C**), EGFP+ myocytes per total nuclei (**D**), and EGFP+ myocytes per total myocytes (**E**) represented in histograms. n=3 hearts, minimum 10 fields of view per heart.

half of the level observed in CKH2B NMC (5.8±1.1% SD versus 13.8±3.8% SD, respectively; Figure 4C). Interestingly, the EGFP+ population was substantially lower in CKmCm BM and nonmyocyte than in CKH2B (0.04±0.02% SD versus 4.7±2.7% SD nonmyocyte, 2.9% versus 20.4% BM in CKmCM and CKH2B, respectively; Online Figure VIC). Discrepancies in reporter expression may be due in part to differences in mouse strain and reporter induction protocol; however, the lower proportion of EGFP+ cells in CKmCm is also consistent with the c-Kit haploinsufficiency.

H2BEGFP Reporter Is Expressed in CKH2B Adult Cardiac Myocytes

c-Kit expression has been reported in neonatal mouse cardiomyocytes and genetically tagged mouse ACMs[4,9,31,32] and measured in ACM (Figure 2). Therefore, expression of H2BEGFP reporter in myocytes was tested by immunolabeling for EGFP and cardiac myosin light chain in heart tissue from CKH2B mice treated with doxycycline for 1 or 4 days (Figure 5A and 5B). Quantification of H2BEGFP signal in all nuclei and in myocyte nuclei reveals that ≈1.8% of all cardiac nuclei express H2BEGFP after 1 day of induction, increasing to 6% by 4 days of treatment (Figure 5C). Cardiac myocyte nuclei positive for H2BEGFP comprise <0.1% of all nuclei at 1 day, and 0.5% of all nuclei by 4 days of induction (Figure 5D), whereas the proportion of cardiac myocytes expressing H2BEGFP reporter increases from 0.1% to 2.5% between 1 and 4 days, respectively (Figure 5E). ACMs isolated from doxycycline-treated CKH2B hearts exhibit discreet nuclear H2BEGFP fluorescent signal in 9.4% of total myocytes (Online Figure VIIA; Figure 7F). Likewise, naive CKH2B ACM treated with doxycycline postisolation express H2BEGFP (Online Figure VIIB). Taken together, these data confirm c-Kit expression in mouse ACM (Figure 2A) and demonstrate sensitive detection of c-Kit expression in the cardiomyocyte population as revealed by cumulative H2BEGFP expression over time with doxycycline induction. Additionally, paraffin sections of tamoxifen-induced CKmCm were immunolabeled for EGFP and a cardiomyocyte marker to identify EGFP+ myocytes in the knock-in hearts. Between 1 and 5 EGFP+ myocytes were detected per heart section in 3 individual CKmCm hearts (Online Figure VID). Collectively, these data provide further evidence that c-Kit is expressed in adult cardiac myocytes.

H2BEGFP Is Expressed in CKH2B Bone Marrow Stem Cells In Vitro

Bone marrow is an established source of c-Kit–expressing stem cells. c-Kit+ bone marrow stem cells (BMSC) were isolated as previously described[33] from CKH2B mice, expanded, and treated with doxycycline in vitro to assess transgene expression in a c-Kit–enriched stem cell system. As shown by live fluorescence imaging, untreated BMSC express no fluorescent signal (Online Figure IXA), whereas cells exposed to doxycycline exhibit induction of robust, chromatin-associated H2BEGFP fluorescence consistent with expected histone distribution (Online Figure IXB and IXC). Flow cytometry and confocal microscopy analyses of fixed, immunolabeled BMSCs further confirm low baseline reporter signal in untreated BMSCs (Online Figure IXD and IXH) and robust induction of H2BEGFP in doxycycline-treated CKH2B (Online Figure IXE, IXF, and IXI) but not in single transgenic c-KitrtTA BMSC (Online Figure IXG). Coexpression of c-Kit with the H2BEGFP signal is detected in ≈60% of the total c-Kit+ BMSC population, as measured by flow cytometry (Online Figure IXF). BMSCs labeled for flow cytometry and imaged by confocal microscopy exhibit membrane c-Kit and nuclear H2BEGFP signals (Online Figure IXI). Cumulatively, these data demonstrate robust and appropriate induction of the H2BEGFP reporter in a cultured stem cell population enriched for c-Kit expression, consistent with previous publications characterizing the CKH2B promoter construct.[21]

CKH2B CPCs Express c-Kit and H2BEGFP Reporter In Vitro

Nonmyocyte c-Kit+ cardiac cells are an important source of stem and progenitor cells for cardiac regenerative therapy. c-Kit CPCs isolated from CKH2B hearts were induced with doxycycline and probed for c-Kit and H2BEGFP protein expression. H2BEGFP protein is undetectable in untreated CPCs and clearly induced by doxycycline treatment, as indicated by immunoblot (Figure 6A), fluorescence imaging of live and immunostained fixed cells (Figure 6F and 6G; Online Movie I; Online Figure X). c-Kit protein and mRNA levels are substantially lower in CPCs than in BMSCs, and H2BEGFP levels increase 2-fold in CPCs between 1 and 2 days of exposure to doxycycline, whereas endogenous c-Kit levels remain unchanged (Figure 6C and 6E). qPCR confirms that mRNA levels of H2BEGFP but not endogenous c-Kit are augmented after doxycycline induction (Figure 6B and 6D), and live imaging verifies nuclear localization of the fluorescent H2BEGFP signal in CPCs (Figure 6F; Online Figure X). Collectively, these results demonstrate that the CKH2B reporter is induced in 2 cultured adult c-Kit stem cell populations and reflects the heterogeneity of c-Kit expression inherent in the parent tissue from which these cells are derived.

Cardiac c-Kit Expression Increases After Diffuse Injury In Vivo

Diffuse injury induces transient proliferation of CPCs in vivo.[8] Mice received a single injection of 150 mg/kg isoproterenol subcutaneously, and hearts were analyzed by immunostaining or flow cytometry 3 days later. Consistent with previous reports, the c-Kit+ nonmyocyte population increased (12.6%–20.1% in control versus injured hearts) as measured by flow cytometry (Online Figure XIC). CKH2B mice received a single injection of isoproterenol and treated with doxycycline for 3 days, and c-Kit colocalization with H2BEGFP was measured by immunolabeling in paraffin sections or flow cytometry on isolated nonmyocyte to assess the impact of diffuse injury on transgene expression. The H2BEGFP+ nonmyocyte population increased by 63% (4.9%–8.0% of ungated nonmyocyte), whereas the proportion of c-Kit+ H2BEGFP NMC declined from 29.5% to 20.7% in uninjured versus injured hearts, respectively (Online Figure XIC). The proportion of mesenchymal/stromal cells, as marked by CD105, CD90.1, and PDGFRα, all increased within the total nonmyocyte and EGFP+ nonmyocyte populations (Online Figure XID and XIE), supported by clear colocalization of vimentin with EGFP+ in damaged regions of cardiac CKH2B tissue sections

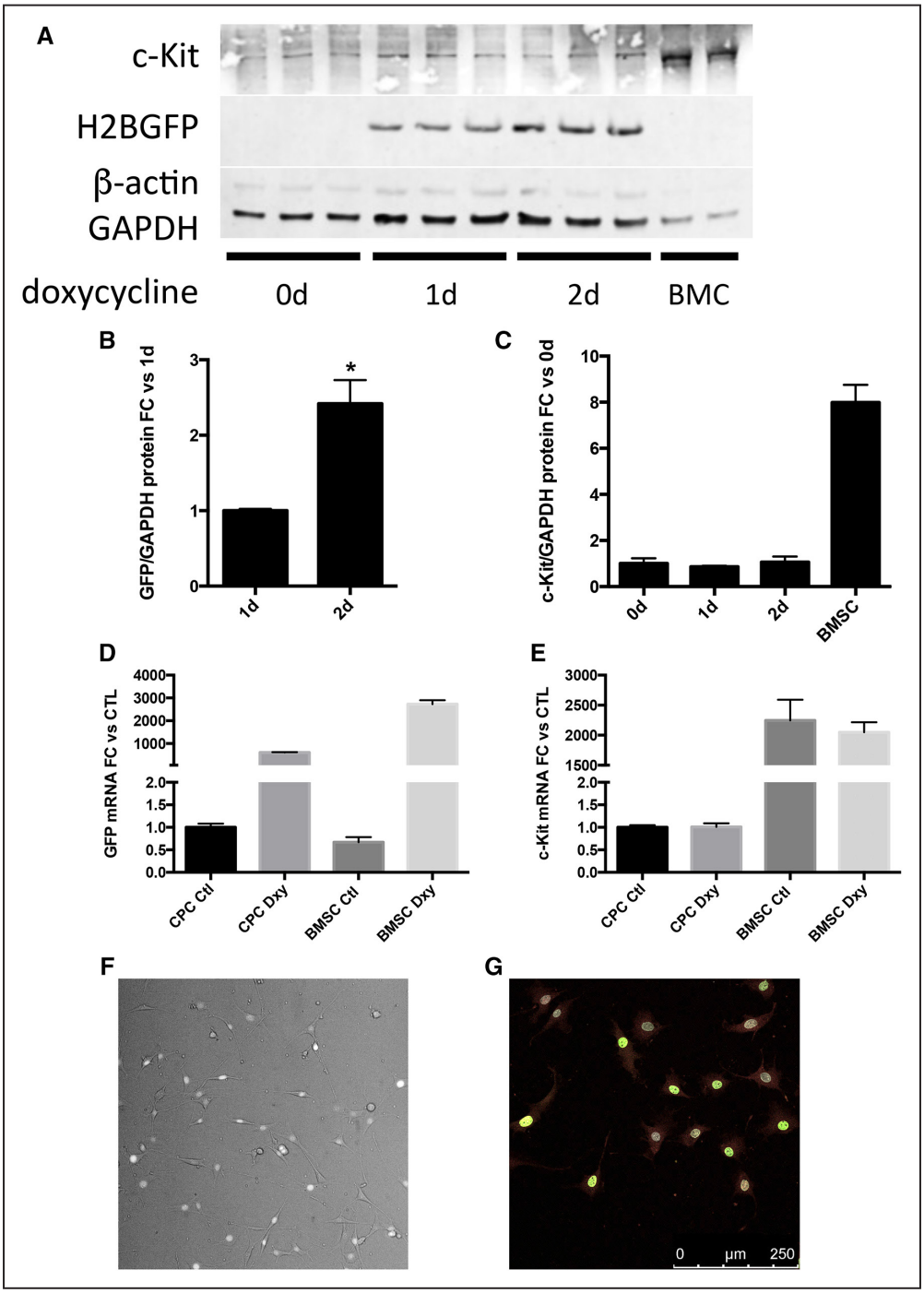

Figure 6. H2BEGFP reporter is induced in CKH2B c-Kit+ cardiac progenitor cells (CPCs) in vitro. CKH2B CPCs express c-Kit and accumulate H2BEGFP after treatment with doxycycline (**A**). BMC indicates c-KitrtTA whole bone marrow. Quantification of H2BEGFP protein levels in **A** relative to 1 d of doxycycline treatment (**B**) and of c-Kit relative to untreated CPCs (**C**). Quantification of mRNA levels of EGFP (enhanced green fluorescent protein; **D**) and c-Kit (**E**) relative to untreated CPCs. H2BEGFP fluorescence in c-Kit+ CKH2B CPCs after doxycycline induction in live cells (**F**) and fixed cells immunolabeled for c-Kit (**G**, red=c-Kit, green=EGFP, and gray=DAPI [4',6-diamidino-2-phenylindole]).

(Online Figure XIA). The percentage of c-Kit+ cells labeled for H2BEGFP in injured heart was comparable to uninjured controls (75.7% vs 71.9%, respectively; Figure 7A, 7B, and 7D). Cells coexpressing CD45 and EGFP were detected in injured areas of cardiac tissue sections (Online Figure XIB), while flow cytometry analysis indicates a decrease in the CD45+/H2BEGFP+ nonmyocyte population from 27% to 11% in uninjured versus injured hearts. The total number of c-Kit cells per area was 3.1 versus 1.1 per mm^2 in injured versus uninjured heart sections (Figure 7C), consistent with flow cytometry data and previous reports of elevated c-Kit cell numbers in isoproterenol-treated hearts 3 days after injury.[8]

Prior studies have reported evidence for c-Kit expression in myocytes.[4,9,10,31,32] Therefore, expression of H2BEGFP was

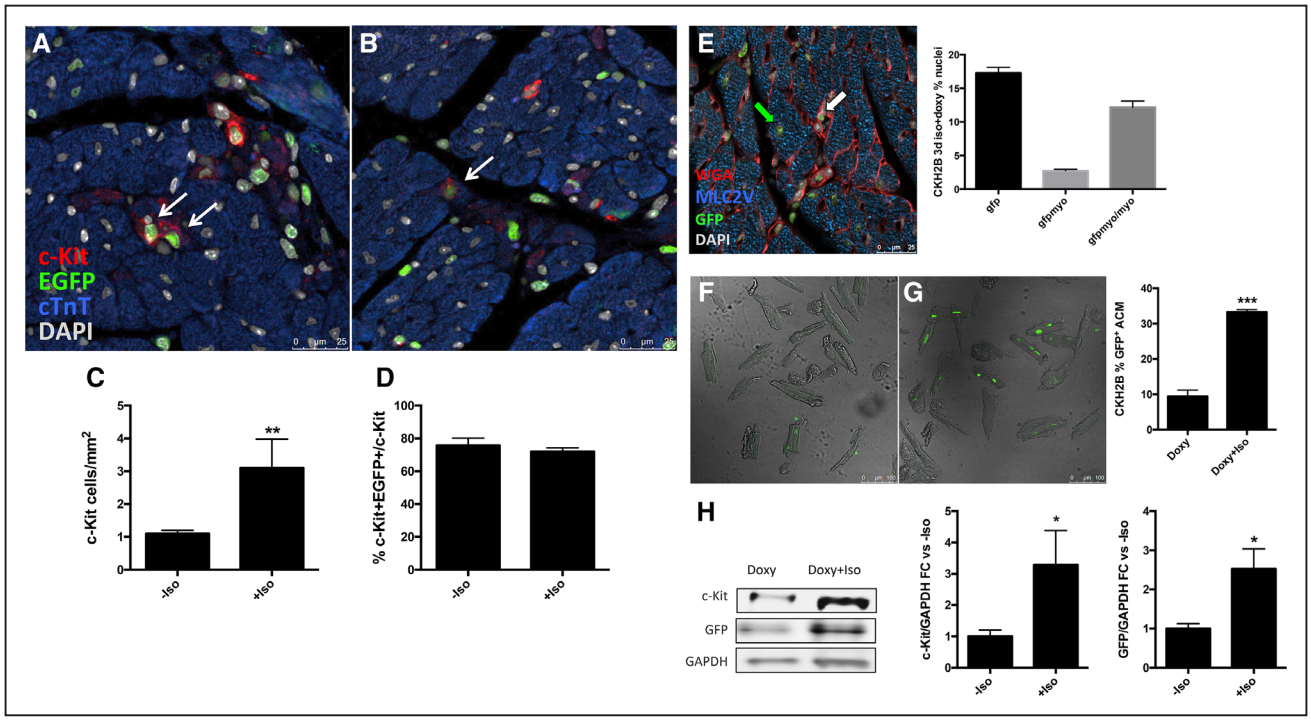

Figure 7. Cardiac c-Kit+ expression increases after diffuse injury in vivo. H2BEGFP expression in cardiac c-Kit+ cells visualized by immunostaining and confocal microscopy (**A** and **B**; red=c-Kit, green=EGFP (enhanced green fluorescent protein), blue=cTnT [cardiac troponin T], gray=DAPI [4',6-diamidino-2-phenylindole], and white arrows indicate c-Kit+/EGFP+ cells). Quantification of c-Kit+ immunolabeled cells per area of tissue (**C**) and percentage of c-Kit+ cells expressing H2BEGFP reporter in uninjured vs injured CKH2B hearts (**D**). H2BEGFP expression in adult cardiac myocytes in hearts from doxycycline- and isoproterenol-treated CKH2B revealed and quantified by immunostaining (**E**; red=WGA [wheat germ agglutinin], green=EGFP, blue=MyLC2V, gray=DAPI, white arrow indicates H2BEGFP in nonmyocyte, and green arrow indicates H2BEGFP in cardiomyocyte). Adult cardiac myocytes (ACMs) isolated from CKH2B mice treated with doxycycline only (**F**) or doxycycline and isoproterenol (**G**) for 3 d as imaged and quantified by confocal microscopy. Protein levels of c-Kit and EGFP quantified in ACM isolated from Doxy- or Doxy+Iso-treated CKH2B hearts (**H**). Bright field=ACM; green=H2BEGFP fluorescence. n=3 mice (**F** through **H**), n=4 isolations (**I**).

assessed in cardiac myocytes isolated from hearts of CKH2B mice receiving a single injection of isoproterenol and treated with doxycycline for 3 days. H2BEGFP signal increased overall in isoproterenol-treated hearts as measured by immunolabeling for EGFP and cardiac myosin light chain (Figure 7E). Total EGFP-positive nuclei rose from 6% in unchallenged hearts to 17% after injury, the EGFP-positive myocytes increased from 0.5% to 3% of total nuclei, and the proportion of EGFP-labeled myocytes was 13% of the myocyte population versus 3% in control hearts (Figures 3E and 7F), consistent with the upregulation of c-Kit in ACMs treated with isoproterenol in vitro (Figure 2C). Furthermore, the percentage of H2BEGFP+ ACM isolated from isoproterenol-injured CKH2B hearts was >3-fold higher than those from uninjured controls (33.3% versus 9.4%, respectively; Figure 7F and 7G), and protein levels of c-Kit and H2BEGFP were also elevated in ACM from isoproterenol-treated animals (Figure 7H). These data strongly support evidence for c-Kit expression in adult cardiac myocytes in vivo and in vitro and emphasize a previously underappreciated and potentially important role for c-Kit signaling in the cardiomyocyte response to stress.

Discussion

Over a decade of cumulative research supports the important biological role of c-Kit+ cells in cardiac development, homeostasis, and repair,[2,8,22,34,35] although recent studies using genetically modified knock-in mice have challenged certain aspects of c-Kit–mediated contribution to myocardial regeneration.[9,36] Knock-in mouse models thus far commonly focus on the property of c-Kit as a canonical stem cell marker originally identified in the hematopoietic context but devote relatively little attention to the critical biological role of c-Kit–dependent signal transduction. Regarding c-Kit as a perfunctory marker of stem cells overlooks substantial evidence that c-Kit signaling is an important determinant of myocardial biology and the molecular response to pathological injury.[19,37] Findings presented here report biologically relevant c-Kit function in CPCs and myocytes, with important implications for the role of c-Kit expression and signaling in the cardiac injury response.

c-Kit is a type III receptor tyrosine kinase comprised an extracellular ligand-binding domain, transmembrane region, and intracellular kinase signaling domain. Binding of c-Kit ligand SCF initiates receptor dimerization, autophosphorylation, and activation of intracellular signaling cascades such as PI3K (phosphatidylinositide 3-kinase)/AKT and Ras/MAPK (mitogen-activated protein kinase)/ERK. AKT and ERK signaling downstream of c-Kit confers powerful protective and proliferative effects in the heart and other tissues.[14,15,37,38] In the myocardial context, SCF-mediated activation of c-Kit or overexpression of constitutively active c-Kit protects against cardiomyopathic challenge,[38] whereas defective c-Kit

signaling leads to compromised cardiac function in response to age and stress.[39–41] Consistent with published literature, findings obtained using isolated ACM demonstrate that c-Kit protein is functionally present and responsive to SCF exposure (Figure 2A through 2C; Online Figure II). Furthermore, c-Kit expression increases in ACMs after adrenergic stress (Figure 2C), potentially contributing to a protection of the myocardium from pathological injury.

Concluding that c-Kit expression in cardiomyocytes is a normal biological process is reinforced by studying genetically engineered mouse models using 3 distinct c-Kit promoter systems including transgenic c-Kit-BAC (bacterial artificial chromosome) reporter[4] and c-Kit locus knock-in systems.[9,18,31,42] Instant on c-Kit expression tagging in a c-Kit knock-in model demonstrated reporter expression in adult cardiac myocytes,[31] consistent with H2BEGFP tagging of myocytes in CKH2B hearts after 4 days of doxycycline treatment (Figure 4). In the wake of pathological damage to the myocardium, EGFP signal in c-Kit-BAC border zone myocytes after cryoinjury indicates activation of c-Kit expression in stressed cardiomyocytes[4] is consistent with higher incidence of H2BEGFP in ACMs isolated from isoproterenol-injured CKH2B hearts (Figure 7E through 7H) and elevated c-Kit protein levels in isoproterenol-treated ACMs (Figure 2C). Sample preparation and detection method influence outcomes of quantitative assessments, as exemplified by comparing findings using immunolabeled paraffin sections versus freshly isolated ACM. The percentage of EGFP+ cardiomyocytes in paraffin sections (2.5%) represents an in situ view of the heart in which tissue content and context are preserved, yet epitope availability to antibodies may be diminished because of tissue processing. In comparison, the percentage of freshly isolated EGFP+ ACM from CKH2B hearts (9%) represents the end product of a multistep preparation that selects for cardiomyocytes that survive myocardial digestion and enrichment procedures. Furthermore, c-Kit protein is not detected in all EGFP+ cells in CKH2B cardiac cells because levels of c-Kit protein versus mRNA expression do not necessarily directly correlate (Online Figure VG). Another contributing factor in this observed discrepancy is sensitivity of c-Kit detection. For example, directly conjugated c-Kit antibody is used for detection of c-Kit in unfixed EGFP+ cells (Figure 3D and 3E). However, fixation and permeabilization of cells increases the proportion of c-Kit+ cells in the population because some c-Kit protein is intracellular.[16] Furthermore, applying unconjugated c-Kit primary antibody followed by a fluorescently tagged secondary yields higher sensitivity for detection of c-Kit protein because of increased fluorophore labeling. These methodological considerations can also contribute to variation in correlation between c-kit protein and EGFP reporter detection. Thus, derivation of quantitative findings using multiple approaches as performed in this study marginalizes bias in experimental design and helps to reconcile discrepant observations from prior publications. Consistent documentation of c-Kit in ACM supports a regulatory role in biological processes and validates appearance of the CKH2B reporter in the present study as a reasonable and relevant indicator for c-Kit expression in ACMs. Differential induction of the 2 mouse models is an important discussion point. Although tagging efficiency of c-Kit+ cells is comparable in the 2 mouse models, the underlying genetics and induction protocols are dramatically different. To generate the EGFP+ tag in c-Kit+ cells in the knock-in model, CKmCm mice ingest tamoxifen in their feed for 4 weeks to affect permanent Cre-mediated recombination, whereas CKH2B animals imbibe doxycycline in their water for 4 days to drive expression of the H2BEGFP+ reporter. In the first system, EGFP+ cannot accumulate after recombination, unlike the tet-inducible system directly driving expression of H2BEGFP. These differences in reporter expression mechanisms influence reporter induction dynamics between the 2 models, in addition to the distinct c-Kit promoters used for tissue-specific expression.

Induction and activation of c-Kit in CPCs echo findings in ACMs. c-Kit signaling confers protective, proliferative, and promigratory effects through induction of ERK and AKT in adult human and rat CPCs.[19,41] Likewise, the SCF/c-Kit pathway promotes proliferation in CPCs stimulated by coculture with MSCs.[43] Consistently, c-Kit levels increase in mouse CPCs after cellular stress (Figure 1A and 1B). Interestingly, in human CPCs, c-Kit protein levels decrease and recover after 5 days in low serum, whereas c-Kit mRNA increases steadily from 1 to 5 days in low serum (Figure 1C and 1D). Furthermore, SCF-mediated activation of c-Kit promotes CPC proliferation and blunts cell death in both mCPC and hCPC (Figure 1E through 1J), demonstrating the functional biological role of c-Kit in CPCs. Again, as is true for ACM, genetically engineered fluorescent tag reporter models contribute support for relevance of c-Kit cell biology through visualization and tracking of cardiac c-Kit+ cells in vivo and in vitro.[3,4,9,10,31] The tetracycline-responsive H2BEGFP reporter was deliberately chosen for our study based on literature precedents as a long-lived, easily identifiable chromatin-associated fluorescent tag originally designed for stem cell–tracking studies.[23,44] Combined with the transgenic c-KitrtTA promoter, the resultant CKH2B reporter system presented in this report provides a sensitive, inducible readout for c-Kit expression without impacting endogenous c-Kit function consequential to targeted knock-in approaches that take advantage of the endogenous promoter but, by inherent necessity of experimental design, inactivate normal transcriptional activity of the c-Kit locus.

Another critical aspect of further validating the H2BEGFP model as a tool for investigating cardiac c-Kit cell biology is in consistency with numerous reports detailing phenotypic and morphological properties of CPCs.[2,3,8,22,45,46] H2BEGFP-tagged cells in transgenic hearts exhibit typical morphology of small, round c-Kit+ cells embedded in the myocardium (Figure 3A). Induction of H2BEGFP expression revealed by confocal analyses of paraffin sections and flow cytometry of freshly isolated nonmyocyte cardiac cells (Figure 3B through 3E) matches reports with other c-Kit reporter models.[9] Likewise, CPCs isolated and expanded from CKH2B hearts exhibit classic CPC spindle morphology, express c-Kit, and upregulate H2BEGFP after doxycycline treatment (Figure 6; Online Movie I; Online Figure X). These fundamental characterizations together with concurrence between our findings and prior publications[2,46] reinforce the fidelity and authenticity of c-Kit properties as revealed in the H2BEGFP transgenic model.

Cardiac c-Kit cell expansion occurs in diffuse injury models in vivo.[47,48] Analysis of c-Kit+ cells in isoproterenol-injured CKH2B hearts revealed sites of c-Kit+/H2BEGFP+ clusters and, interestingly, significantly more H2BEGFP+ cardiomyocytes in vivo and in vitro (Figure 7), consistent with elevated c-Kit expression in isoproterenol-treated ACMs (Figure 2C) and reminiscent of EGFP-positive myocytes in border zone myocytes of c-Kit-BAC-EGFP hearts.[4] Upregulation of c-Kit in CKH2B myocytes in response to stress further substantiates a previously unrecognized or underappreciated biologically relevant role for c-Kit signaling in cardiac myocytes.

c-Kit+ cells constitute a highly heterogeneous population with broad distribution and diverse function throughout the body postulated to possess a range of phenotypic and biological properties.[35] The cardiac c-Kit+ cell subpopulation likewise comprises a diverse cell pool purported to participate in both direct contribution to tissue formation by lineage commitment and indirect paracrine-mediated signaling.[35,49–51] Tagging efficiency of such a heterogenous cell population will inevitably vary with promoter expression levels, whether endogenous or transgenic, and may be affected by the hemizygous state of current c-Kit knock-in reporter models. Interestingly, up to 35% of cardiac c-Kit+ cells do not express a genetic reporter tag in either system, as measured by flow cytometry and immunolabeing of paraffin sections (Figures 3 and 4),[9] further highlighting the complexity of c-Kit expression dynamics. Although ≈70% of H2BEGFP+ NMC are negative for c-Kit protein by flow cytometry (Online Figure VE and VF), these EGFP+/c-Kit NMC possess c-Kit mRNA by real-time qPCR (Online Figure VG) consistent with CKH2B transgenic promoter activity reflecting endogenous c-Kit mRNA expression. EGFP+ NMC diversity is readily apparent from immunoprofiling that shows heterogeneity of immune cell, interstitial cell, and mesenchymal/stromal markers including FceR1, F4/80, CD206, vimentin, CD105, CD90.1, and PDGFRα (Online Figures ID and VE). Such heterogeneity warrants cautious interpretation of c-Kit+ cell biology consistent with the existence of multiple distinct subpopulations possessing nuanced differential characteristics that are lost on imposition of assessments focused on average measurements.

Genetic knock-in models that disrupt the c-Kit locus by necessity confer a hemizygous genotype for c-Kit. Given the proliferative and protective roles of c-Kit signaling in CPCs and evidence for survival signaling in ACMs, it is important to consider the potential impact of the hemizygous c-Kit phenotype on cardiac function and repair. Indeed, frequency of c-Kit cells decreased ≈50% in myocardial tissue sections from knock-in versus transgenic samples (Figure 4B), perhaps a consequence of differences in c-Kit gene dosage (hemizygosity in the CKmCm knock-in mice), strain (FVB for CKH2B and C57Bl/6 for CKmCm), or reporter system (direct TRE-mediated induction in CKH2B versus Cre-mediated recombination in CKmCm). One explanation for the difference in cell labeling between the knock-in and the transgenic models could be a feed-forward mechanism whereby disruption of one copy of c-Kit expression in the knock-in model leads to reduced c-Kit levels in all cells that express c-Kit. Impairment of c-Kit function leads to unequivocal phenotypic consequences in Wv (white spotting variant) c-Kit mutant mice that exhibit impaired cardiac recovery after infarction, diminished cardiac function with advanced age, and compromised c-Kit cell terminal differentiation into cardiomyocytes.[32,39–41] Circumspection is reasonable when considering the myocardial response to injury in c-Kit hemizygous mice that could compromise reparative capacity of c-Kit+ cells in myocardial regeneration. Reporter models that do not disrupt the endogenous locus, such as the previously described c-Kit-BAC-EGFP transgenic[4] or the inducible CKH2B system described here, bypass interference with endogenous c-Kit expression and associated changes in cellular function. Given the preponderance of evidence as cited in preceding paragraphs to substantiate the biological role for c-Kit in the normal and injured myocardium, inescapable c-Kit allele inactivation should not be readily dismissed or deemed irrelevant from interpretation of results using genetically engineered knock-in models.

Together with the advantage of preserving normal endogenous c-Kit regulation, the CKH2B tagging system uses a transgenic c-Kit promoter to express rtTA transcription factor combined with a tet-responsive ubiquitous H2BEGFP reporter line. Doxycycline-mediated transgene induction can be performed at any stage of development without the potential adverse side effects of tamoxifen treatment in pregnant dams.[52–57] Protein stability of H2BEGFP, with a reported half-life of several months in vivo,[44,58] provides long-term tagging of c-Kit+ cells in CKH2B mice, while allowing for reversibility in mitotically active systems. Permanent tagging of c-Kit cells allowing for long-term lineage tracing of cells has been initiated through combining the c-KitrtTA transgenic construct with a tetracycline-responsive Cre line[59] and the ROSA$^{mT/mG}$ reporter mouse.[60] Future studies using various c-KitrtTA transgenic models will establish distribution of c-Kit+ cells in the heart and clarify participation of c-Kit+ cells in response to cardiac injury.

In summary, the biological role of cardiac c-Kit is an important one that may be underappreciated because of an overemphasis on the use of c-Kit as a marker of stem cells. Proproliferative and protective effects of c-Kit signaling in cardiac cells are central to their regenerative potential and should be considered when designing experimental models to assess their role in cardiac formation and repair. All genetic lineage-tracing models have inherent limitations. Knock-ins frequently disrupt expression of the gene of interest and impair normal biological regulation, whereas transgenic promoter constructs may lack regulatory elements of the endogenous gene. Multicomponent lineage-tracing models designed to mark cells temporally and spatially harbor inducible or regulatable elements or rely on enzymatic recombination for tagging, introducing further layers of complexity and inescapable variables in efficiency, specificity, or even toxicity. In the final analysis, all experimental models are tools, with even the most sophisticated promoter-driven reporter models unable to precisely capture post-transcriptional regulation of c-Kit expression. For example, recent studies reveal that c-Kit translation, but not transcription, is regulated by Pim1 kinase in the hematopoetic stem cell pool.[61] Similarly, retinoic acid controls c-Kit translation through PI3K/Akt/mTOR

(mammalian target of rapamycin) during spermatogonial differentiation.[62,63] Additionally, microRNA 221 downregulates c-Kit protein expression in melanoma, hyperglycemic HUVECs (human umbilical vein endothelial cells), and PDGF (platelet-derived growth factor receptor)-stimulated vascular smooth muscle cells.[64–67] Multiple layers of c-Kit protein regulation dependent on posttranslational modification, ubiquitination, internalization, and degradation rate all contribute to dynamic c-Kit expression beyond the reach of any one reporter system to reflect endogenous c-Kit biology. Acknowledging that there is much still to learn and embracing variations in perspectives rooted in divergent experimental models will resolve discrepancies, unify the cardiovascular research community, and provide new avenues for exploration moving forward with a renewed respect for the complexity of myocardial c-Kit biology.

Acknowledgments

We gratefully acknowledge Dr Roland Wolkowicz and Cameron Smurthwaite from the San Diego State University flow cytometry core facility, the SDSU OLAC vivarium and veterinary staff for animal care, Chris Kohlmeyer, RN, of the San Diego Cardiac Center, Dr Robert Adamson, MD, and Sharp Memorial Hospital staff for providing the Sussman lab with human heart biopsy samples, and Sussman lab members for thoughtful discussion and feedback on this study.

Sources of Funding

M.A. Sussman is supported by National Institutes of Health (NIH) grants: R01HL067245, R37HL091102, R01HL105759, R01HL113647, R01HL117163, P01HL085577, and R01HL122525, as well as an award from the Fondation Leducq. N.A. Gude is supported by the NIH grants R37HL091102, R01HL117163, R01HL105759, and U54CA132384. M.M. Monsanto is supported by NIH grant R01HL122525, Rees Stealy Research Foundation, Achievement Rewards for College Scientists, and Elliott Family Fund Scholarship. K.M. Broughton is supported by NIH grant F32HL136196. F.G. Khalafalla is supported by NIH grant F32HL131299. J.van Berlo is supported by NIH grants R00HL112852 and R01HL130072.

Disclosures

M.A. Sussman is a founding member of CardioCreate, Inc. The other authors report no conflicts.

References

1. Orlic D, Kajstura J, Chimenti S, Limana F, Jakoniuk I, Quaini F, Nadal-Ginard B, Bodine DM, Leri A, Anversa P. Mobilized bone marrow cells repair the infarcted heart, improving function and survival. *Proc Natl Acad Sci USA*. 2001;98:10344–10349.
2. Beltrami AP, Barlucchi L, Torella D, Baker M, Limana F, Chimenti S, Kasahara H, Rota M, Musso E, Urbanek K, Leri A, Kajstura J, Nadal-Ginard B, Anversa P. Adult cardiac stem cells are multipotent and support myocardial regeneration. *Cell*. 2003;114:763–776.
3. Fransioli J, Bailey B, Gude NA, Cottage CT, Muraski JA, Emmanuel G, Wu W, Alvarez R, Rubio M, Ottolenghi S, Schaefer E, Sussman MA. Evolution of the c-kit-positive cell response to pathological challenge in the myocardium. *Stem Cells*. 2008;26:1315–1324. doi: 10.1634/stemcells.2007-0751.
4. Tallini YN, Greene KS, Craven M, Spealman A, Breitbach M, Smith J, Fisher PJ, Steffey M, Hesse M, Doran RM, Woods A, Singh B, Yen A, Fleischmann BK, Kotlikoff MI. c-kit expression identifies cardiovascular precursors in the neonatal heart. *Proc Natl Acad Sci USA*. 2009;106:1808–1813.
5. Miyamoto S, Kawaguchi N, Ellison GM, Matsuoka R, Shin'oka T, Kurosawa H. Characterization of long-term cultured c-kit+ cardiac stem cells derived from adult rat hearts. *Stem Cells Dev*. 2010;19:105–116. doi: 10.1089/scd.2009.0041.
6. Bolli R, Chugh AR, D'Amario D, et al. Cardiac stem cells in patients with ischaemic cardiomyopathy (SCIPIO): initial results of a randomised phase 1 trial. *Lancet*. 2011;378:1847–1857. doi: 10.1016/S0140-6736(11)61590-0.
7. Fischer KM, Cottage CT, Konstandin MH, Völkers M, Khan M, Sussman MA. Pim-1 kinase inhibits pathological injury by promoting cardioprotective signaling. *J Mol Cell Cardiol*. 2011;51:554–558. doi: 10.1016/j.yjmcc.2011.01.004.
8. Ellison GM, Vicinanza C, Smith AJ, et al. Adult c-kit(pos) cardiac stem cells are necessary and sufficient for functional cardiac regeneration and repair. *Cell*. 2013;154:827–842. doi: 10.1016/j.cell.2013.07.039.
9. van Berlo JH, Kanisicak O, Maillet M, Vagnozzi RJ, Karch J, Lin SC, Middleton RC, Marbán E, Molkentin JD. c-kit+ cells minimally contribute cardiomyocytes to the heart. *Nature*. 2014;509:337–341. doi: 10.1038/nature13309.
10. Hatzistergos KE, Takeuchi LM, Saur D, Seidler B, Dymecki SM, Mai JJ, White IA, Balkan W, Kanashiro-Takeuchi RM, Schally AV, Hare JM. cKit+ cardiac progenitors of neural crest origin. *Proc Natl Acad Sci USA*. 2015;112:13051–13056.
11. Chen Z, Zhu W, Bender I, Gong W, Kwak IY, Yellamilli A, Hodges TJ, Nemoto N, Zhang J, Garry DJ, van Berlo JH. Pathologic stimulus determines lineage commitment of cardiac c-kit+ cells. *Circulation*. 2017;136:2359–2372. doi: 10.1161/CIRCULATIONAHA.117.030137.
12. Vicinanza C, Aquila I, Scalise M, et al. Adult cardiac stem cells are multipotent and robustly myogenic: c-kit expression is necessary but not sufficient for their identification. *Cell Death Differ*. 2017;24:2101–2116. doi: 10.1038/cdd.2017.130.
13. Morrison-Graham K, Takahashi Y. Steel factor and c-kit receptor: from mutants to a growth factor system. *Bioessays*. 1993;15:77–83. doi: 10.1002/bies.950150202.
14. Rönnstrand L. Signal transduction via the stem cell factor receptor/c-kit. *Cell Mol Life Sci*. 2004;61:2535–2548. doi: 10.1007/s00018-004-4189-6.
15. Lennartsson J, Rönnstrand L. Stem cell factor receptor/c-kit: from basic science to clinical implications. *Physiol Rev*. 2012;92:1619–1649. doi: 10.1152/physrev.00046.2011.
16. Shi H, Drummond CA, Fan X, Haller ST, Liu J, Malhotra D, Tian J. Hiding inside? Intracellular expression of non-glycosylated c-kit protein in cardiac progenitor cells. *Stem Cell Res*. 2016;16:795–806. doi: 10.1016/j.scr.2016.04.017.
17. Hesse M, Fleischmann BK, Kotlikoff MI. Concise review: the role of c-kit expressing cells in heart repair at the neonatal and adult stage. *Stem Cells*. 2014;32:1701–1712. doi: 10.1002/stem.1696.
18. Hatzistergos KE, Hare JM. Murine models demonstrate distinct vasculogenic and cardiomyogenic cKit+ lineages in the heart. *Circ Res*. 2016;118:382–387. doi: 10.1161/CIRCRESAHA.115.308061.
19. Vajravelu BN, Hong KU, Al-Maqtari T, Cao P, Keith MC, Wysoczynski M, Zhao J, Moore JB IV, Bolli R. C-Kit promotes growth and migration of human cardiac progenitor cells via the PI3K-AKT and MEK-ERK pathways. *PLoS One*. 2015;10:e0140798. doi: 10.1371/journal.pone.0140798.
20. Gupta SK, Shukla P. Gene editing for cell engineering: trends and applications. *Crit Rev Biotechnol*. 2017;37:672–684. doi: 10.1080/07388551.2016.1214557.
21. Cairns LA, Moroni E, Levantini E, Giorgetti A, Klinger FG, Ronzoni S, Tatangelo L, Tiveron C, De Felici M, Dolci S, Magli MC, Giglioni B, Ottolenghi S. Kit regulatory elements required for expression in developing hematopoietic and germ cell lineages. *Blood*. 2003;102:3954–3962. doi: 10.1182/blood-2003-04-1296.
22. Ferreira-Martins J, Ogórek B, Cappetta D, et al. Cardiomyogenesis in the developing heart is regulated by c-kit-positive cardiac stem cells. *Circ Res*. 2012;110:701–715. doi: 10.1161/CIRCRESAHA.111.259507.
23. Tumbar T, Guasch G, Greco V, Blanpain C, Lowry WE, Rendl M, Fuchs E. Defining the epithelial stem cell niche in skin. *Science*. 2004;303:359–363. doi: 10.1126/science.1092436.
24. Joshi M, Keith Pittman H, Haisch C, Verbanac K. Real-time PCR to determine transgene copy number and to quantitate the biolocalization of adoptively transferred cells from EGFP-transgenic mice. *Biotechniques*. 2008;45:247–258. doi: 10.2144/000112913.
25. Yamamoto M, Shook NA, Kanisicak O, Yamamoto S, Wosczyna MN, Camp JR, Goldhamer DJ. A multifunctional reporter mouse line for Cre- and FLP-dependent lineage analysis. *Genesis*. 2009;47:107–114. doi: 10.1002/dvg.20474.
26. Kubli DA, Cortez MQ, Moyzis AG, Najor RH, Lee Y, Gustafsson ÅB. PINK1 is dispensable for mitochondrial recruitment of parkin and activation

of mitophagy in cardiac myocytes. *PLoS One*. 2015;10:e0130707. doi: 10.1371/journal.pone.0130707.
27. Monsanto MM, White KS, Kim T, Wang BJ, Fisher K, Ilves K, Khalafalla FG, Casillas A, Broughton K, Mohsin S, Dembitsky WP, Sussman MA. Concurrent isolation of 3 distinct cardiac stem cell populations from a single human heart biopsy. *Circ Res*. 2017;121:113–124. doi: 10.1161/CIRCRESAHA.116.310494.
28. Young SM, Cambareri AC, Ashman LK. Role of c-Kit expression level and phosphatidylinositol 3-kinase activation in survival and proliferative responses of early myeloid cells. *Cell Signal*. 2006;18:608–620. doi: 10.1016/j.cellsig.2005.06.005.
29. Agarwal S, Kazi JU, Rönnstrand L. Phosphorylation of the activation loop tyrosine 823 in c-Kit is crucial for cell survival and proliferation. *J Biol Chem*. 2013;288:22460–22468. doi: 10.1074/jbc.M113.474072.
30. Yang L, Wu Z, Yin G, Liu H, Guan X, Zhao X, Wang J, Zhu J. Stem cell factor (SCF) protects osteoblasts from oxidative stress through activating c-Kit-Akt signaling. *Biochem Biophys Res Commun*. 2014;455:256–261. doi: 10.1016/j.bbrc.2014.11.002.
31. Liu Q, Yang R, Huang X, Zhang H, He L, Zhang L, Tian X, Nie Y, Hu S, Yan Y, Zhang L, Qiao Z, Wang QD, Lui KO, Zhou B. Genetic lineage tracing identifies in situ kit-expressing cardiomyocytes. *Cell Res*. 2016;26:119–130. doi: 10.1038/cr.2015.143.
32. Li M, Naqvi N, Yahiro E, Liu K, Powell PC, Bradley WE, Martin DI, Graham RM, Dell'Italia LJ, Husain A. c-kit is required for cardiomyocyte terminal differentiation. *Circ Res*. 2008;102:677–685. doi: 10.1161/CIRCRESAHA.107.161737.
33. Quijada P, Toko H, Fischer KM, Bailey B, Reilly P, Hunt KD, Gude NA, Avitabile D, Sussman MA. Preservation of myocardial structure is enhanced by pim-1 engineering of bone marrow cells. *Circ Res*. 2012;111:77–86. doi: 10.1161/CIRCRESAHA.112.265207.
34. Anversa P, Kajstura J, Rota M, Leri A. Regenerating new heart with stem cells. *J Clin Invest*. 2013;123:62–70. doi: 10.1172/JCI63068.
35. Keith MC, Bolli R. "String theory" of c-kit(pos) cardiac cells: a new paradigm regarding the nature of these cells that may reconcile apparently discrepant results. *Circ Res*. 2015;116:1216–1230. doi: 10.1161/CIRCRESAHA.116.305557.
36. Sultana N, Zhang L, Yan J, Chen J, Cai W, Razzaque S, Jeong D, Sheng W, Bu L, Xu M, Huang GY, Hajjar RJ, Zhou B, Moon A, Cai CL. Resident c-kit(+) cells in the heart are not cardiac stem cells. *Nat Commun*. 2015;6:8701. doi: 10.1038/ncomms9701.
37. Di Siena S, Gimmelli R, Nori SL, et al. Activated c-Kit receptor in the heart promotes cardiac repair and regeneration after injury. *Cell Death Dis*. 2016;7:e2317. doi: 10.1038/cddis.2016.205.
38. Ishikawa K, Fish K, Aguero J, Yaniz-Galende E, Jeong D, Kho C, Tilemann L, Fish L, Liang L, Eltoukhy AA, Anderson DG, Zsebo K, Costa KD, Hajjar RJ. Stem cell factor gene transfer improves cardiac function after myocardial infarction in swine. *Circ Heart Fail*. 2015;8:167–174. doi: 10.1161/CIRCHEARTFAILURE.114.001711.
39. Ye L, Zhang EY, Xiong Q, Astle CM, Zhang P, Li Q, From AH, Harrison DE, Zhang JJ. Aging Kit mutant mice develop cardiomyopathy. *PLoS One*. 2012;7:e33407. doi: 10.1371/journal.pone.0033407.
40. Fazel S, Cimini M, Chen L, Li S, Angoulvant D, Fedak P, Verma S, Weisel RD, Keating A, Li RK. Cardioprotective c-kit+ cells are from the bone marrow and regulate the myocardial balance of angiogenic cytokines. *J Clin Invest*. 2006;116:1865–1877. doi: 10.1172/JCI27019.
41. Cimini M, Fazel S, Zhuo S, Xaymardan M, Fujii H, Weisel RD, Li RK. c-kit dysfunction impairs myocardial healing after infarction. *Circulation*. 2007;116:I77–I82. doi: 10.1161/CIRCULATIONAHA.107.708107.
42. Wallner M, Duran JM, Mohsin S, et al. Acute catecholamine exposure causes reversible myocyte injury without cardiac regeneration. *Circ Res*. 2016;119:865–879. doi: 10.1161/CIRCRESAHA.116.308687.
43. Hatzistergos KE, Saur D, Seidler B, Balkan W, Breton M, Valasaki K, Takeuchi LM, Landin AM, Khan A, Hare JM. Stimulatory effects of mesenchymal stem cells on cKit+ cardiac stem cells are mediated by SDF1/CXCR4 and SCF/cKit signaling pathways. *Circ Res*. 2016;119:921–930.
44. Foudi A, Hochedlinger K, Van Buren D, Schindler JW, Jaenisch R, Carey V, Hock H. Analysis of histone 2B-GFP retention reveals slowly cycling hematopoietic stem cells. *Nat Biotechnol*. 2009;27:84–90. doi: 10.1038/nbt.1517.
45. Gude N, Muraski J, Rubio M, Kajstura J, Schaefer E, Anversa P, Sussman MA. Akt promotes increased cardiomyocyte cycling and expansion of the cardiac progenitor cell population. *Circ Res*. 2006;99:381–388. doi: 10.1161/01.RES.0000236754.21499.1c.
46. Smith AJ, Lewis FC, Aquila I, Waring CD, Nocera A, Agosti V, Nadal-Ginard B, Torella D, Ellison GM. Isolation and characterization of resident endogenous c-Kit+ cardiac stem cells from the adult mouse and rat heart. *Nat Protoc*. 2014;9:1662–1681. doi: 10.1038/nprot.2014.113.
47. Ellison GM, Torella D, Karakikes I, Purushothaman S, Curcio A, Gasparri C, Indolfi C, Cable NT, Goldspink DF, Nadal-Ginard B. Acute beta-adrenergic overload produces myocyte damage through calcium leakage from the ryanodine receptor 2 but spares cardiac stem cells. *J Biol Chem*. 2007;282:11397–11409. doi: 10.1074/jbc.M607391200.
48. Nadal-Ginard B, Ellison GM, Torella D. The cardiac stem cell compartment is indispensable for myocardial cell homeostasis, repair and regeneration in the adult. *Stem Cell Res*. 2014;13:615–630. doi: 10.1016/j.scr.2014.04.008.
49. Chamuleau SA, Vrijsen KR, Rokosh DG, Tang XL, Piek JJ, Bolli R. Cell therapy for ischaemic heart disease: focus on the role of resident cardiac stem cells. *Neth Heart J*. 2009;17:199–207.
50. Ellison GM, Galuppo V, Vicinanza C, Aquila I, Waring CD, Leone A, Indolfi C, Torella D. Cardiac stem and progenitor cell identification: different markers for the same cell? *Front Biosci (Schol Ed)*. 2010;2:641–652.
51. Nigro P, Perrucci GL, Gowran A, Zanobini M, Capogrossi MC, Pompilio G. c-kit(+) cells: the tell-tale heart of cardiac regeneration? *Cell Mol Life Sci*. 2015;72:1725–1740. doi: 10.1007/s00018-014-1832-8.
52. Danielian PS, Muccino D, Rowitch DH, Michael SK, McMahon AP. Modification of gene activity in mouse embryos in utero by a tamoxifen-inducible form of Cre recombinase. *Curr Biol*. 1998;8:1323–1326.
53. Halakivi-Clarke L, Cho E, Onojafe I, Liao DJ, Clarke R. Maternal exposure to tamoxifen during pregnancy increases carcinogen-induced mammary tumorigenesis among female rat offspring. *Clin Cancer Res*. 2000;6:305–308.
54. Park EJ, Sun X, Nichol P, Saijoh Y, Martin JF, Moon AM. System for tamoxifen-inducible expression of cre-recombinase from the Foxa2 locus in mice. *Dev Dyn*. 2008;237:447–453. doi: 10.1002/dvdy.21415.
55. Huh WJ, Khurana SS, Geahlen JH, Kohli K, Waller RA, Mills JC. Tamoxifen induces rapid, reversible atrophy, and metaplasia in mouse stomach. *Gastroenterology*. 2012;142:21.e7–24.e7. doi: 10.1053/j.gastro.2011.09.050.
56. Lee S, Lee MS, Park J, Zhang JY, Jin DI. Oxidative stress in the testis induced by tamoxifen and its effects on early embryo development in isogenic mice. *J Toxicol Sci*. 2012;37:675–679.
57. Lizen B, Claus M, Jeannotte L, Rijli FM, Gofflot F. Perinatal induction of Cre recombination with tamoxifen. *Transgenic Res*. 2015;24:1065–1077. doi: 10.1007/s11248-015-9905-5.
58. Busche A, Schmitz S, Fleige H, Robbins SH, Walzer T, Stewart CA, Förster R, Messerle M, Prinz I. Genetic labeling reveals altered turnover and stability of innate lymphocytes in latent mouse cytomegalovirus infection. *J Immunol*. 2011;186:2918–2925. doi: 10.4049/jimmunol.1003232.
59. Perl AK, Wert SE, Nagy A, Lobe CG, Whitsett JA. Early restriction of peripheral and proximal cell lineages during formation of the lung. *Proc Natl Acad Sci USA*. 2002;99:10482–10487.
60. Muzumdar MD, Tasic B, Miyamichi K, Li L, Luo L. A global double-fluorescent Cre reporter mouse. *Genesis*. 2007;45:593–605. doi: 10.1002/dvg.20335.
61. An N, Cen B, Cai H, Song JH, Kraft A, Kang Y. Pim1 kinase regulates c-Kit gene translation. *Exp Hematol Oncol*. 2016;5:31. doi: 10.1186/s40164-016-0060-3.
62. Zhang L, Tang J, Haines CJ, Feng H, Lai L, Teng X, Han Y. c-kit expression profile and regulatory factors during spermatogonial stem cell differentiation. *BMC Dev Biol*. 2013;13:38. doi: 10.1186/1471-213X-13-38.
63. Busada JT, Chappell VA, Niedenberger BA, Kaye EP, Keiper BD, Hogarth CA, Geyer CB. Retinoic acid regulates Kit translation during spermatogonial differentiation in the mouse. *Dev Biol*. 2015;397:140–149. doi: 10.1016/j.ydbio.2014.10.020.
64. Igoucheva O, Alexeev V. MicroRNA-dependent regulation of cKit in cutaneous melanoma. *Biochem Biophys Res Commun*. 2009;379:790–794. doi: 10.1016/j.bbrc.2008.12.152.
65. Godshalk SE, Paranjape T, Nallur S, et al. A variant in a microRNA complementary site in the 3' UTR of the KIT oncogene increases risk of acral melanoma. *Oncogene*. 2011;30:1542–1550. doi: 10.1038/onc.2010.536.
66. Li Y, Song YH, Li F, Yang T, Lu YW, Geng YJ. MicroRNA-221 regulates high glucose-induced endothelial dysfunction. *Biochem Biophys Res Commun*. 2009;381:81–83. doi: 10.1016/j.bbrc.2009.02.013.
67. Davis BN, Hilyard AC, Nguyen PH, Lagna G, Hata A. Induction of microRNA-221 by platelet-derived growth factor signaling is critical for modulation of vascular smooth muscle phenotype. *J Biol Chem*. 2009;284:3728–3738. doi: 10.1074/jbc.M808788200.

Circulation Research
JOURNAL OF THE AMERICAN HEART ASSOCIATION

Cardiac c-Kit Biology Revealed by Inducible Transgenesis

Natalie A. Gude, Fareheh Firouzi, Kathleen M. Broughton, Kelli Ilves, Kristine P. Nguyen, Christina R. Payne, Veronica Sacchi, Megan M. Monsanto, Alexandria R. Casillas, Farid G. Khalafalla, Bingyan J. Wang, David E. Ebeid, Roberto Alvarez, Walter P. Dembitsky, Barbara A. Bailey, Jop van Berlo and Mark A. Sussman

Circ Res. 2018;123:57-72; originally published online April 10, 2018;
doi: 10.1161/CIRCRESAHA.117.311828
Circulation Research is published by the American Heart Association, 7272 Greenville Avenue, Dallas, TX 75231

Print ISSN: 0009-7330. Online ISSN: 1524-4571

SUPPLEMENTAL MATERIAL

Detailed Methods.

Cell proliferation assays: BrdU incorporation was detected in mouse CPCs as follows: 5000 mCPCs or hCPCs were plated per well in a 2 well chamber slide. The following day, cells were subjected to low serum conditions (2.5% ES-FBS) containing 40 mM BrdU with or without 200 ng/ml SCF for 72 hours. Cells were fixed for 20 minutes in 4% paraformaldehyde, washed three times in PBS/0.1% Tween-20, blocked in PBS/10% horse serum and immunolabeled for BrdU overnight at 4^{o}C, then labeled with Alexa 488-conjugated secondary antibody. For hCPC, prior to applying primary antibody, cells were subjected to 30 minutes of 2N HCl to facilitate access of antibody to chromatin-incorporated BrdU. Images were acquired using an SP8 confocal microscope. BrdU^{+} cells were counted per total DAPI labeled nuclei. Approximately 100 cells were counted per treatment condition. A two-tailed t-test was used to determine statistical significance between Low serum and Low serum+SCF sample groups. $p<0.05$ was considered significant. For cell counting assays, 20,000 mCPCs or hCPCs were plated per well of a 12-well plate. Cells were pre-starved in 2.5% ES-FBS and treated with vehicle or SCF (Peprotech 200 ng/ml) for 3 days. Cells were dissociated and counted every day using a hemocytometer, and doubling time calculated for each condition using a population doubling time online calculator (http://www.doubling-time.com/compute.php).
Cell numbers were normalized to day 1. CPCs derived from two different mice were used, experiments were repeated three times, and statistical analysis to compare two groups was performed using a two-tailed t-test. $p<0.05$ was considered statistically significant.

c-Kit antibody neutralization:
100,000 mCPCs were plated per well of a 6-well plate in mCPC growth medium. Following cell attachment after 5-6 hours, growth medium was replaced with low serum medium containing %2.5 ES-FBS. After approximately 16 hours in low serum, a group of cells was treated with c-Kit antibody (10 μg/ml) for 2 hours followed by SCF treatment (200 ng/ml) for 5 minutes. Protein lysate was collected for immunoblotting analysis. n=3. Significance was determined by unpaired t-test, $p<0.05$ was considered statistically significant, *=$p<0.05$.
Adult human CPCs between passages 6 and 10 were cultured on a 6-well plate (50K cells/well) in hCPC growth media for 24 hours. Cells were exposed to low serum media (2.5% ES-FBS/ 1% PSG in F-12/Ham) for 24 hours, treated with c-Kit antibody (15 μg/ml) for 2 hours followed by SCF treatment (200 ng/ml, 5 minutes). Protein lysates were collected for for immunoblotting analysis.

Cell death assay: 10,000 mCPCs were plated per well of a 6 well dish in mCPC growth media, treated with vehicle or 200 ng/mL mSCF (Peprotech #250-03) for 24 hours, then subjected to 4 hours serum starvation (0% ES-FBS). Experiments were repeated three times and mCPCs from at least two different mice were analyzed. Human CPCs were plated at a density of 20,000 cells per well of a 6 well dish in hCPC growth media. Vehicle or hSCF 200ng/mL (Peprotech, #300-07) was added after two hours, and on the following day media was changed to hCPC medium lacking serum and supplements with vehicle or 200ng/mL hSCF for three days. Cells were dissociated and labeled with Annexin V (BD Biosciences 1:175) and Propidium Iodide (10mg/ml) to detect apoptosis and necrosis, respectively, by flow cytometry.

Flow cytometric analysis of bone marrow and nonmyocyte cell isolates: Whole bone marrow suspensions were created as follows: marrow was flushed from freshly dissected femurs through a 40mm mesh using PBS+1%FBS+1mM EDTA, centrifuged at low speed for three minutes and resuspended in PBS+5% FBS prior to labeling with antibodies. Nonmyocyte

suspensions were isolated from collagenase digested hearts as described for mCPC isolation. Whole bone marrow and nonmyocyte cardiac cell suspensions isolated from doxycycline treated CKH2B mice were labeled with fluorophore conjugated antibodies for 30 minutes, washed in PBS+1%FBS+1mM EDTA and analyzed for coincidence of EGFP and antibody signal using a Canto II flow cytometer and FloJo software. See Supplemental Table II for specific antibody information.

Immunoblotting: Protein lysates were collected from samples and loaded on 4-12% NuPAGE Novex Bis-Tris Gels (Invitrogen). Proteins were transferred to a Millipore Immobilon-P PVDF membrane, blocked with Odyssey Blocking Buffer (TBS), and probed overnight at 4°C with primary antibodies targeting c-Kit, phospho-c-Kit, AKT, phospho-AKT, ERK, phospho-ERK and GAPDH at the dilutions indicated in Table II. Secondary antibodies conjugated to LI-COR IRDye680 or IRDye800 fluorophores were applied for 2 hours at room temperature. Fluorescence signal was detected using an Odyssey CLx Imaging System and quantified using Image Studio or ImageJ software.

Immunohistochemistry and confocal microscopy: Tissues collected from transgenic and control mice were fixed in formalin and processed for paraffin embedding as previously described [31]. Paraffin sections (5μm) were deparaffinized, subjected to antigen retrieval in 10mM citrate pH 6.0 and quenched for endogenous peroxidase activity in 3% H2O2 in TN buffer (150mM NaCl, 100mM Tris pH 7.6) for 30 minutes. Tissues were immunolabeled with antibodies to c-Kit (RND cat# AF1356), EGFP (Molecular Probes, A-11122), and cardiac troponin T (cTnT clone 13-11, Thermofisher MA5-12960) overnight at 4°C. Fluorescently conjugated secondary antibodies were used to detect EGFP and cTnT (Donkey anti-rabbit 488 Thermofisher cat# A-21206, Donkey anti-mouse 647 Thermofisher cat# A-31571). Peroxidase (HRP) conjugated secondary antibody was used to detect c-Kit in paraffin sections (Bovine anti-goat HRP Jacksonimmuno cat #805-035-180) a developed with a tyramide-555 fluorescent substrate according to manufacturer's instructions (Perkin/Elmer). Biotinylated wheat germ agglutinin (WGA-bio, Vector Labs #B-1025) was revealed with Streptavidin Alexa Fluor 700 (SA-700, Thermofisher #S21383) to define cell boundaries. DAPI was applied in the final wash step at 0.1μg/ml to label nuclei. Antibody concentrations are listed in Table II. Images were collected using a Leica SP8 confocal microscope and processed with Leica and Photoshop software. c-Kit cell analysis was performed on at least three animals from each group when available. Three tissue and technical replicates were performed per animal. Using an SP8 confocal microscope, c-Kit+ cells were imaged in base, midsection and apex regions of the heart. Tile scan images were also taken to analyze total tissue area. Cells were counted for c-Kit+/gfp+ and c-Kit+/gfp- to determine recombinant efficiency. Total c-Kit+ cell number was divided by total tissue area to determine average cells per area. A linear mixed model analysis was used to determine statistical significance, as described below in Statistics. $p<0.05$ was considered significant.

Immunocytochemistry: CPCs were fixed in 4% paraformaldehyde for 20 minutes, washed in 1% Tween/PBS, blocked in 10% horse serum and immunolabeled for c-Kit (Polyclonal Goat IgG, RND Systems, AF1356) and EGFP (Polyclonal chicken IgY, Thermofisher, A10262) at 4°C overnight. Flourescently conjugated secondary antibodies (Donkey anti-goat cy3 and Donkey anti-GFP 488) were applied for 90 minutes at room temperature. All washes were performed in 1% Tween/PBS. Nuclei were stained with DAPI (1 mg/ml stock, 1:5000 in PBS), slides were coverslipped with Vectashield mounting media, and stained cells visualized using a Leica SP8 confocal microscope. Images were processed with Leica and Photoshop software. Antibodies and dilutions used for all applications are listed in Supplemental Table II. ACM were fixed in 4% PFA for 10 minutes, washed in 0.1% Tween20/PBS twice for 5 minutes, permeabilized in 0.1% Triton-X-100/PBS for 30 minutes, blocked in 10% horse serum/PBS for 1 hour, and incubated

overnight at 4^{o}C with goat anti-c-Kit diluted 1:50 in blocking buffer. Washes were in 0.1% Tween20/PBS, c-Kit and sarcomeres were visualized by staining with with donkey anti-goat CY3 1:300, Phalloidin 633 1:500 for two hours in blocking buffer, and nuclei stained with DAPI 1:5000 in PBS. Images were acquired with a Leica SP8 confocal microscope and images processed with Leica and Adobe Photoshop software.

Supplemental Statistical Analysis of c-Kit EGFP tagging efficiency (Figure 4):

GFP Tagging Efficiency Statistical Analysis: To test the difference in the two mice strains, the repeated measures of CKIT for each animal are modeled using a linear mixed model. The linear mixed-effects model allows us to make inferences about the fixed effects, which are the mean intercept, experiment, and mice strain. The random effect for the intercept describes the variability associated with each animal using the three repeated experiments. There are 3 Experiments. There are 3 animals in mice strain H2B-GFP Do and 4 animals in mice strain CKIT-CRE – TX, for a total number of 7 animals. The experiments and mice strains are categorical variables and are modeled using indicator variables. The reference experiment is Experiment 1 and the reference mice strain is CKIT-CRE - TX.

Let CKIT_ij model the the individual animal response for animal i in experiment j, where i=1,..., 9, and j=1,…,3.

The final model can be written as:

CKIT_ij = beta_0 + beta_1*MouseStrain2_i + beta_2*Experiment2_ij + beta_3*Experiment3_ij + u_0i + epsilon_ij

The parameters beta_0 and beta_1 represents the fixed effect associated with the two mouse strains and beta_2 and beta_3 represent fixed effects associated with the three experiments. Recall, the random effects are represented by u_0i and epsilon_ij. The u_0i term represents the random intercept associated with animal i and is assumed to be a mean zero variance sigma^2_intercept normal random variable. The epsilon_ij are the residuals for animal i for experiment j and they are assumed be mean zero normal random variables. The full model that included fixed effects associated with the interaction between experiment and mice strain were not significant and therefore dropped from the full model (P=0.5870)

The final model was fit with the R function lme by Restricted Maximum Likelihood (REML).

The summary of the fixed effects is given by:

Fixed effects: CKIT ~ MiceStrain + Experiment

	Value	Std.Error	DF	t-value	P-value
(Intercept)	0.6850619	0.05752175	12	11.909616	0.0000
MiceStrain2	0.1361222	0.07872177	5	1.729156	0.1443
Experiment2	-0.0347429	0.04425530	12	-0.785055	0.4476
Experiment3	-0.1581429	0.04425530	12	-3.573422	0.0038

The p-value associated with the mice strain factor indicates there is a non-significant effect of mice strain (P=0.14). Since the sample size is small in this analysis, a test for the difference in means of the two mice strains using a post-hoc Tukey test for multiple comparisons of means while controlling the family wise error rate was performed using the final model is given below. The post-hoc test p-value of 0.08 (P < 0.1) indicates that there is some evidence to suggest there is a difference in means of the two mice strains.

Linear Hypotheses:

	Estimate	Std. Error	z value	Pr(>|z|)
1 - 0 == 0	0.13612	0.07872	1.729	0.0838 .

A likelihood ratio test indicated that the random intercept should be included in the final model (P < 0.05). Examination of the final model summary and diagnostic plots indicated that the model assumptions were satisfied.

The summary of the random effects is given by:

Random effects formula: ~1 | animal		
	(Intercept)	Residual
Std.Dev	0.09131635	0.08279409

Ckit+ Cells per unit Area Statistical Analysis: To test the difference in the three mice strains, the repeated measures of CKIT for each animal are modeled using a linear mixed model. The linear mixed-effects model allows us to make inferences about the fixed effects, which are the mean intercept, experiment, and mice strain. The random effect for the intercept describes the variability associated with each animal using the three repeated experiments. There are 3 Experiments. There are 2 animals from mice strain CKIT-CRE - No TX, 3 animals from mice strain H2B-GFP Do, and 4 animals from mice strain CKIT-CRE – TX, for a total number of 9 animals. The experiments and mice strains are categorical variables and are modeled using indicator variables. The reference experiment is Experiment 1 and the reference mice strain is CKIT-CRE - No TX.

Let CKIT_ij model the the individual animal response for animal i in experiment j, where i=1,..., 9, and j=1,…,3.

The final model can be written as:

CKIT_ij = beta_0 + beta_1*MiceStrain2_i + beta_2*MiceStrain3_i + u_0i + epsilon_ij

The parameters beta_0, beta_1 and beta_2 represents the fixed effect associated with the three mouse strains. MiceStrain2 is H2B-GFP Do and MiceStrain3 is CKIT-CRE – TX. The random effects are represented by u_0i and epsilon_ij. The u_0i term represents the random intercept associated with animal i and is assumed to be a mean zero variance sigma^2_intercept normal random variable. The epsilon_ij are the residuals for animal i for experiment j and they are assumed be mean zero normal random variables. It should be noted that the final model includes only the fixed effects associated with the three mouse strains. The full model that included fixed effects associated with the three experiments and the interaction between experiment and mice strain were not significant and therefore dropped from the full model (P=0.2944, P=0.6293)

The final model was fit with the R function lme by Restricted Maximum Likelihood (REML).

The summary of the fixed effects is given by:

Fixed effects: CKIT ~ MiceStrain.

	Value	Std.Error	DF	t-value	P-value
(Intercept)	0.3944388	0.1817506	18	2.1702202	0.0436
MiceStrain2	0.7027529	0.2346390	6	2.9950385	0.0242
MiceStrain3	0.0941051	0.2225981	6	0.4227579	0.6872

The small p-value (P=0.0337) associated with the ANOVA mice strain factor indicates there is a significant effect of mice strain. To test for the difference in means of the three mice strains a post-hoc Tukey test for multiple comparisons of means while controlling the family wise error rate was performed using the final model.

Linear Hypotheses R-code output:

```
       Estimate Std. Error z value Pr(>|z|)
1 - 0 == 0  0.70275    0.23464   2.995  0.00759 **
2 - 0 == 0  0.09411    0.22260   0.423  0.90577
2 - 1 == 0 -0.60865    0.19631  -3.100  0.00541 **
---
Signif. codes:  0 ‘***’ 0.001 ‘**’ 0.01 ‘*’ 0.05 ‘.’ 0.1 ‘ ’ 1
```

A likelihood ratio test indicated that the random intercept should be included in the final model ($P < 0.05$). Examination of the final model summary and diagnostic plots indicated that the model assumptions were satisfied.

The summary of the random effects is given by:

Random effects formula: ~1 | animal

	(Intercept)	Residual
Std.Dev	0.2077059	0.2622488

Online Figure I. SCF specifically activates c-Kit signaling in CPCs

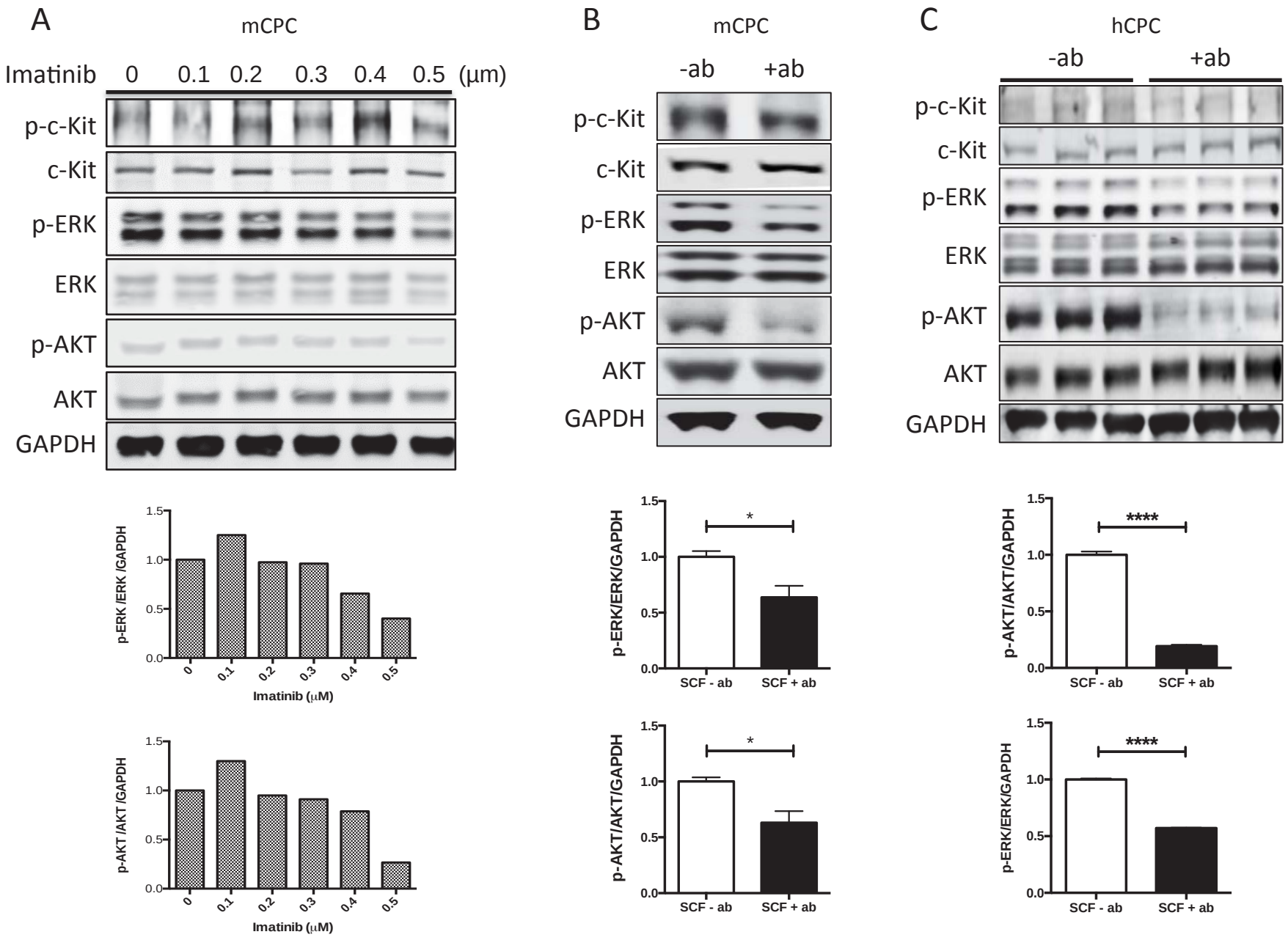

Online Figure I. SCF specifically activates c-Kit signaling in CPCs

D

Marker	% of NMC
FceR1	8.3 +/- 2.4, n=3
F4/80	7.4 +/- 2.0, n=3
CD206	9.9 +/- 3.2, n=2
CD45	9.8 +/- 2.5, n=3

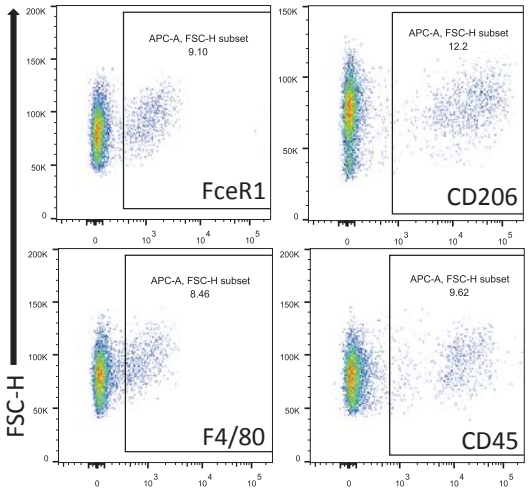

E

Marker	% of mCPC p12
FceR1	1.2 +/- 0.3, n=3
F4/80	1.0 +/- 0.7, n=3
CD206	0.8 +/- 0.3, n=3
CD45	2.0 +/- 1.2, n=3
CD105	94.6 +/- 3.2, n=3
CD90.1	45.1 +/- 6.3, n=3
PDGFRα	47.7 +/- 31.7, n=3

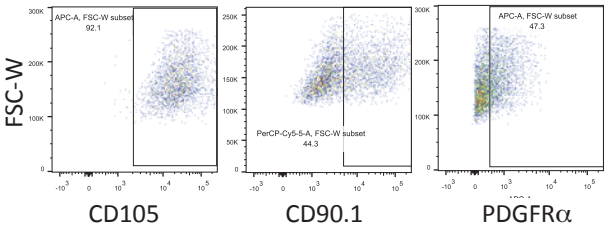

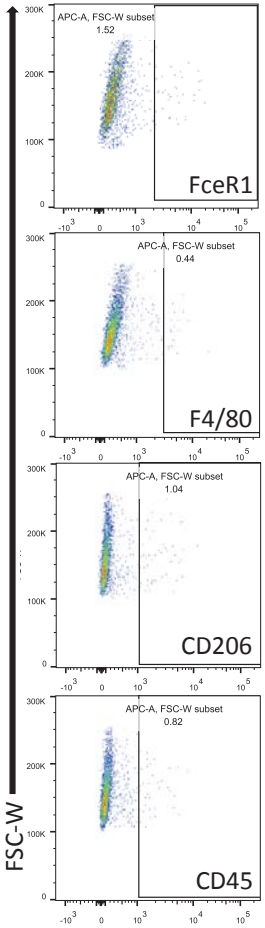

F

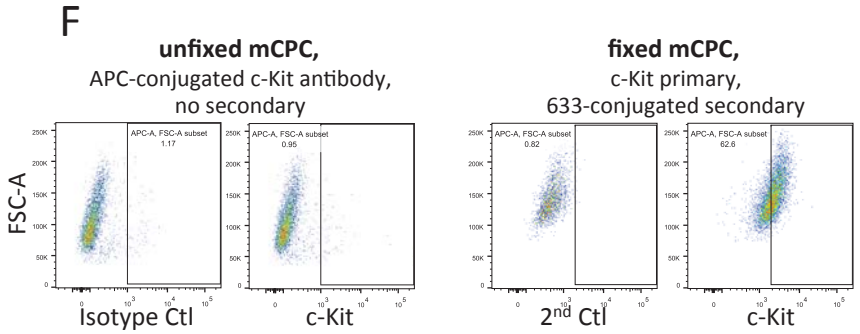

Online Figure II. ACM possess active c-Kit signaling.

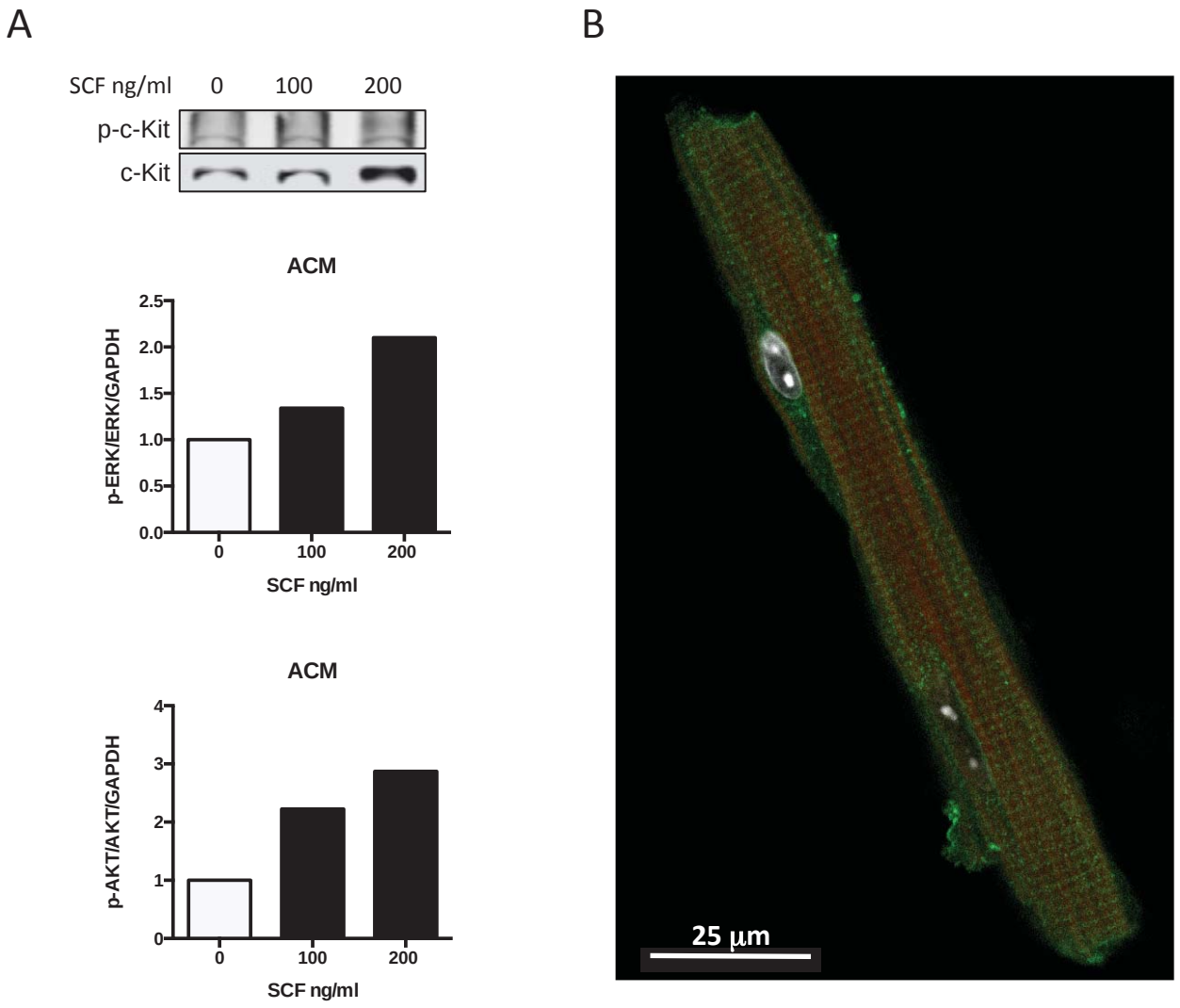

Online Figure II. ACM possess active c-Kit signaling.

C

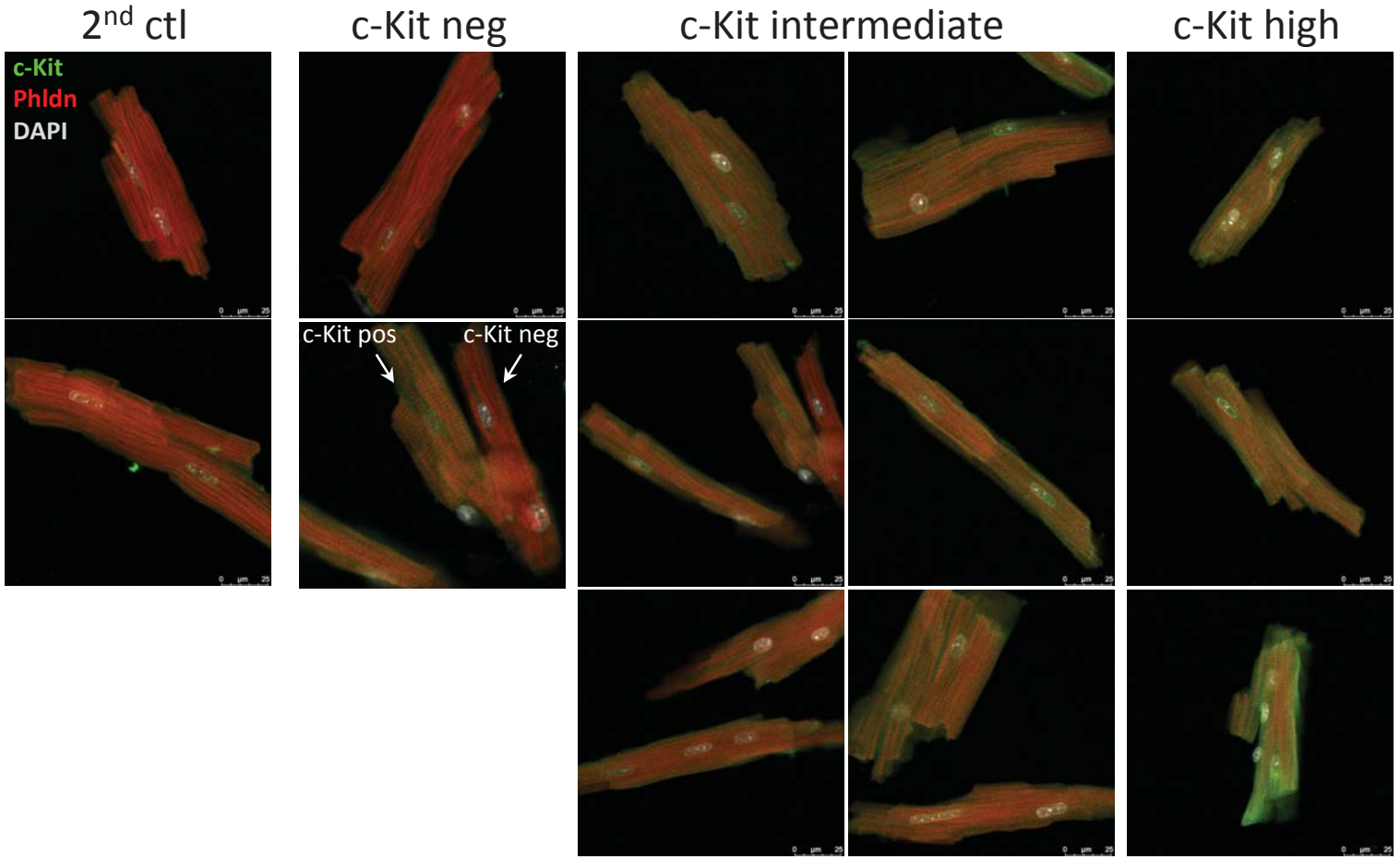

Online Figure III. Constructs, transgenic mouse lines and crosses for c-Kit reporter expression

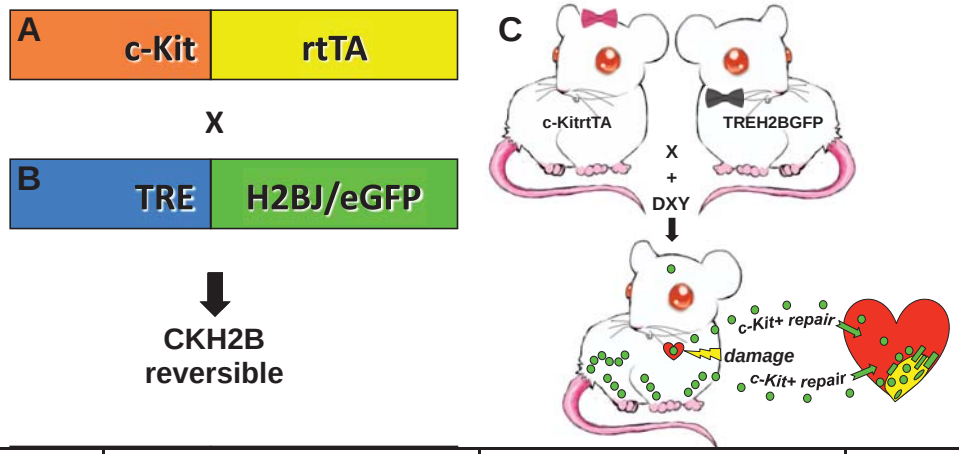

D

c-Kit promoter	Reporter	Inducible Tag	Treatment
c-KitrtTA	TREH2BEGFP (Jackson #005104)	c-KitrtTA/H2BEGFP = **CKH2B**	Doxycycline induces reversible expression of Histone2BEGFP in c-Kit+ cells

Online Figure IV. Quantitation of c-KitrtTA transgene by qPCR.

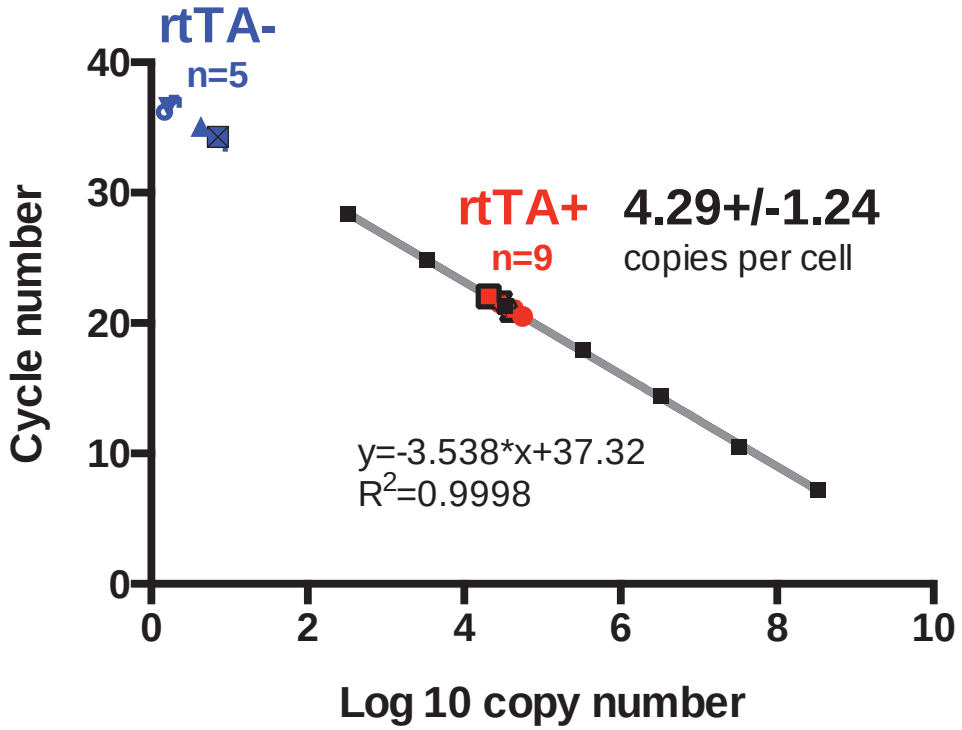

Online Figure V. Identification of non-myocyte cardiac cells labeled by H2BEGFP reporter

A

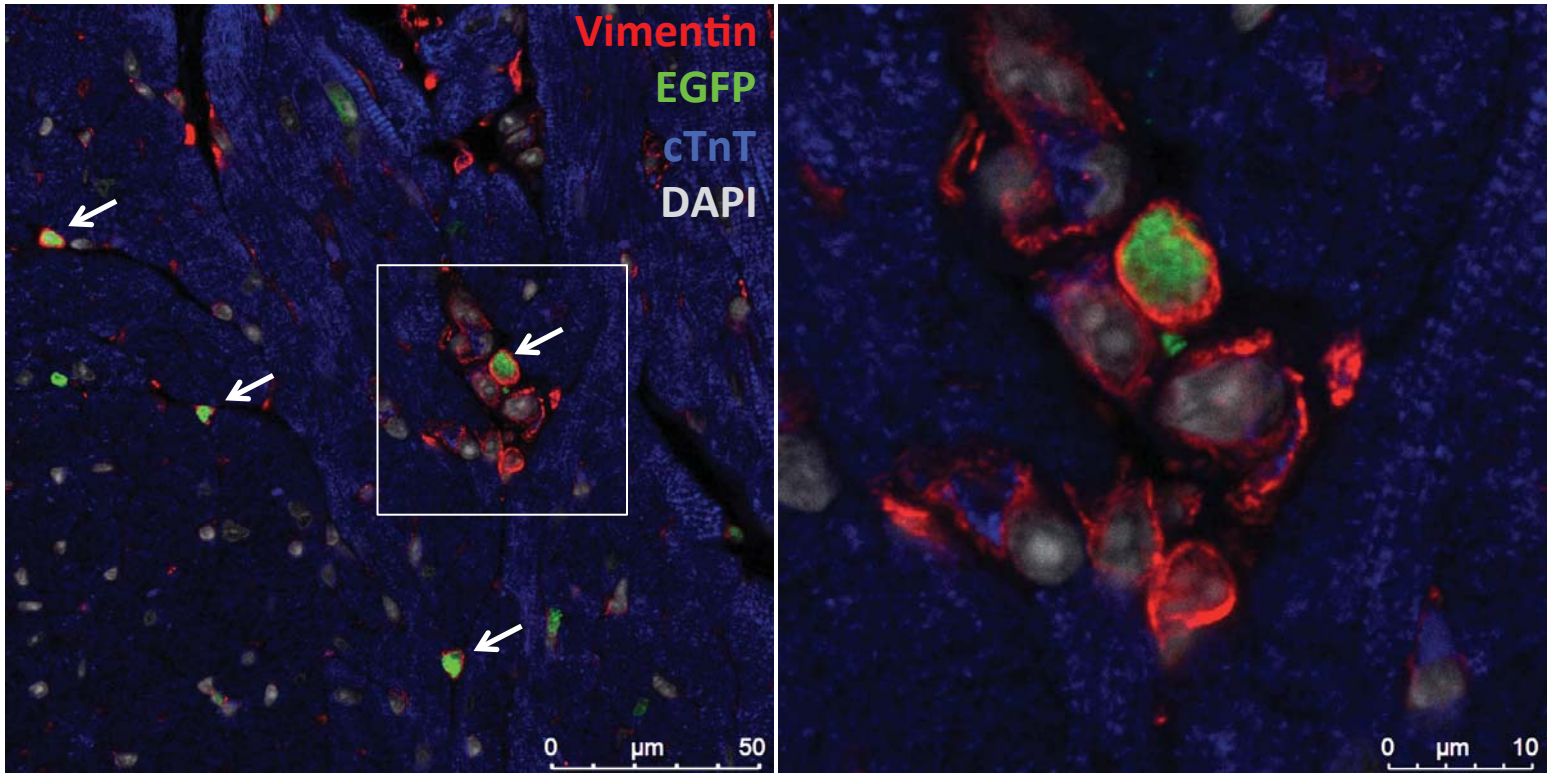

Online Figure V. Identification of non-myocyte cardiac cells labeled by H2BEGFP reporter

B

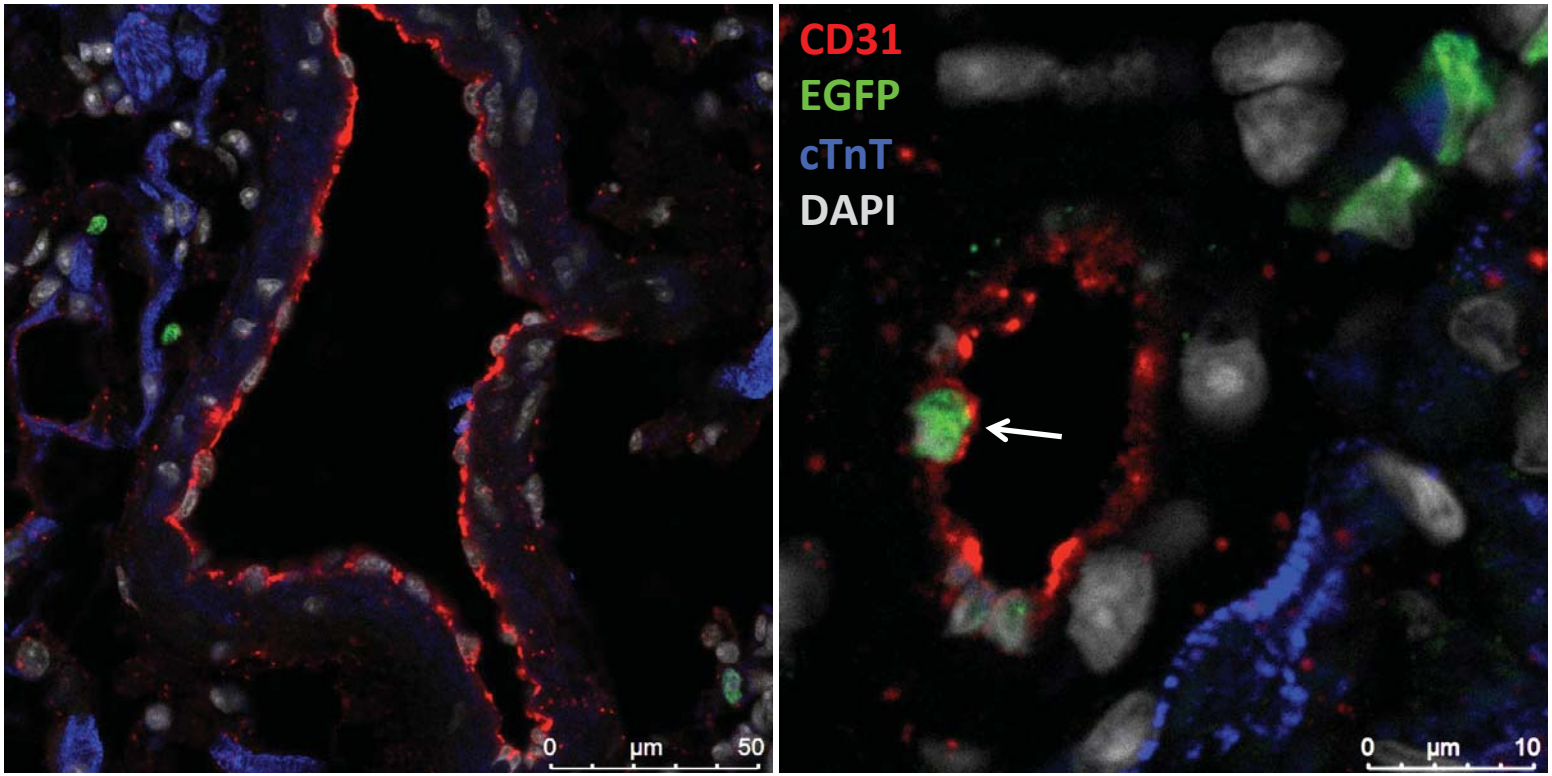

Online Figure V. Identification of non-myocyte cardiac cells labeled by H2BEGFP reporter

C

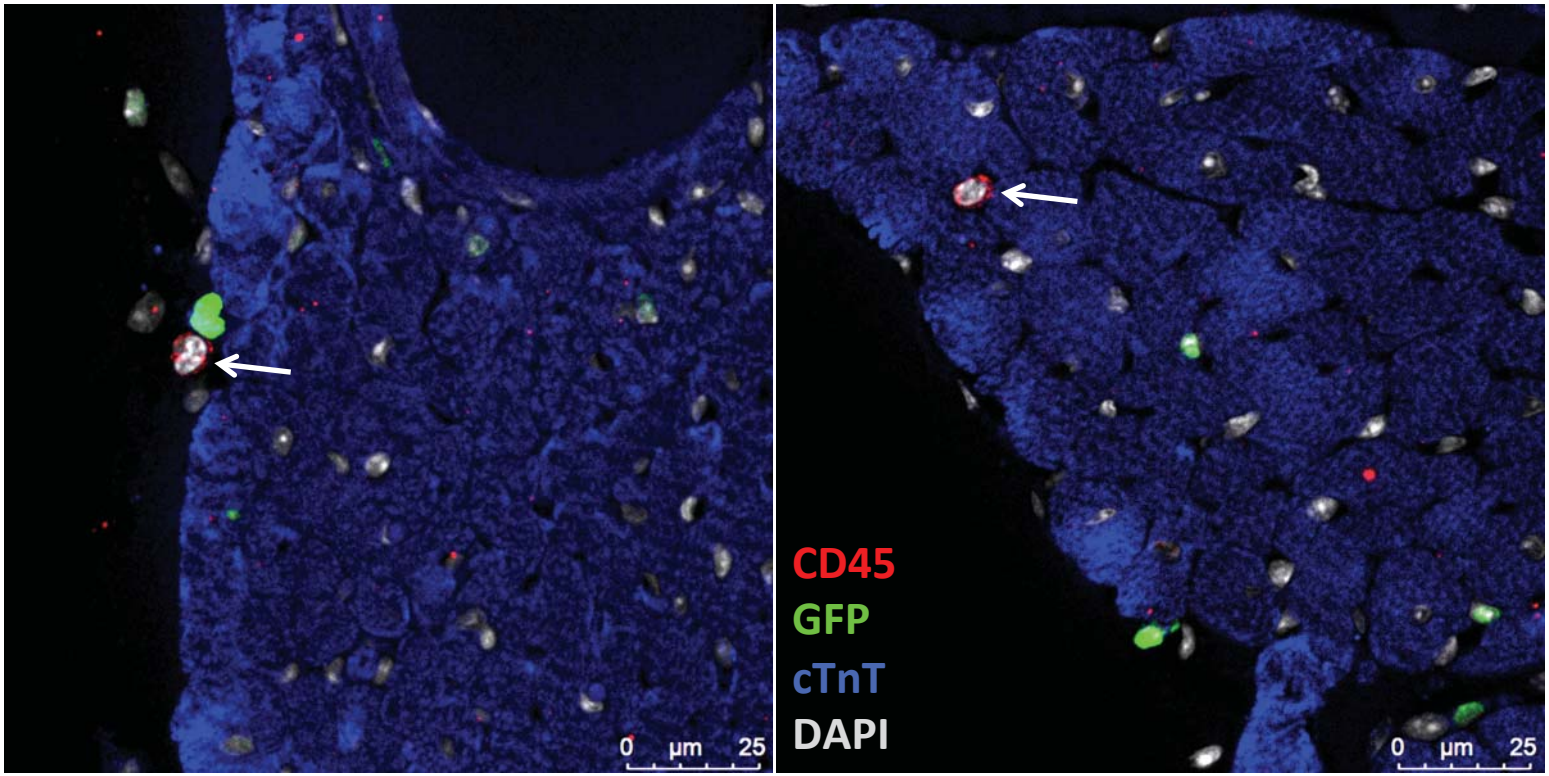

Online Figure V. Identification of non-myocyte cardiac cells labeled by H2BEGFP reporter

D

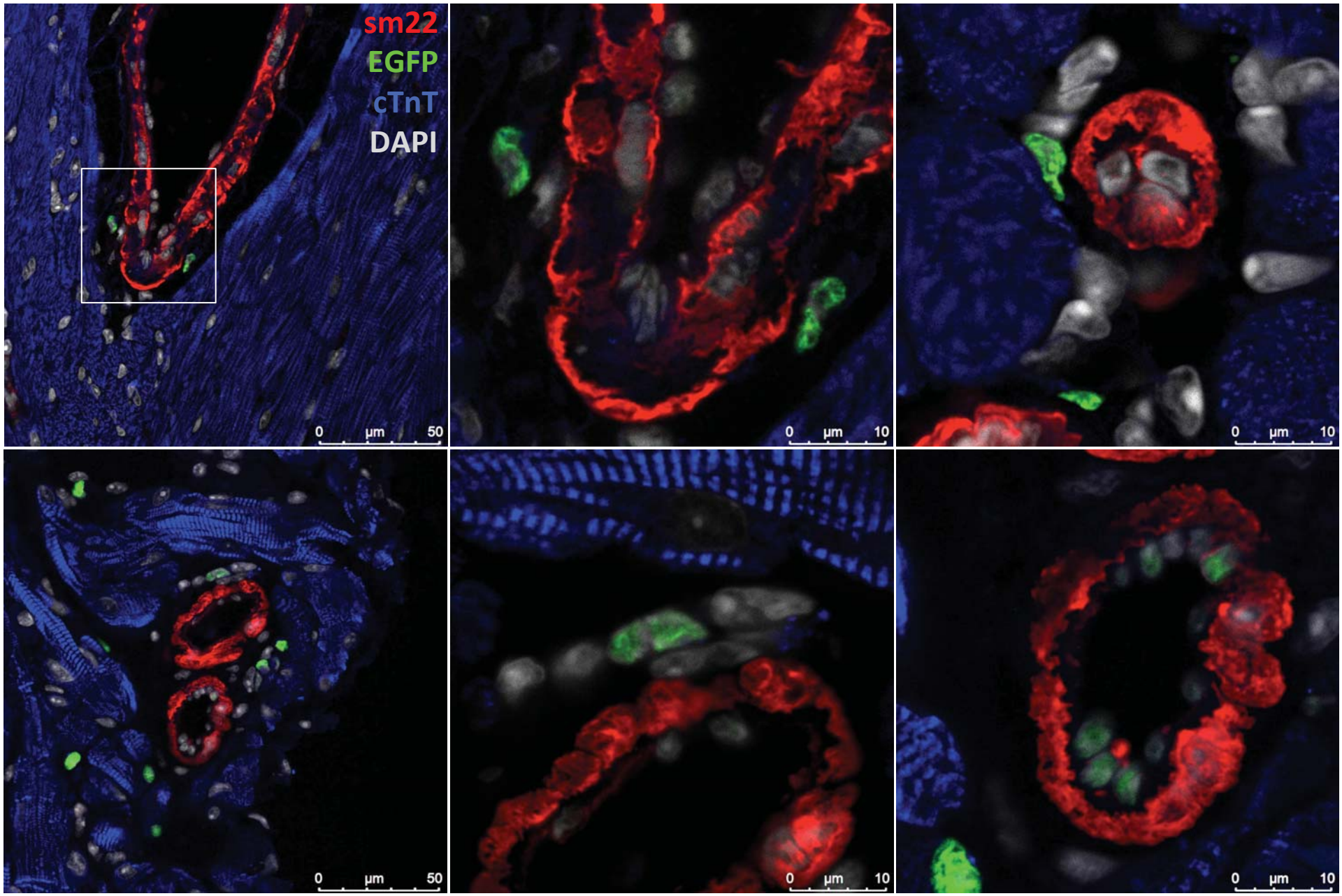

Online Figure V. Identification of non-myocyte cardiac cells labeled by H2BEGFP reporter

E

Marker	% of EGFP+ NMC
c-Kit	29.5 +/- 6.2, n=10
CD31	8.9 +/- 4.6, n=2
CD45	27 +/- 1.6, n=2
CD105	62.4 +/- 1.9, n=2
CD90.1	72.0 +/- 0.64, n=2
PDGFRα	49.0 +/- 10.4, n=2

Marker	% of EGFP+ BM
c-Kit	82.4 +/- 10.8, n=14
CD31	67.9 +/- 35.5, n=2
CD45	99.0 +/- 0.07, n=2

F

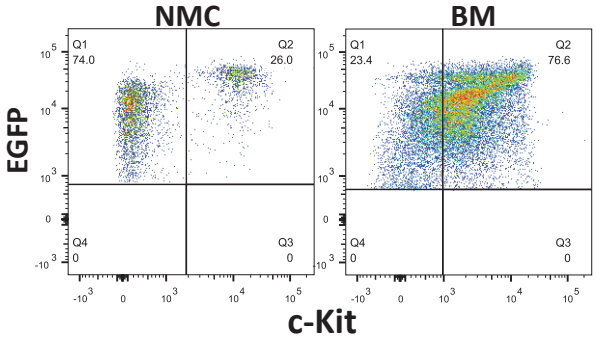

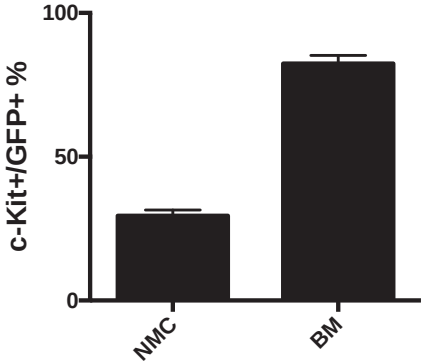

G

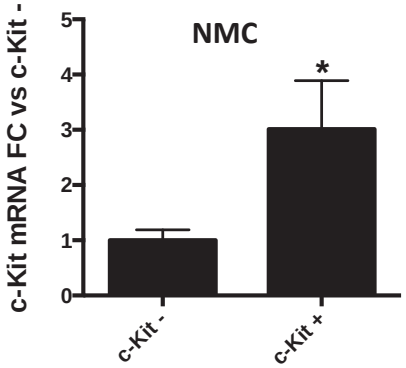

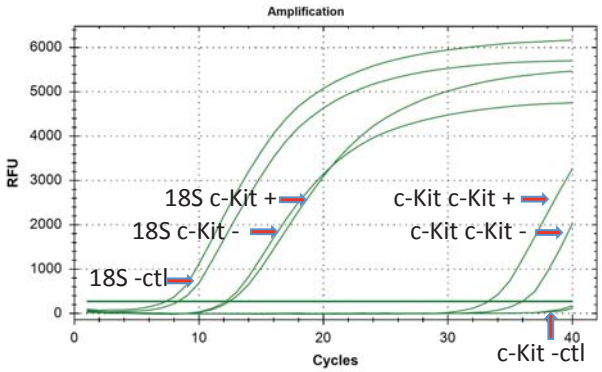

Online Figure VI. EGFP+ is expressed in c-Kit+ cells of induced CKmCm and CKH2B hearts.

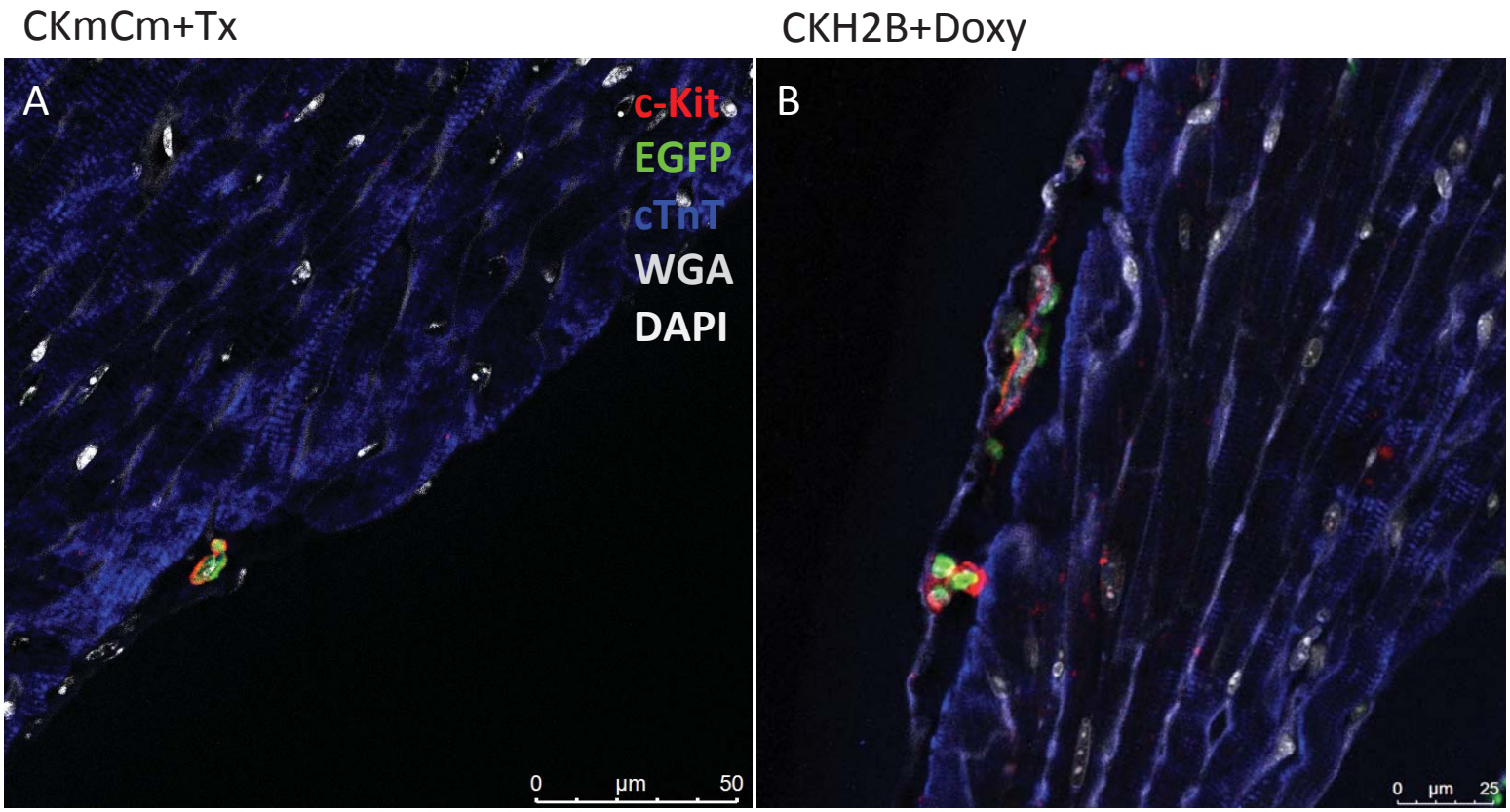

Online Figure VI. EGFP+ is expressed in c-Kit+ cells ofinduced CKmCm and CKH2B hearts.

C

NMC EGFP+ % total

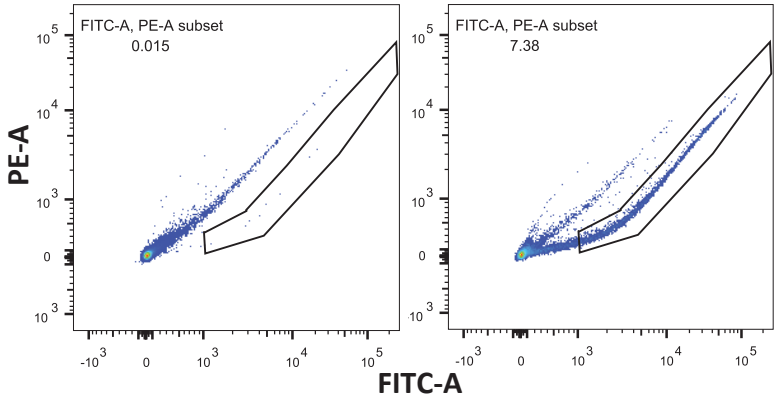

	CKmCm NMC	CKH2B NMC
EGFP+ gate	0.04% +/- 0.02 n=3	4.7% +/- 2.7 n=9

BM EGFP+% total

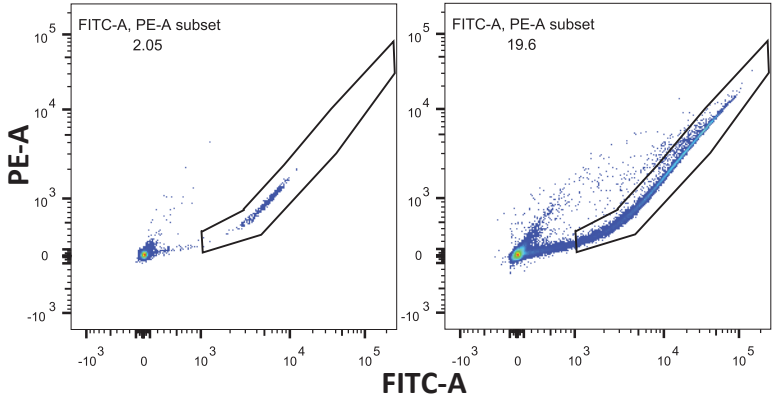

	CKmCm BM	CKH2B BM
EGFP+ gate	2.9% +/- 1.2 n=4	20.4% +/- 7.0 n=10

Online Figure VI. EGFP+ is expressed in c-Kit+ cells of induced CKmCm and CKH2B hearts.

D

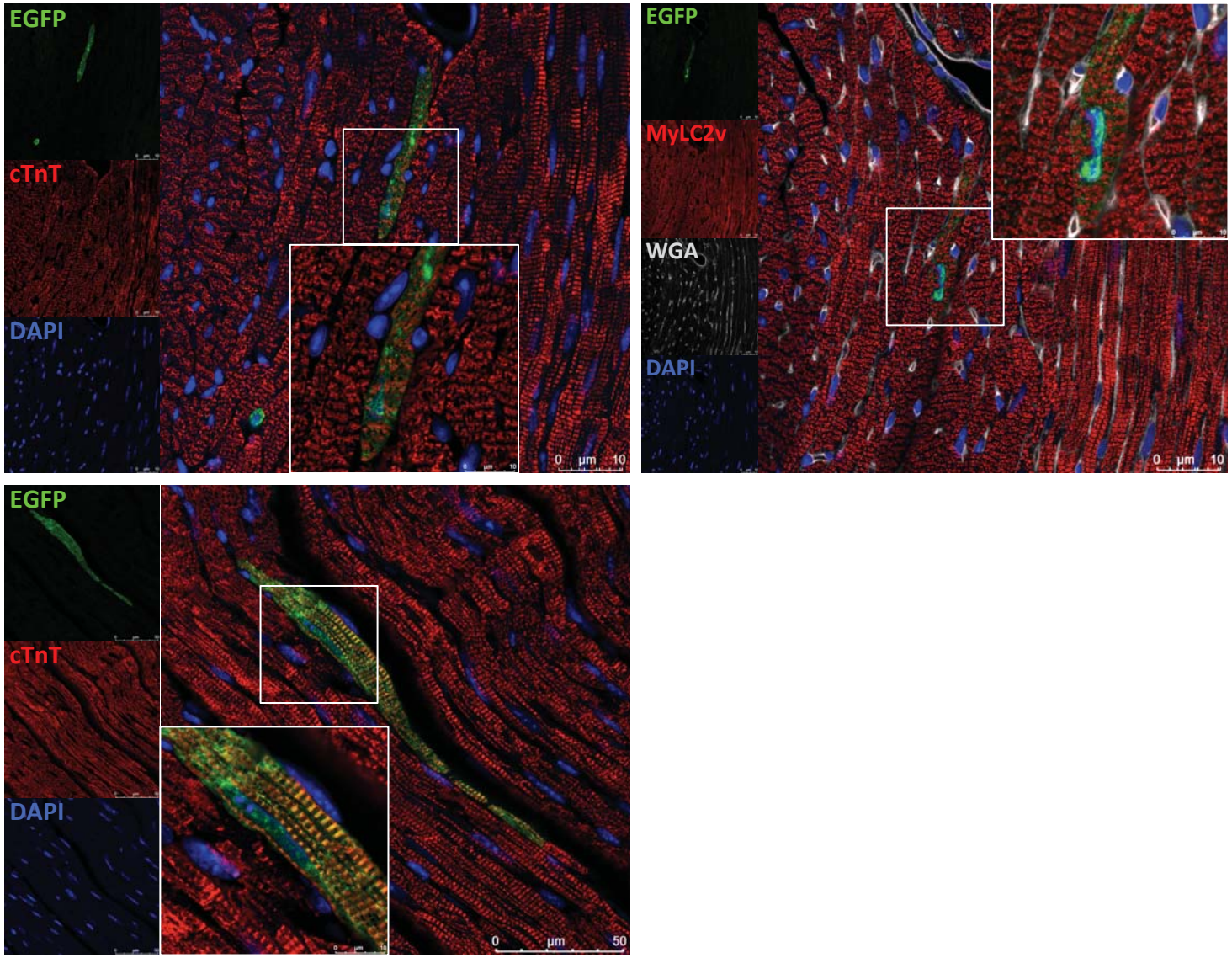

Online Figure VII. H2BEGFP reporter is expressed in ACM isolated from CKH2B hearts

A

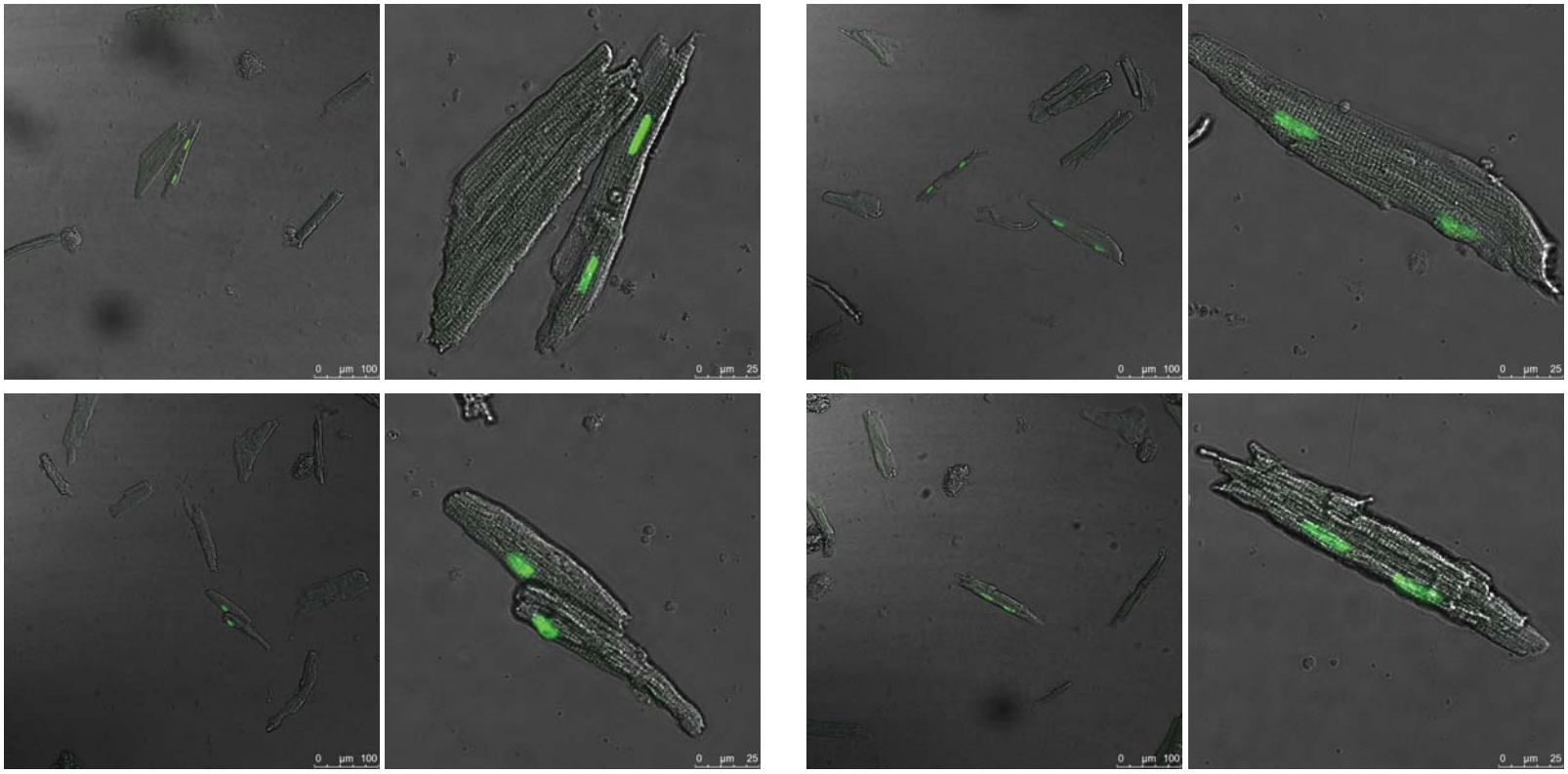

Online Figure VII. H2BEGFP reporter is expressed in ACM isolated from CKH2B hearts

B

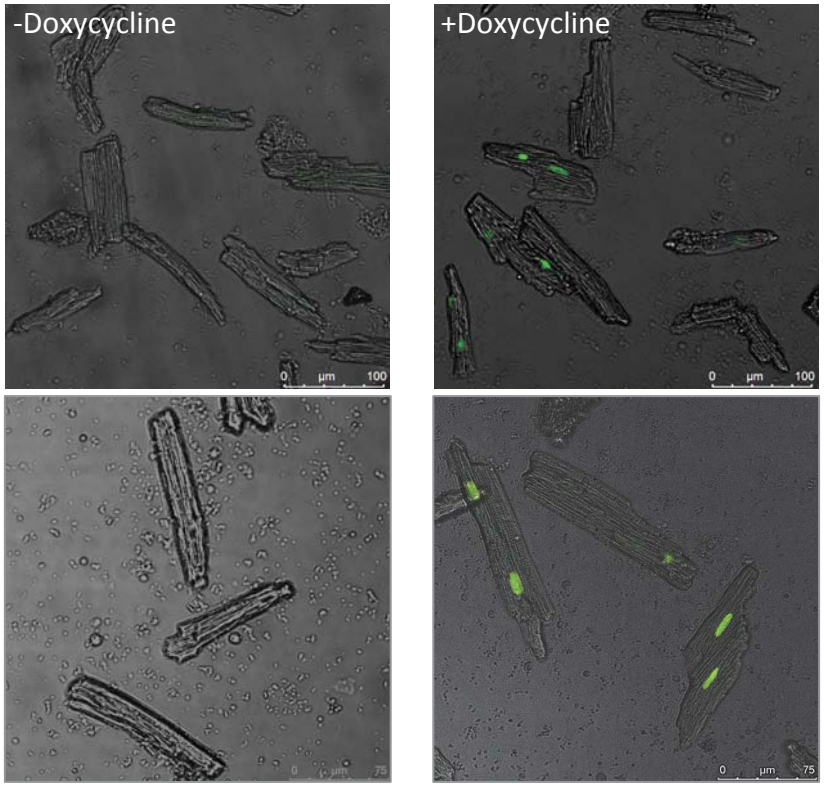

Online Figure VIII: H2BEGFP reporter is expressed in non-cardiac c-Kit+ cells.

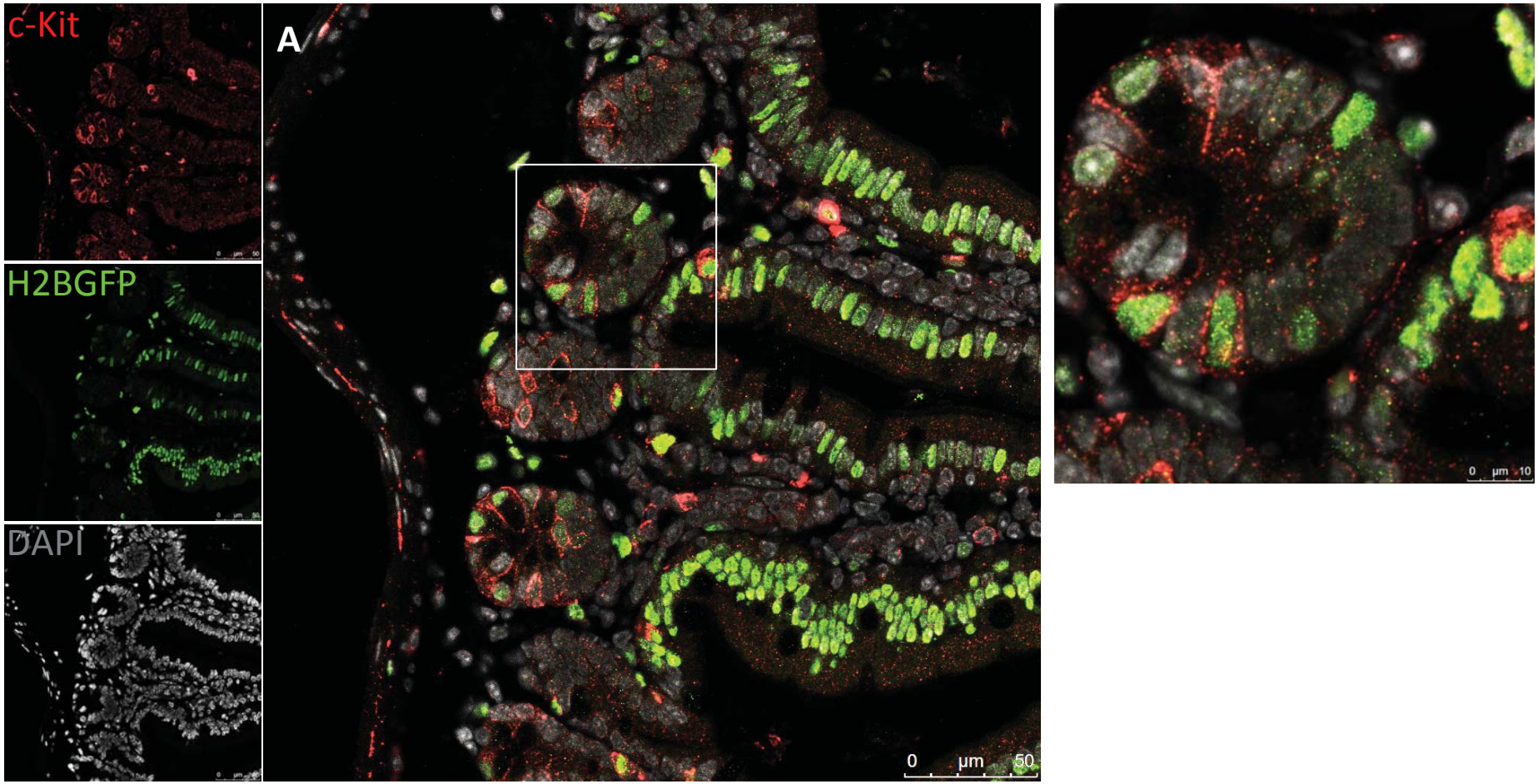

Online Figure VIII: H2BEGFP reporter is expressed in non-cardiac c-Kit+ cells.

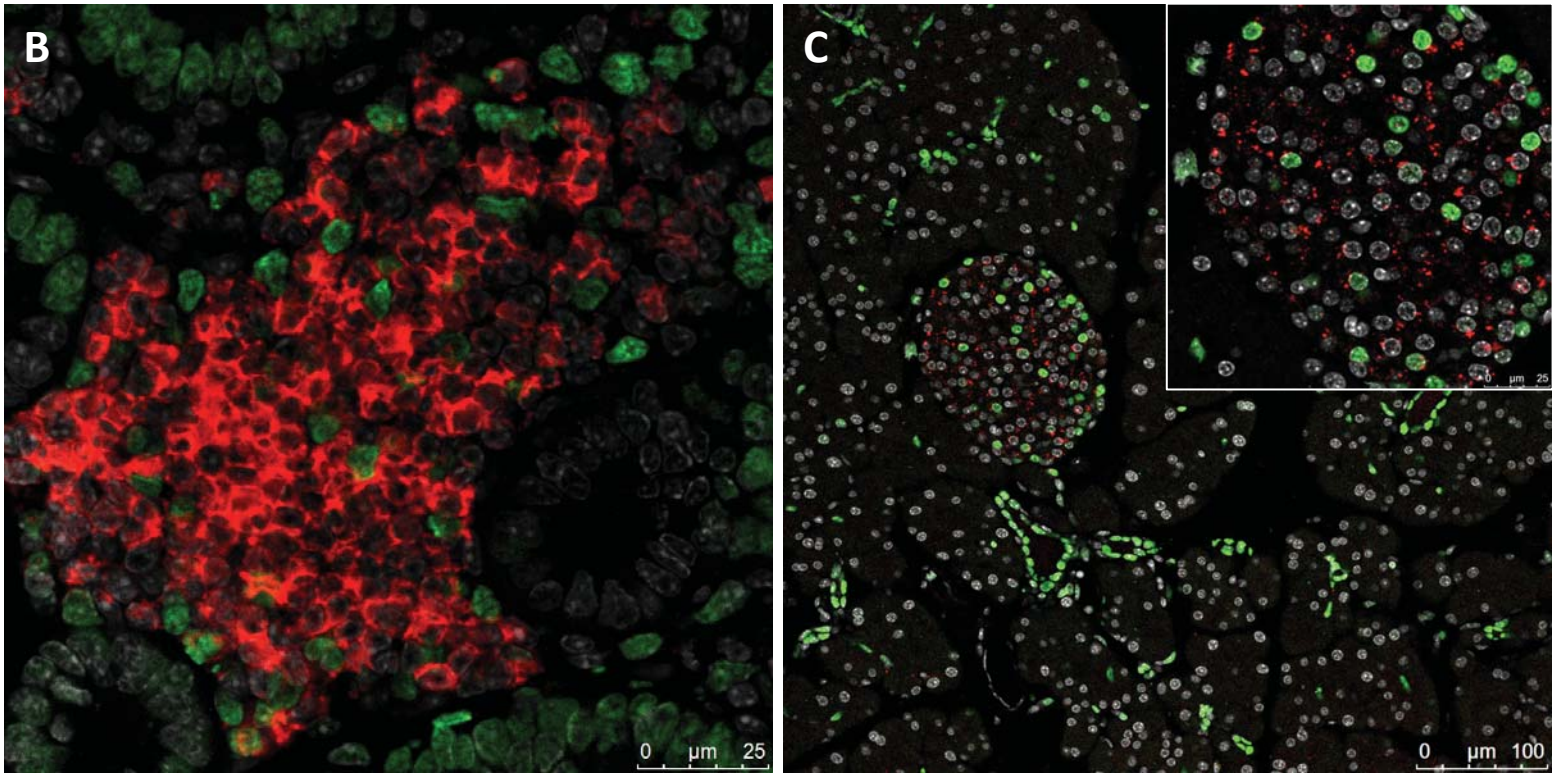

Online Figure IX. H2BEGP reporter is induced in CKH2B c-Kit+ bone marrow stem cells (BMSCs) *in vitro*.

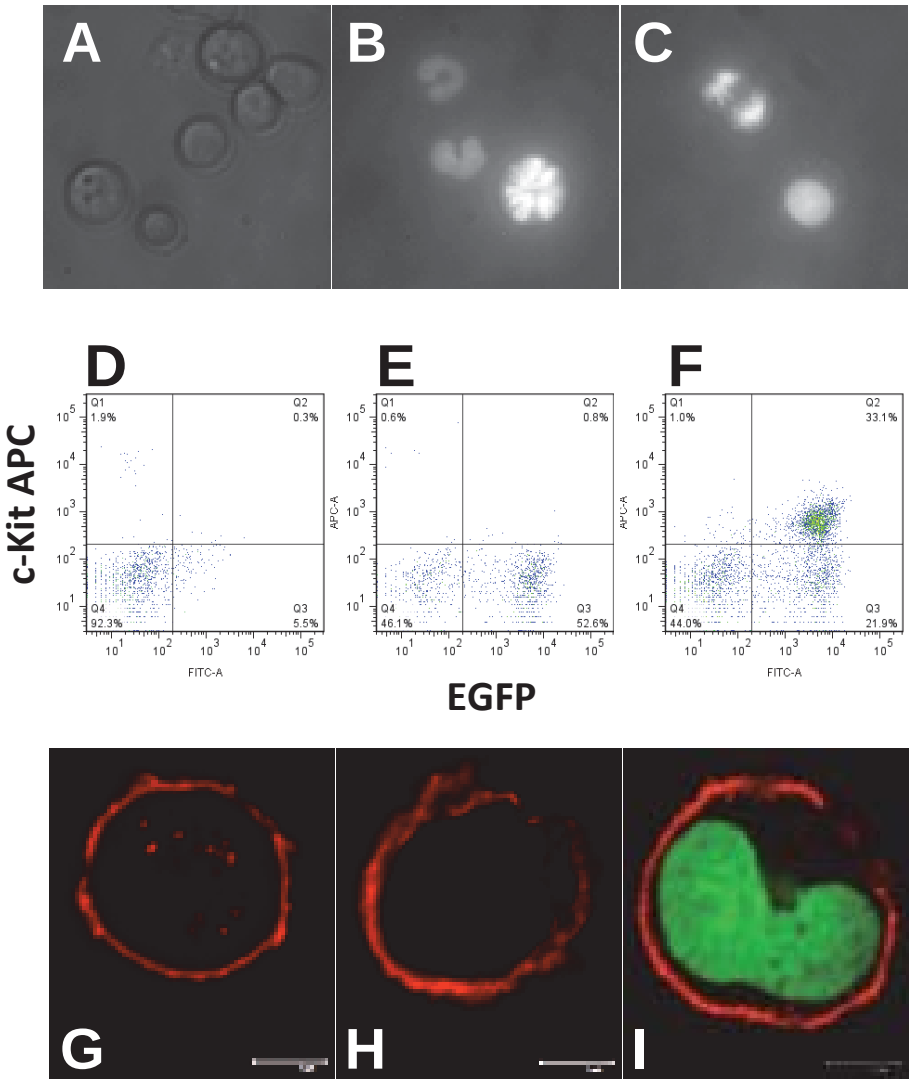

Online Figure X. H2BEGFP reporter accumulates in doxycycline treated CKH2B CPCs *in vitro*.

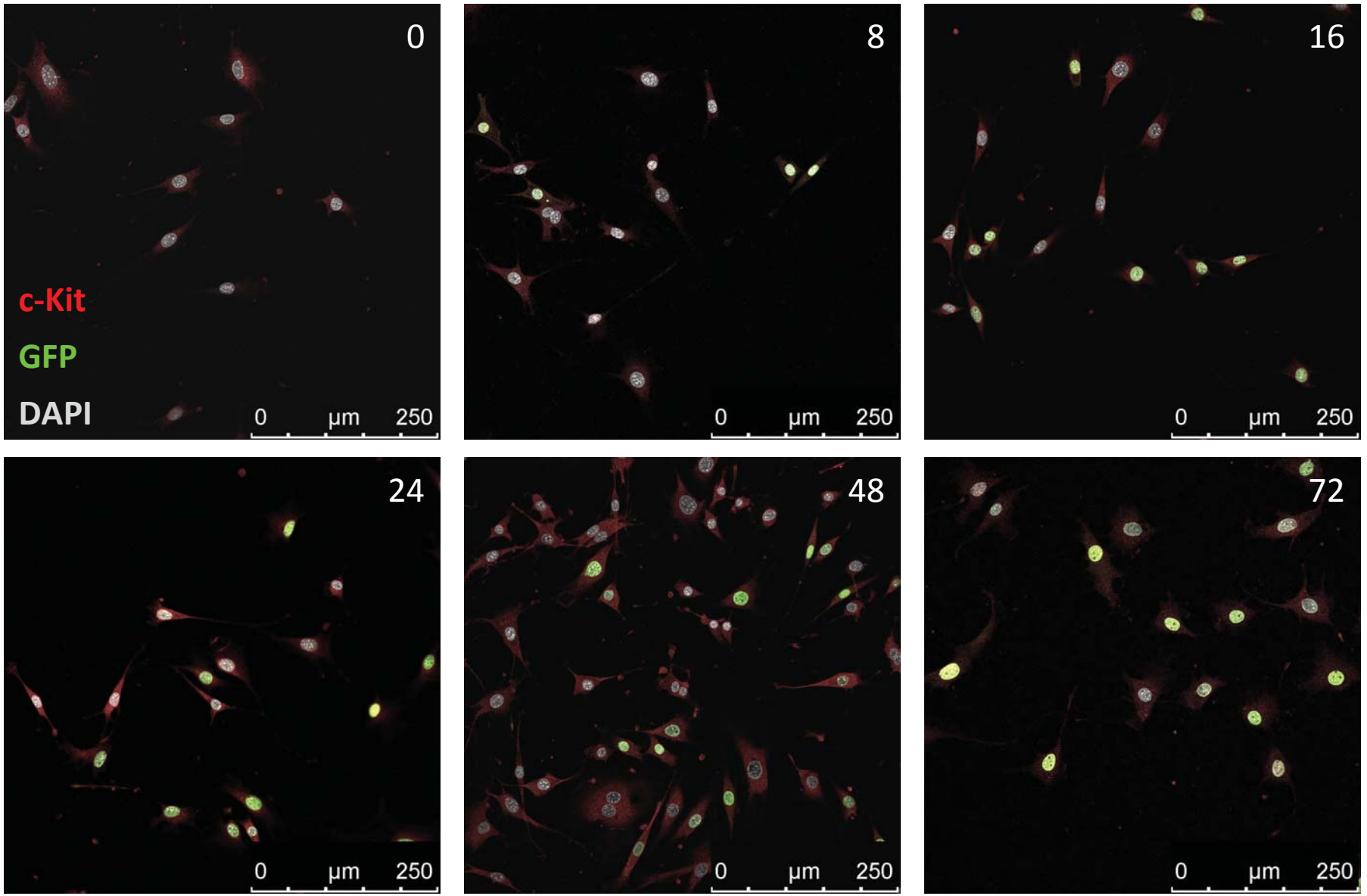

Online Figure XI. Identification of EGFP+ cells in isoproterenol treated CKH2B hearts

A

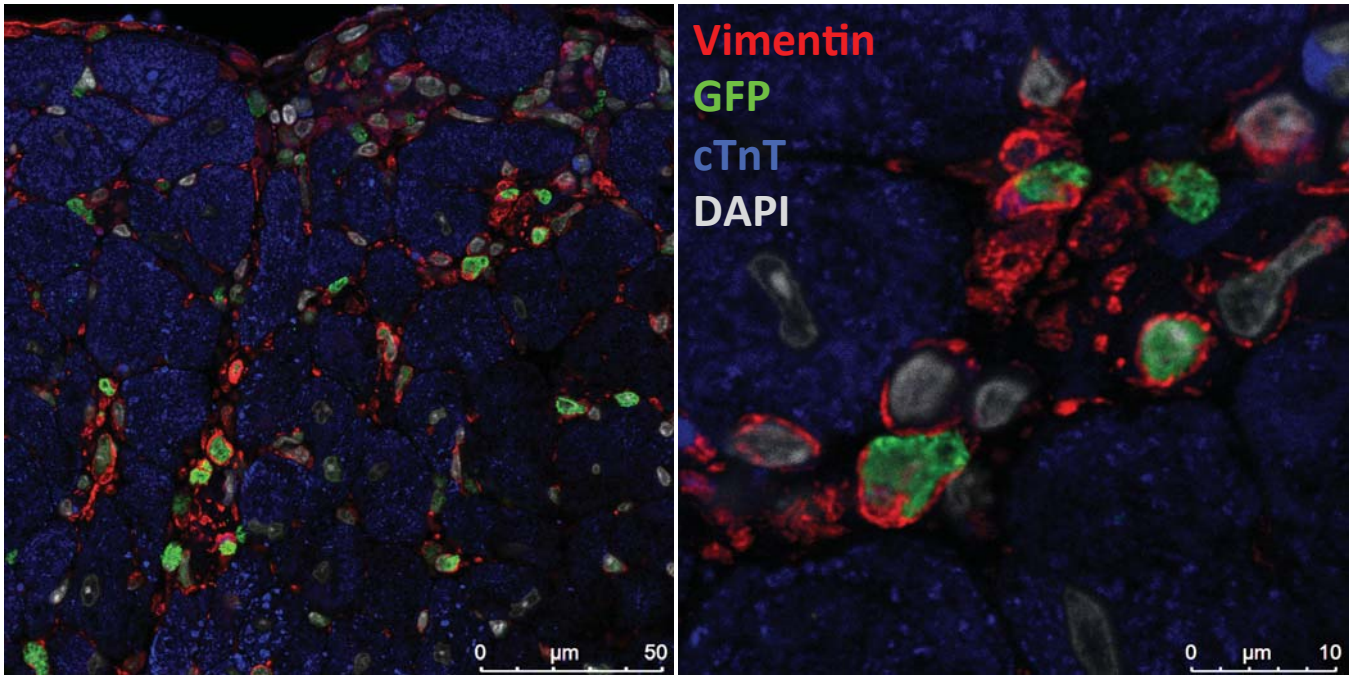

Online Figure XI. Identification of EGFP+ cells in isoproterenol treated CKH2B hearts

B

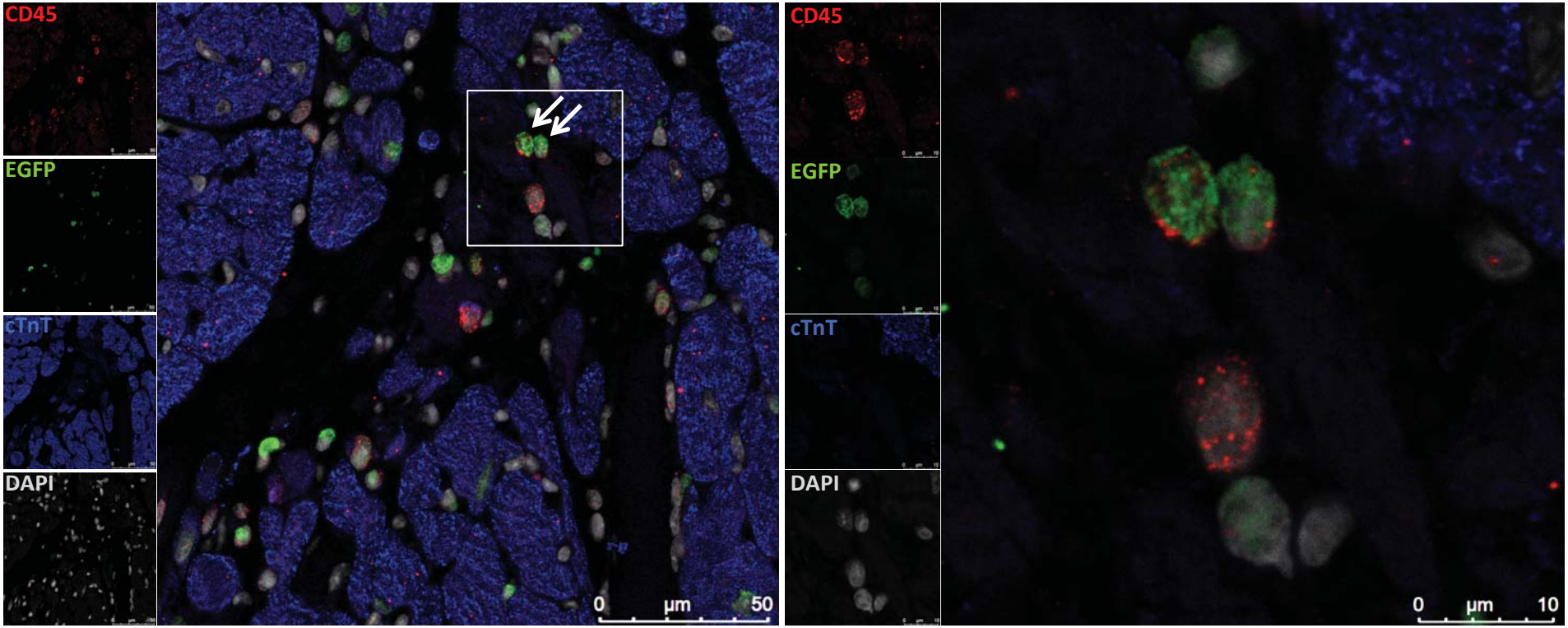

Online Figure XI. Identification of EGFP+ cells in isoproterenol treated CKH2B hearts

C

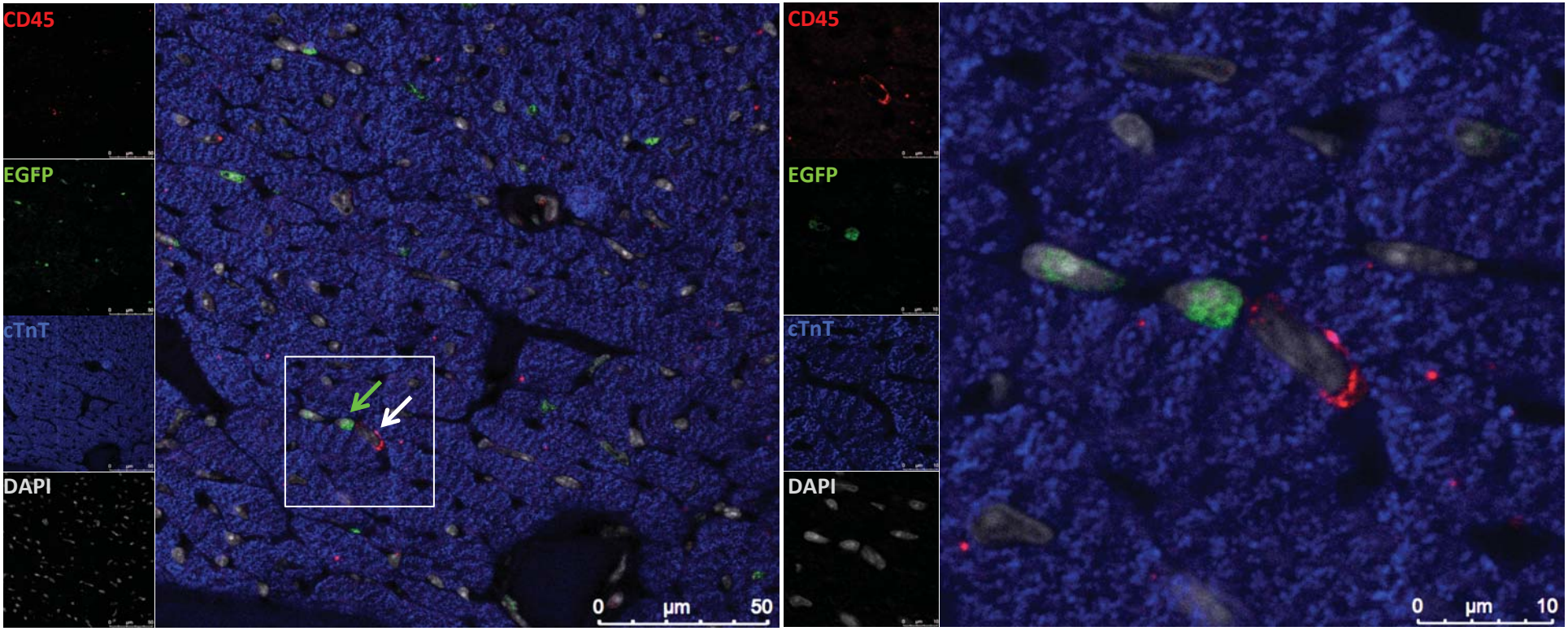

Online Figure XI. Identification of EGFP+ cells in isoproterenol treated CKH2B hearts

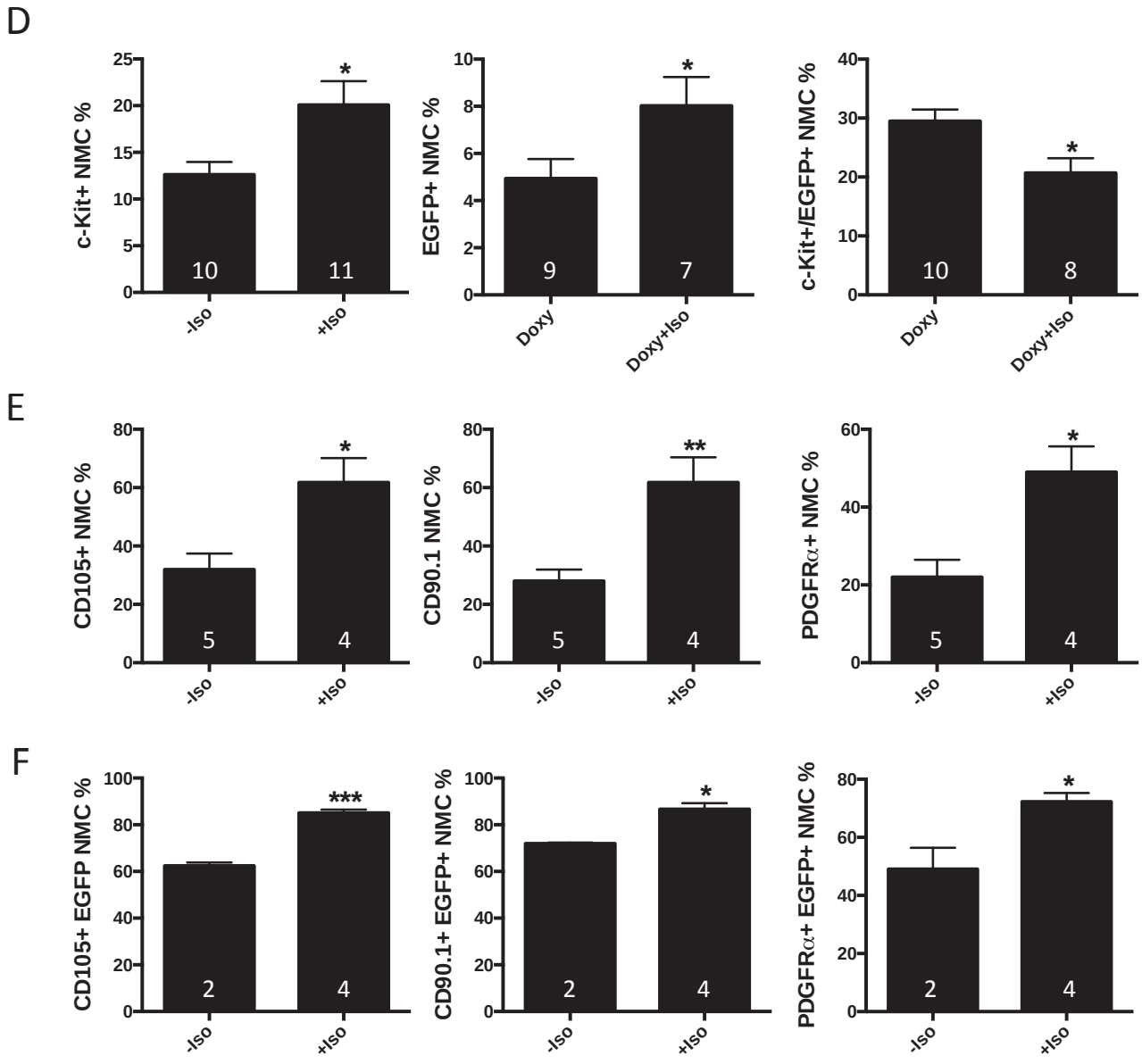

Online Figure I. SCF specifically activates c-Kit signaling in CPCs. SCF-induced phosphorylation of c-Kit, ERK and AKT is blunted in mCPCs pretreated with Imatinib in a dose dependent manner, as measured by immunoblot analysis (A). c-Kit antibody blunts SCF-induced activation of c-Kit, ERK and AKT in mCPCs (B) and hCPCs (C) as quantified from immunoblot analysis. Freshly isolated NMCs contain macrophage and mast cell populations (D). mCPCs at passage 12 express stromal surface markers (CD105, CD90.1 and PDGFRα) but not macrophage (F4/80, CD206) or mast cell proteins (FceR1) as measured by flow cytometry (E). c-Kit is detected by flow cytometry in fixed mCPCs immunolabeled with primary and secondary antibodies, but not in unfixed mCPCs directly immunolabeledwith fluorophore conjugated c-Kit antibody (F). mCPCs were expanded in culture for 12 passages. n=3 experimental replicates for B-E unless otherwise indicated. Statistical significance measured by two-tailed t-test, *=$p<0.05$, ***=$p<0.001$.

Online Figure II. ACMs possess active c-Kit signaling. Immunoblot of c-Kit and phospho-c-Kit in ACMs treated with 0, 100 and 200 ng/ml SCF (A). ACM immunolabeled with c-Kit (green) co-stained with phalloidin (red) and DAPI (white) (B). Freshly isolated ACM express c-Kit protein in 79% of the population, as measured by immunolabeling. Secondary controls in left panel (2^{nd} ctl), ACM negative for c-Kit staining in second panel (c-Kit neg), and ACM positive for c-Kit in right-hand panels (c-Kit intermediate and c-Kit high).

Online Figure III. Constructs, transgenic mouse lines and crosses for c-Kit reporter expression. c-Kit promoter clone 2 [21] drives expression of the reverse tetracycline-controlled transcription factor, rtTA, (A). pTRE-H2BEGFP transgenic reporter mice in which the tetracycline responsive element (TRE) and minimal CMV promoter control expression of Histone 2BJ/EGFP fusion protein (B, JaxMice #005104). Double transgenic mice bearing the c-Kit/rtTA and pTRE-H2BEGFP constructs are expected to express H2BEGFP in c-Kit+ cells following exposure to doxycycline (C). Table defining mouse lines and crosses (D).

Online Figure IX. Quantitation of c-KitrtTA transgene by qPCR. rtTA signal detected in genomic DNA (gDNA) purified from transgenic (red) and non-transgenic (blue) liver samples is plotted on a standard curve determined by serial dilutions of c-KitrtTA plasmid (A). rtTA transgene copy number is approximately 4 per cell in CKH2B mice hemizygous for rtTA. n =9 c-KitrtTA and 5 nontransgenic gDNA samples.

Online Figure V. Identification of non-myocyte cardiac cells labeled by H2BEGFP reporter. Hearts from CKH2B mice treated with doxycycline were harvested for immunolabeling of paraffin sections or flow cytometry analysis. H2BEGFP+ cells (EGFP, green) were colocalized with vimentin (A), cardiac troponin T (cTnT, blue) and DAPI (white). White arrows indicate EGFP+/vimentin+ cells (A). Colocalization of CD31 (red) with EGFP (green) indicated by white arrow (B). Colocalization of CD45 (red) with EGFP (green) indicated by white arrows (C). Immunolabeling of sm22 (red) and EGFP (green) (D). Flow cytometry of dissociated CKH2B EGFP+ nonmyocyte cardiac population immunolabeled with c-Kit, CD31, CD45, CD105, CD90.1 and PDGFRα (top table, E) or EGFP+ bone marrow immunolabeled with c-Kit, CD31 and CD45 (bottom table, E). Comparative quantitation of c-Kit+EGFP+ nonmyocyte and bone marrow populations (F). Detection of c-Kit mRNA in EGFP+ NMC sorted by flow cytometry into c-Kit- and c-Kit+ populations, as measured by qPCR analysis (G). c-Kit+ cells have more c-Kit mRNA, however c-Kit- cells express detectable levels of message compared to cells negative for c-Kit signal, as shown in bottom panel depicting relative amplification curves. 18S=housekeeping gene (G).

Online Figure VI. EGFP+ is expressed in c-Kit+ cells of induced CKmCm and CKH2B hearts. Representative confocal micrograph of paraffin section from tamoxifen induced CKmCm heart (A) and doxycycline treated CKH2B heart (B) immunolabeled for c-Kit (red), EGFP (green), Wheat Germ Agglutinin (WGA, gray), Cardiac Troponin T (cTnT, blue) and DAPI (gray) used for quantitation of c-Kit+GFP+ cells in Figure 5. NMC (left) and BM (right) were isolated from CKmCm+Tx and CKH2B+doxycycline mice and analyzed by flow cytometry for EGFP+ reporter expression. Gating for EGFP+ as shown in upper panels reveals fewer EGFP+ cells in both populations from CKmCm mice, as tabulated below (C). Paraffin sections of CKmCm+Tx hearts were immunolabeled for EGFP+ (green) myocyte markers (red), DAPI (blue) and WGA (white). EGFP+ myocytes are shown at higher magnification in boxes (D).

Online Figure VII. H2BEGFP reporter is expressed in ACM isolated from CKH2B hearts. ACMs (bright field) from doxycycline treated CKH2B hearts exhibit nuclear H2BEGFP signal (green) as revealed by confocal microscopy (A). ACM isolated from untreated CKH2B hearts treated with doxycycline express nuclear H2BEGFP reporter only in doxycycline treated samples (B).

Online Figure VIII. H2BEGFP reporter is expressed in non-cardiac c-Kit+ cells. Immunostaining of noncardiac tissues from doxycycline treated CKH2B mice indicates colocalization of c-Kit (red) and H2BEGFP (green) in intestinal crypts (A), intestinal cryptopatches (B) and pancreatic islets of Langerhans (C). DAPI=gray.

Online Figure IX. H2BEGFP reporter is induced in CKH2B c-Kit+ bone marrow stem cells (BMSC) *in vitro*. Live images of CKH2B BMSCs reveal fluorescent histone in the nucleus in doxycycline treated (B,C) versus vehicle treated cells (A). H2BEGFP expression is induced in c-Kit+ BMSCs as measured by immunolabeling of fixed cells and flow cytometry (D-F) and confocal microscopy (G-I). Absence of H2BEGFP in vehicle treated CKH2B BMSC (A,D,H) and doxycycline treated single transgenic c-KitrtTA BMSC (G) validates doxycycline mediated control of reporter expression. Isotype antibody control (E) verifies specificity of c-Kit signal in F. H2BEGFP is shown in white (B,C) or green (I). red=c-Kit (G-I).

Online Figure X. H2BEGFP accumulates in doxycycline treated CKH2B CPCs *in vitro*. CPCs isolated and expanded from CKH2B hearts were treated with doxycycline for 0, 8, 16, 24, 48 and 72 hours, then fixed and immunolabeled for c-Kit (red), EGFP (green) and DAPI (gray). Time points are indicated in the upper right corner of each micrograph. Scale bar = 250 microns.

Online Figure XI. Identification of EGFP+ cells in isoproterenol treated CKH2B hearts. Hearts from nontransgenic or CKH2B mice treated with doxycycline or doxycycline and isoproterenol 150mg/kg were harvested after three days for immunolabeling of paraffin sections or flow cytometry analysis. H2BEGFP+ cells (EGFP, green) were colocalized with vimentin (A), cardiac troponin T (cTnT, blue) and DAPI (white) (A). Colocalization of CD45 (red) with EGFP (green) in injured tissue indicated by white arrows (B) and magnified in right panel. CD45+/EGFP- (white arrow) and CD45-/EGFP+ (green arrow) cells shown in uninjured region of heart (C), maginifed in right panel. Flow cytometry of dissociated nonmyocyte population from uninjured (-Iso) or injured (+Iso) hearts immunolabeled with c-Kit (D) CD105, CD90.1 or PDGFRα (E) colocalized with EGFP+ (F, D). white numbers indicate n of heart, statistical significance assessed by unpaired t-test, $p<0.05$ considered significant. *=$p<0.05$, **=$p<0.01$, ***=$p<0.01$

Supplemental Tables

Primer sequences		
Target gene	**Application**	
	qPCR	**Genotyping**
mouse c-Kit Forward 1	ACGATGTGGGCAAGAGTTCC	
mouse c-Kit Forward 2	GATCTGCTCTGCGTCCTGTT	
mouse c-Kit Reverse 1	GCCTGGATTTGCTCTTTGTTGT	
mouse c-Kit Reverse 2	ATTGTGCTGGATGGATGGAT	
human c-Kit Forward	ATTCAAGCACAATGGCACGG	
human c-Kit Reverse	AGGGTGTGGGGATGGATTTG	
rtTA Forward	GAAGGCCTGACGACAAGGAA	GCC GAA TTC CCA TGG CCAC CAT GTC TAG ACT GGA CAAG
rtTA Reverse	GTCGCGATGTGAGAGGAGAG	CTG ACA CAG GAA CGC GAG CTG
18S Forward	CGAGCCGCCTGGATACC	
18S Reverse	CATGGCCTCAGTTCCGAAAA	
GAPDH Forward	CATGGCCTTCCGTGTTCCTA	
GAPDH Reverse	CCTGCTTCACCACCTTCTTGAT	
GFP Forward	CGGCGACGTAAACGGCCACAA	TAC GGC AAG CTG ACC CTG AA
GFP Reverse	CACGCCGTAGGTCAGGGTGG	TGT GAT CGC GCT TCT CGT TG

Supplemental Table l. Primer sequences for quantitative real time PCR and genotyping of transgenic mouse lines.

Primary Antibodies and Cellular Stains					
Target	**Catalog #**	**IHC-P**	**WB**	**IF**	**FACS**
c-Kit	RND Systems AF1356	1/50 4 μg/ml	1/200 0.4 μg/ml	1/50 5 μg/ml	
Phospho-c-Kit pY703	Abcam Ab62154		1/200		
Rat anti-c-Kit-APC	Miltenyi 130-102-492				1/10 3 μg/ml
Rat IgG2b-APC	Miltenyi 130-102-664				1/10 3 μg/ml
Rat IgG2ak-APC	Thermofisher 17-4321-81				0.125 μg/test
Rat IgG2bk-APC	Thermofisher 17-4031-81				0.125 μg/test
Mouse IgG2ak-PerCP-Cy5.5	Thermofisher 45-4724-80				0.06 μg/test
Goat IgG-APC	RND Systems IC108A				1/10
Rat anti-CD31-APC	Thermofisher 17-0311-80				0.5 μg/test
Rat anti-CD45-APC	Thermofisher 17-0451-82				0.125 μg/test
Rat anti-CD105-APC	Thermofisher 17-1051-82				0.125 μg/test
Mouse anti-CD90.1-PerCP-Cy5.5	Thermofisher 45-0900-80				0.06 μg/test
Goat anti-PDGFRα-APC	RND Systems FAB1062A				1/10
Rat anti-CD206-APC	Thermofisher 17-2061-80				0.25 μg/test
Rat anti-F4/80-APC	Thermofisher 17-4801-80				2.0 μg/test
Hamster anti-FceR1-APC	Thermofisher 17-5898-80				0.125 μg/test
Rabbit anti-CD45	Abcam ab10558	1/200			
Chicken-anti-Vimentin	Abcam ab39376	1/500			
Goat anti-CD31	Santa Cruz sc-1506	1/40			
Rat anti-c-Kit	Novus NBP-1-43359	10μg/ml for *in vitro* c-Kit neutralization in mCPCs			

Mouse anti-c-Kit	RND Systems MAB332	15μg/ml for *in vitro* c-Kit neutralization in hCPCs			
Rabbit anti-EGFP	Thermofisher A11122	1/200	1/500		
Chicken anti-EGFP	Thermofisher A10262			1/100	
cTnT	Thermofisher MA5-12960	1/200			
BrdU	Abcam AB6326			1/500	
GAPDH	Millipore		1/3000		
b-Actin	Santa Cruz sc-81178		1/1000		
AKT	Santa Cruz sc-1619		1/100		
Phospho-AKT	Cell Signaling 9271		1/500		
ERK1/2	Cell Signaling 9102		1/200		
Phospho-ERK1/2	Cell Signaling 9101		1/500		
Myosin Light Chain 2V	Santa Cruz sc-34490	1/100			
Membrane, WGA-555	Thermofisher W32464	1/100			
Membrane, WGA-biotin	Vector Labs B-1025	1/100			
Streptavidin Alexa Fluor 700	Thermofisher S21383	1/100			
Nucleus, DAPI	Sigma D8417	1/10,000 0.1 μg/ml		1/5000 0.2 μg/ml	

Supplemental Table II. Antibodies and cellular stains used for immunohistochemistry (IHC-P), immunofluorescence (IF), immunoblotting (WB) flow cytometry (FACS) and functional neutralization assays.

Cardiac c-Kit and EGFP Colocalization Efficiency			
	Exp 1	**Exp 2**	**Exp 3**
CKH2B+Doxy 1	0.7414	0.7	0.4776
CKH2B+Doxy 2	0.7955	0.7769	0.667
CKH2B+Doxy 3	0.8372	0.8936	0.9231
CKmCm+Tx1	0.68	0.6486	0.4038
CKmCm+Tx2	0.7857	0.6154	0.4062
CKmCm+Tx3	0.7778	0.7806	0.6875
CKmCm+Tx4	0.5862	0.5455	0.5319

Supplemental Table III: Fractional co-expression values for c-Kit and EGFP in paraffin sections from two c-Kit reporter models.

Online Video I. H2BEGFP accumulates in doxycycline treated CKH2B CPC *in vitro***.** CPCs isolated and expanded from CKH2B hearts (bright field) treated with doxycycline acquire H2BEGFP reporter signal (green) over time, as demonstrated by time-lapse fluorescence images converted into video. Time of video =14 hours 45 minutes.

*** Long In Vivo Checklist**

Circulation Research - Preclinical Animal Testing: A detailed checklist has been developed as a prerequisite for every publication involving preclinical studies in animal models. ***Checklist items must be clearly presented in the manuscript, and if an item is not adhered to, an explanation should be provided.*** *If this information (checklist items and/or explanations) cannot be included in the main manuscript because of space limitations, please include it in an online supplement. If the manuscript is accepted, this checklist will be published as an online supplement. See the explanatory editorial for further information.*

This study involves use of animal models:

Yes

Study Design

The experimental group(s) have been clearly defined in the article, including number of animals in each experimental arm of the study.	Yes
An overall study timeline is provided.	N/A
The protocol was prospectively written	N/A
The primary and secondary endpoints are specified	N/A
For primary endpoints, a description is provided as to how the type I error multiplicity issue was addressed (e.g., correction for multiple comparisons was or was not used and why). (Note: correction for multiple comparisons is not necessary if the study was exploratory or hypothesis-generating in nature).	N/A
A description of the control group is provided including whether it matched the treated groups.	Yes

Inclusion and Exclusion criteria

Inclusion and exclusion criteria for enrollment into the study were defined and are reported in the manuscript.	N/A
These criteria were set *a priori* (before commencing the study).	N/A

Randomization

Animals were randomly assigned to the experimental groups. If random assignment was not used, adequate explanation has been provided.	N/A
Type and methods of randomization have been described.	N/A
Allocation concealment was used.	N/A
Methods used for allocation concealment have been reported.	N/A

Blinding

Blinding procedures with regard to masking of group/treatment assignment from the experimenter were used and are described. The rationale for nonblinding of the experimenter has been provided, if such was not performed.	N/A
Blinding procedures with regard to masking of group assignment during outcome assessment were used and are described.	N/A
If blinding was not performed, the rationale for nonblinding of the person(s) analyzing outcome has been provided.	N/A

Sample size and power calculations

Formal sample size and power calculations were conducted before commencing the study based on *a priori* determined outcome(s) and treatment effect(s), and the data are reported.	N/A
If formal sample size and power calculation was not conducted, a rationale has been provided.	N/A

Data Reporting

Baseline characteristics (species, sex, age, strain, chow, bedding, and source) of animals are reported.	Yes
The number of animals in each group that were randomized, tested, and excluded and that died is reported. If the experimentation involves repeated measurements, the number of animals assessed at each time point is provided is provided for all experimental groups.	N/A
Baseline data on assessed outcome(s) for all experimental groups are reported.	N/A
Details on important adverse events and death of animals during the course of the experiment are reported for all experimental groups.	N/A
Numeric data on outcomes are provided in the text or in a tabular format in the main article or as supplementary tables, in addition to the figures.	Yes
To the extent possible, data are reported as dot plots as opposed to bar graphs, especially for small sample size groups.	Yes
In the online Supplemental Material, methods are described in sufficient detail to enable full replication of the study.	Yes

Statistical methods

The statistical methods used for each data set are described.	Yes
For each statistical test, the effect size with its standard error and *P* value is presented. Authors are encouraged to provide 95% confidence intervals for important comparisons.	Yes
Central tendency and dispersion of the data are examined, particularly for small data sets.	N/A
Nonparametric tests are used for data that are not normally distributed.	N/A
Two-sided *P* values are used.	Yes
In studies that are not exploratory or hypothesis-generating in nature, corrections for multiple hypotheses testing and multiple comparisons are performed.	N/A
In "negative" studies or null findings, the probability of a type II error is reported.	N/A

Experimental details, ethics, and funding statements

Details on experimentation including formulation and dosage of therapeutic agent, site and route of administration, use of anesthesia and analgesia, temperature control during experimentation, and postprocedural monitoring are described.	Yes
Both male and female animals have been used. If not, the reason/justification is provided.	Yes
Statements on approval by ethics boards and ethical conduct of studies are provided.	Yes
Statements on funding and conflicts of interests are provided.	Yes

---

Date completed: 03/24/2018 19:39:03
User pid: 11355